Rocking revisited 4

Analysis of rocking-induced stresses for concrete breakwater armour units

MSc thesis by Thomas Goud

TU Delft

23-01-2020

Thomas Goud

Rocking revisited 4

Analysis of rocking-induced stresses for concrete breakwater armour units

By Thomas Goud

Student ID: 4296613

In partial fulfilment of the requirements for the degree of Master of Science in Civil Engineering, tracks Hydraulic Engineering and Structural Engineering, at the Delft University of Technology

Assessment committee

Dr. ir. B. (Bas) Hofland (chair of the committee)	TU Delft, section Hydraulic Engineering
Prof. dr. ir. J.G. (Jan) Rots	TU Delft, section Structural Engineering
Dr. A. (Alessandro) Antonini	TU Delft, section Hydraulic Engineering
Ir. P.A. (Paul) Korswagen Eguren	TU Delft, section Structural Engineering

Preface

This MSc thesis report is the final part of my studies at the Delft University of Technology. It presents my research to the stresses in concrete breakwater armour units due to rocking under wave attack.

This is a good place to express my gratitude to everyone who has contributed to my studies and MSc thesis, even if it is only a tiny contribution, though I doubt that anyone ever reads this. First of all, I want to thank my entire committee (Bas Hofland, Paul Korswagen, Alessandro Antonini, and Jan Rots) for their input and help when I needed it, even though I did not actively seek help very often. Special thanks to Cock van der Lem, who let me borrow the CUR reports that were the starting point of my thesis. I am grateful to anyone who has provided me with any information that helped me on my way, even if I do not mention them by name. Furthermore, I want to thank my whole family, just because I can do that in the preface, and because they have supported me throughout my entire life. Last but not least, I want to thank all fellow students who made my studies bearable and enjoyable, most notably Shannon, with whom I spent many hours in Delft, both working on our own thesis, which was enjoyable and motivating even though we were sometimes sitting there silently.

Thomas Goud
Alblasserdam, the Netherlands. January 2020

Contents

Summary

Concrete breakwater armour units sometimes collide with each other under heavy wave attack. This process, called rocking, leads to stresses in the concrete units, which can become so high that the concrete units break. This is problematic for the stability of the breakwater, but it is not yet incorporated in the design practice. This report provides a probabilistic method to determine the breakage probability of concrete breakwater armour units, elaborated for Xbloc®s. The starting point is to determine the impact velocity, which is then used as input to determine the impact force. By identifying the critical failure mechanism, and with the impact force as input, the relevant stresses can be determined. This stress is compared with the impact strength of concrete, to predict crack formation in the concrete. By performing a Monte Carlo simulation of this process, it is possible to quantify exceedance probabilities and to give an expected failure percentage. Figure 1 provides a flow chart of all the required steps to reach the goal of predicting breakage of an armour unit, including the parameters and variables that are needed in each step.

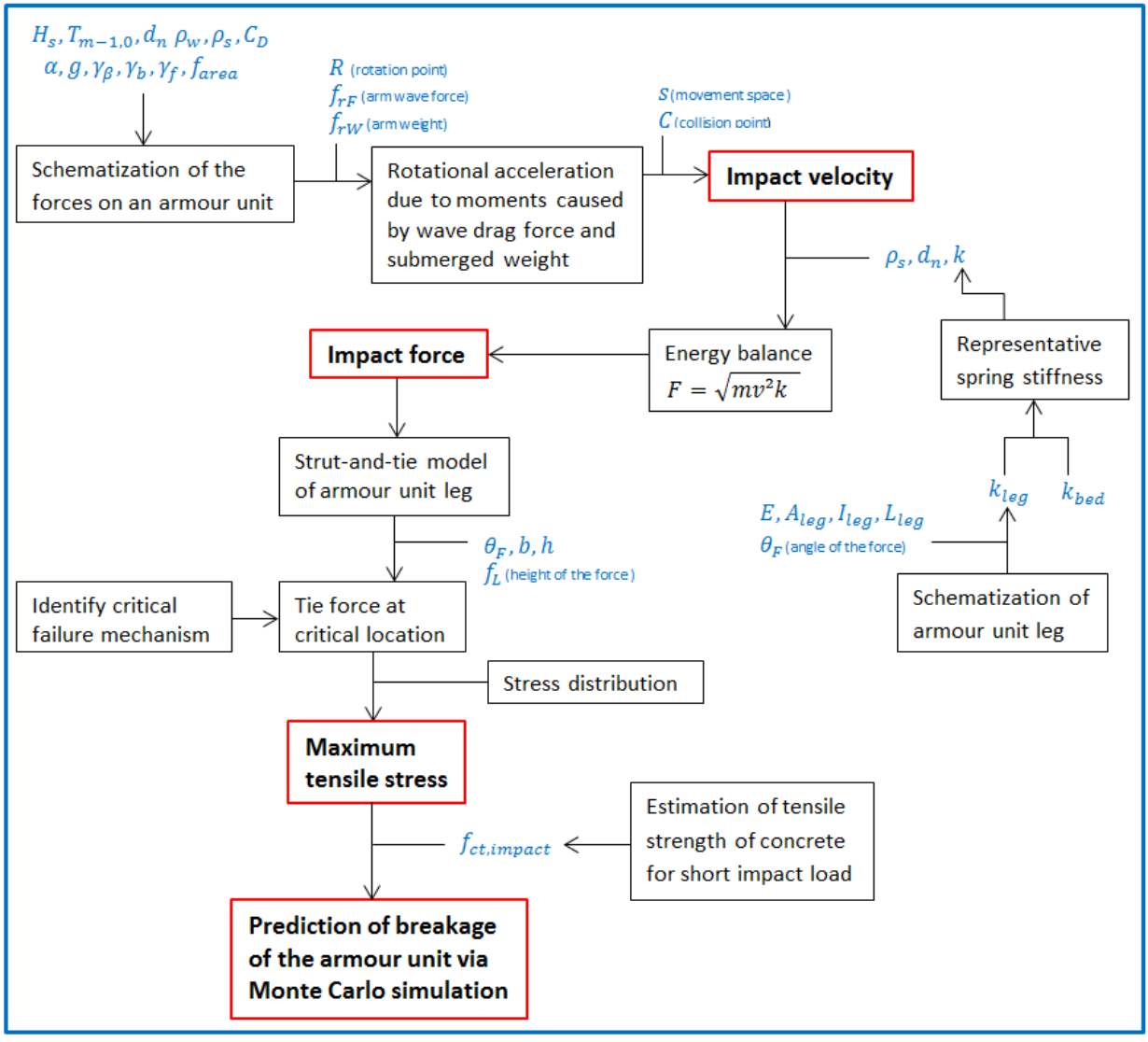

Figure 1: Flow chart of the whole model

The impact velocity is based on a 2D schematization of the forces on an armour unit under wave attack. The wave drag force is determined using the run-up velocity, and the submerged weight is used. From the moments that result from these forces, the rotational acceleration is determined, which can be translated to an impact velocity, by taking into account the travelled distance up to impact. Only rotation is considered for the movement, since it is often observed that rocks and blocks rotate instead of undergoing a translation. In the derivation of the impact velocity formula, it is assumed that the acceleration is constant, but this is not the case, so a correction factor is established to reduce this error. The impact velocity and its parameters and variables are elaborated for both cubes and Xbloc®s. A validation is performed by comparing it with physical model test results, which shows that the modelled impact velocity is in the right order of magnitude.

The impact force is based on an energy balance between the kinetic energy of the moving block and the potential energy in the form of a spring stiffness. This energy balance does not include kinetic energy of the stricken armour unit, nor energy losses due to local crushing of the concrete. Though both could potentially be significant in some situations, they are neglected, because they are unknown. The force is thus determined from the spring energy, for which the spring stiffness is based on a system of two springs in series: one spring represents the armour unit stiffness, the other represents the stiffness of the gravel bed beneath the armour unit. The armour unit stiffness itself is based on the compressive stiffness and bending stiffness of an armour unit leg. A validation is performed by comparing the modelled impact force with physical model test results, although the physical test did not include the breakwater bed, so it is temporarily excluded from the model as well, to make a fair comparison. For this comparison, the modelled impact force is in the right order of magnitude, but it is not validated if the representation of the breakwater bed is correct.

In order to determine the stresses, it is important to first find the failure mechanism. Failure due to tensile bending stresses is identified as the most important failure mechanism, with the base of the leg as critical cross section. Some other failure mechanisms may occur, such as local crushing or chipped off corners, but these are not taken into account because they generally do not have a severe effect on the overall state of the breakwater. The stresses at the critical location are determined from a strut-and-tie model, which gives a 2D representation of the armour unit leg. A FEM model is used to find the stress distribution at the critical location, which, together with the tie force from the strut-and-tie model, results in an expression for the maximum tensile stress. The stress is then compared with the tensile impact stress of the concrete, to evaluate if the concrete fails. Predicted failure in the model is thus defined as the formation of cracks, which is assumed to eventually lead to complete rupture of the leg, due to the repeated loading by the waves.

All the derived expressions are implemented in the eventual model, for which values are estimated for each parameter, and stochastic variables are given a probabilistic distribution. The model then needs only the significant wave height and the armour unit diameter as input, in order to perform a Monte Carlo simulation that determines distributions of the impact velocity, the impact force, and the maximum tensile stresses, and predicts failure for N independent cases. The model results show that failure of the concrete happens more frequently as waves and armour units get larger, up to predicted failure in 15.8% of the simulated cases for a case of H_s = 10.01 m and d_n = 2.71 m. Failure of armour units generally is more problematic in cases with larger waves and armour units, so it is good that the model represents this.

List of symbols

a	Acceleration	[m/s²]
a_R	Rotational acceleration	[rad/s²]
A	Reference area (in drag formula)	[m²]
b	Cross section width	[m]
C_D	Drag coefficient	[-]
d_n	Nominal diameter	[m]
d_{n50}	Nominal median diameter	[m]
E	Young's modulus	[N/m²]
F	Force, subscript H or V indicate horizontal or vertical components	[N]
f_{area}	Area affected by waves, as a fraction of d_n^2	[m^{-2}]
f_{ck}	Characteristic concrete strength	[N/mm²]
f_{cor}	Correction factor for acceleration not being constant	[-]
f_{ctm}	Mean tensile concrete strength	[N/mm²]
$f_{inertia}$	Factor for mass moment of inertia, such that $I = f_{inertia}\rho d_n^5$	[m^{-3}]
g	Gravitational acceleration	[m/s²]
h	1. Cross section height	[m]
	2. Height at which the force acts on the armour unit leg	[m]
H	Wave height	[m]
H_s	Significant wave height	[m]
H_{m0}	Significant wave height obtained from wave spectrum	[m]
I	1. Mass moment of inertia	[kg·m²]
	2. Area moment of inertia	[m^4]
k	Elastic stiffness	[N/m]
K	Contact stiffness	[$kN/mm^{3/2}$]
K_D	'Dustbin' parameter in Hudson's formula	[-]
M	(Bending) moment	[N·m]

N	1. Number of waves	[-]
	2. Number of repetitions (Monte Carlo simulation)	[-]
	3. Normal force	[N]
P	Notional permeability coefficient in Van der Meer's formula	[-]
p	Probability (of exceedance)	[-]
R_u	Run-up level relative to still water level	[m]
S	Damage level, as used in Van der Meer's formula	[-]
T	Wave period	[s]
u	Fluid velocity	[m/s]
v	1. Armour unit velocity	[m/s]
	2. Impact velocity	[m/s]
W	Weight	[N]
z_A	Level on the slope relative to still water level (in run-up formula)	[m]
α	1. Slope angle	[rad]
	2. Effective mass, as used in the CUR reports	[kg]
γ_b	Influence factor for a berm (in run-up formula)	[-]
γ_f	Influence factor for roughness of the slope (in run-up formula)	[-]
γ_β	Influence factor for oblique waves (in run-up formula)	[-]
δ	Deformation	[mm]
Δ	Relative mass density, $\Delta = \frac{\rho_s - \rho_w}{\rho_w}$	[-]
θ	Orientation angle of the armour unit	[°]
θ_F	Angle of the incoming force	[°]
ρ_s	Density of rock or concrete	[kg/m³]
ρ_w	Density of water	[kg/m³]
μ	Friction coefficient	[-]
ξ	Iribarren parameter or breaker parameter	[-]

1. Introduction

1.1 Background of the problem

Many coasts and harbours are protected against waves by means of breakwaters. Usually, the breakwater is the first line of defence against the water and is thus subjected to the heaviest waves. Several types of breakwaters have been developed to withstand those waves. A commonly applied type, and the subject of this MSc thesis, is the rubble mound breakwater, which has an armour layer of large rocks or concrete elements to take away the wave energy, and a gravel and sand core to prevent the water from flowing through the breakwater. A schematization of a rubble mound breakwater is given in Figure 1.1.

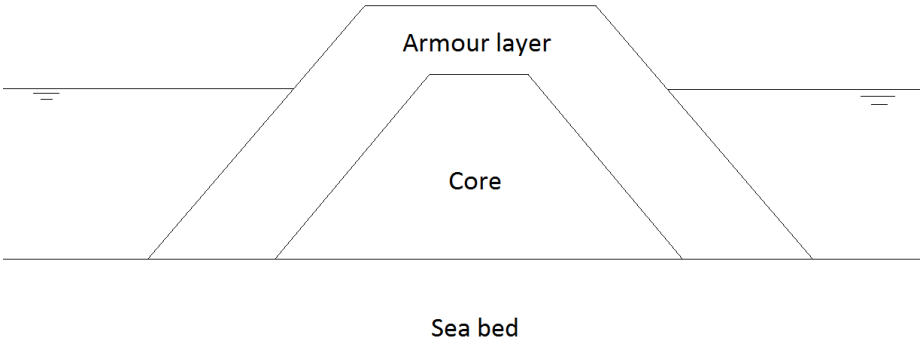

Figure 1.1: Schematized cross-section rubble mound breakwater

Rubble mound breakwaters have been used for many years now, but there are still developments. In the early days, large natural rocks were used in the armour layer, which is still a solid solution in moderate wave climates. However, in heavy conditions, the waves can be so large that it is difficult to find any natural rocks of sufficient size and weight. Therefore, concrete armour units were being developed, as they can be fabricated in the required size. Originally, simple concrete cubes were being used, but people realized that the stability of the armour units could be improved by improving the interlocking between the armour units, leading to the development of armour units with legs. Emphasizing on this feature led to slender armour units with greatly improved interlocking, but then a new problem arose: several breakwaters failed when many armour units broke due to rocking. Rocking is the situation when an armour unit moves due to wave attack and collides with another unit. The general design conventions at the time mainly focussed on hydraulic problems, but it became clear that the structural strength is important as well. The Dutch 'Civieltechnisch Centrum Uitvoering Research en Regelgeving', abbreviated as the CUR, carried out an extensive research to the strength of concrete armour units, after several breakwaters failed in the 1980's (CUR, 1989 – 1, 2 and 1990 – 1, 2). They researched the impact velocity and impact force during rocking, in order to create a prediction for breakage of armour units due to rocking.

Though breakage of armour units due to rocking is nowadays recognized as a failure mechanism of breakwaters, it is still barely incorporated in the standard design procedures, partially because there is not yet enough knowledge about predicting breakage due to rocking. Therefore, this MSc thesis attempts to contribute to this knowledge, in order to eventually obtain a methodology to design breakwaters with low vulnerability to rocking.

1.2 Goal

The goal of this MSc thesis is to determine the rocking-induced stresses in concrete breakwater armour units theoretically, by means of analytical expressions, in order to predict breakage of these units in a probabilistic way.

These rocking-induced stresses are determined in a few separate steps. To start, the impact velocity of a collision between two armour units will be determined. This velocity will then be used as input to determine the impact forces on these units, which in turn will be used as input to determine the stresses. Based on these stresses and the concrete strength under a short impact load, a prediction of failure of the concrete can be made.

The impact velocity will be based on the acceleration that follows from a force balance on an armour unit under wave attack. The impact velocity will be determined for armour units at or around the still water line. This impact velocity will be validated by physical model test results. The impact velocity is an input variable to determine the impact force, which will be done based on an energy balance. The impact force will also be validated by physical model test results. The rocking-induced tensile bending stresses will be determined using the force as input, based on a strut-and-tie model of a deep beam. Eventually, a prediction of breakage can be given, based on the stresses and the concrete strength. Ultimately, each relevant variable will be given a probabilistic distribution, such that a probabilistic breakage prediction is obtained when putting everything together in one model.

1.3 Outline of the report

The structure of this report is presented in a flow chart in Figure 1.2 and will shortly be described here. First, some relevant knowledge from the literature study will be presented, which was used as a starting point for this MSc thesis. Subsequently, an analytical expression will be derived to determine the impact velocity of one armour unit hitting another unit, based on the acceleration that is obtained from a force balance of an armour unit under wave attack. Several parameters and variables needed in this impact velocity expression will also be determined. The impact velocity is then used to determine the impact force during the collision, based on an energy balance. The next chapter, about failure of the concrete, treats the different failure mechanisms of a concrete armour unit, and gives an estimate for the concrete strength under short impact loading. Then, the rocking-induced stresses can be determined based on the impact force, and the identified critical failure mechanism. Now, the whole model is complete and can be put together. An approximated probabilistic distribution will be given to all input parameters, resulting in a probabilistic breakage prediction. Finally, an overview of the conclusions will be given, followed by a short list of recommendations for future research and possible improvements of this research.

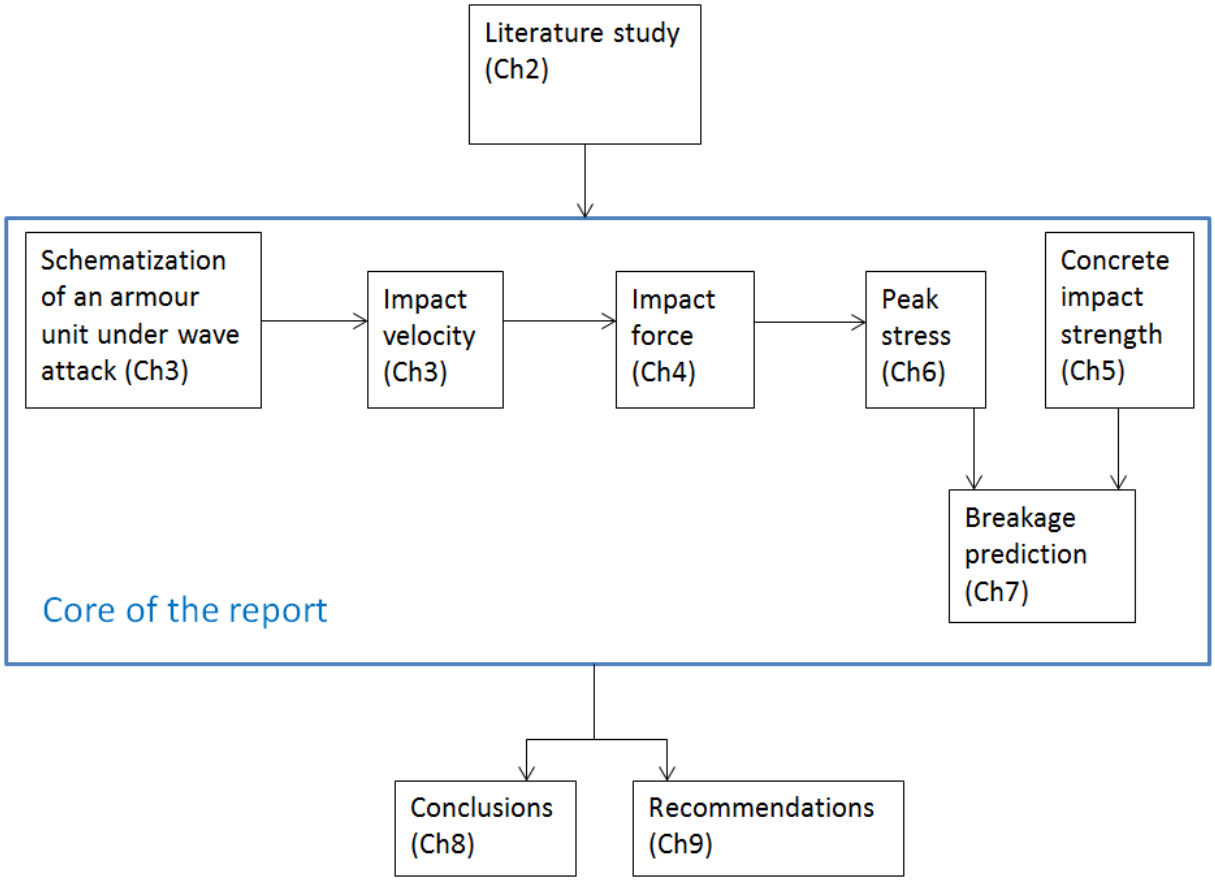

Figure 1.2: Flow chart outline report

2. Study of previous research and knowledge

This chapter is dedicated to finding useful information, either from previous research or knowledge in any other way. An overview of relevant findings is given in this chapter.

2.1 General breakwater information

In order to properly analyse the stresses in concrete armour units due to rocking, a basic understanding of the functioning and design of breakwaters is important. There are a few different types of breakwaters, with the most relevant one for this MSc thesis being the rubble mound breakwater. Rubble mound breakwaters have been used for centuries to protect coasts and harbours. A typical cross-section of a rubble mound breakwater is given in Figure 2.1.

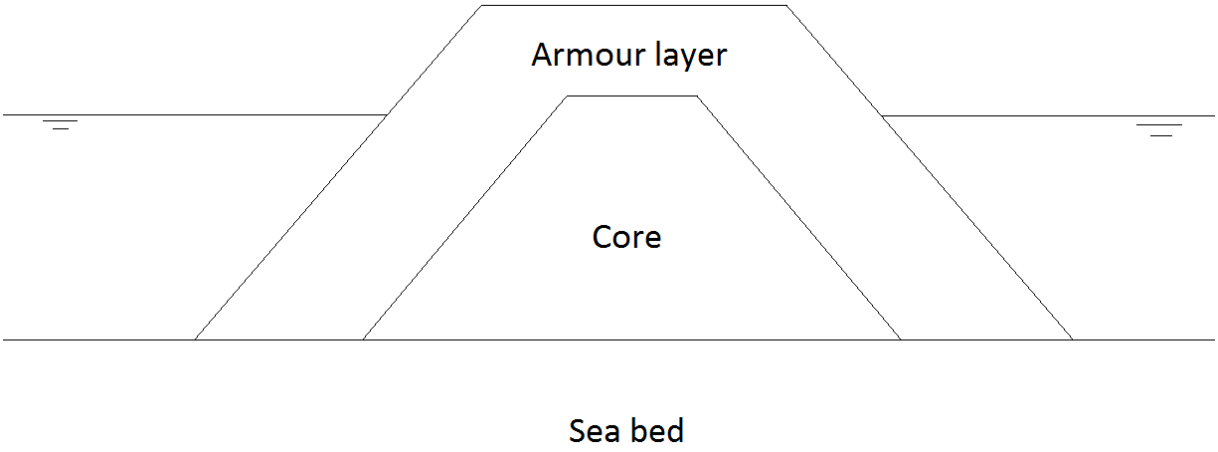

Figure 2.1: Schematized cross-section rubble mound breakwater

A rubble mound breakwater consists of a core and an armour layer on top, possibly with one or more intermediate layers in between. The core of the breakwater usually consists of sand or gravel and prevents water from flowing through the breakwater. The breakwater can be designed to allow for some permeability, as its main function is to nullify the wave energy. The armour layer protects the core and consist of large, heavy rocks that should be able to withstand the waves. The wave energy dissipates as it runs up the slope of the armour layer. The breakwater must be sufficiently high to prevent overflow and overtopping. The rocks must provide enough stability to prevent being washed away by the waves. Logically, the larger the waves, the larger the required rocks to maintain stability. At some point, the waves are so large that it becomes very difficult to find natural rocks that are heavy enough to provide sufficient stability. Therefore, concrete armour units were being developed, as they can be made with the required weight, but for now, the information will be treated without looking specifically at rocks or concrete units.

2.2 Stability formulas

How large and heavy the rocks need to be in order to withstand certain waves has been a topic of many research. Iribarren (1938) considered a force equilibrium for a block on a slope, to derive a formula for calculating the required rock size. He considered four main forces on the rock: own weight, buoyancy, wave force, and frictional resistance. In order to fully understand what is happening, the derivation of the formula is repeated in a similar way, following the lecture notes of Van den Bos and Verhagen (2018). The situation can be schematized as in Figure 2.2.

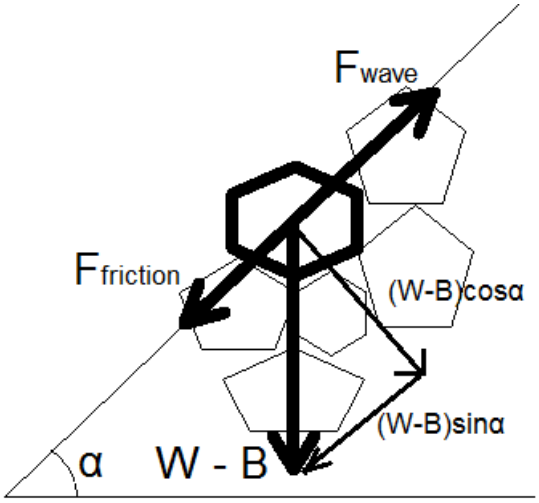

Figure 2.2: Schematization forces on a rock on a breakwater slope

The weight W and buoyancy B both work in vertical direction, but opposite to each other.. Since the weight is larger than the buoyancy, this can be depicted as a net downward force. This net force can be decomposed in a component along the slope and a component perpendicular to the slope, as done in Figure 2.2. Then, a balance can be made of this component along the slope, the friction and the wave force, as in Equation 2.1.

$$F_{wave} = F_{friction} + (W - B)\sin\alpha \qquad \text{Equation 2.1}$$

For the wave force, a relatively simple equation is assumed, similar to uniform flow, where $F = C_i \rho_w u^2 d_n^2$, and $u \approx \sqrt{gH}$ for shallow water waves.

$$F_{wave} = \rho_w g d_n^2 H \qquad \text{Equation 2.2}$$

The weight W and buoyancy B follow from relatively simple expressions:

$$W = \rho_s g d_n^3 \qquad \text{Equation 2.3}$$

$$B = \rho_w g d_n^3 \qquad \text{Equation 2.4}$$

Finally, the friction force is a function of a certain friction coefficient μ and the force perpendicular to the slope.

$$F_{friction} = \mu(W - B)\cos\alpha \qquad \text{Equation 2.5}$$

Putting everything in Equation 2.1 results in:

$$\rho_w g d_n^2 H = \mu(\rho_s g d_n^3 - \rho_w g d_n^3)\cos\alpha + (\rho_s g d_n^3 - \rho_w g d_n^3)\sin\alpha \quad \text{Equation 2.6}$$

Further evaluation leads to:

$$\frac{\rho_w}{\rho_s - \rho_w}\frac{H}{d_n} = \mu\cos\alpha + \sin\alpha \quad \text{Equation 2.7}$$

$$\frac{H}{\Delta d_n} = \mu\cos\alpha + \sin\alpha \quad \text{Equation 2.8}$$

Though the resulting formula Equation 2.8 is not perfect for application in the more complex real world, it is useful to give insight in the relevant parameters. The incoming wave is represented via wave height H, the relative weight of the rock via Δd_n, the friction via μ, and the slope angle via α. The friction μ can also be related to the angle of repose. It is then used as $\mu = \tan\phi$. Many newer formulas also use the form of $\frac{H}{\Delta d_n}$, which is often called the stability number. Some formulas have also been developed specifically for a certain type of concrete armour unit.

Another important formula is proposed by Hudson (1953). He performed many tests and eventually came up with:

$$M = \frac{\rho_s H_{sc}^3}{K_D \Delta^3 cot\alpha} \quad \text{Equation 2.9}$$

More often seen in the rewritten form:

$$\frac{H_{sc}}{\Delta d} = \sqrt[3]{K_D cot\alpha} \quad \text{Equation 2.10}$$

The K_D-value is sometimes called a 'dustbin parameter', in which among others the friction, interlocking and accepted damage level are included. Therefore, different types of armour units will have a different K_D-value. There are artificial elements with increased interlocking between the elements, which increases the stability and they will therefore have a higher K_D-value.

It must be noted that although Hudson's formula is used worldwide, it does have its limitations. The textbook written by Schiereck (Updated by Verhagen, 2016) sums up some limitations. Most importantly, cotα is insufficient to describe friction and equilibrium on a slope. Therefore, the formula is only valid for slope angles of $1.5 < \cot\alpha < 4.0$. Furthermore, the wave period is not included in the formula. Wave period is related to wave steepness and hence the breaking pattern of the wave on the slope, which does affect stability. Next, permeability also plays a role in stability, but is not included in Hudson's formula. A lack of permeability will cause a pressure build-up, which can eventually help to push the stones from their position. Additionally, it appeared from later tests that also the number of waves has some influence, which makes sense, since the more waves, the greater the chance of a large one. That is another limitation, since Hudson did not include the number of waves in his formula. The last limitation mentioned is the damage level, which is supposedly included in the K_D-value to be valid for 5% damage, but it is not clear how damage is defined. Therefore, it is also unclear for what damage you allow when designing a breakwater with Hudson's formula.

Despite all these limitations, Hudson's formula became popular and is used around the world. Thanks to its popularity, many time and research is spent on finding and correcting recommended K_D-values, which helped to maintain utility for the Hudson's formula. Even for newly developed armour units, it is still determined what their K_D-value is.

To overcome the limitations of Hudson's formula, extensive tests were carried out in the Netherlands. Many large and small scale tests were performed, of which the results were curve-fitted to eventually lead to the following formulas by Van der Meer (1988 - 1):

$$\frac{H_{sc}}{\Delta d_{n50}} = 6.2P^{0.18}\left(\frac{S}{\sqrt{N}}\right)^{0.2}\xi^{-0.5} \qquad \text{(plunging breakers)} \qquad \text{Equation 2.11}$$

$$\frac{H_{sc}}{\Delta d_{n50}} = 1.0P^{-0.13}\left(\frac{S}{\sqrt{N}}\right)^{0.2}\xi^{P}\sqrt{cot\alpha} \qquad \text{(surging breakers)} \qquad \text{Equation 2.12}$$

The Van der Meer formulas include the permeability via P, the damage via S, the number of waves via N, and also the wave period is included via the Iribarren parameter ξ, since $\xi = \tan\alpha \,/\, \sqrt{H/L_0}$, in which the deep water wavelength $L_0 = \frac{gT^2}{2\pi}$. The Van der Meer formulas are therefore definitely an improvement from the Hudson's formula, as it covers all of the main limitations of Hudson's formula. Still, even Van der Meer's formulas are not perfect, particularly because they are empirically curve-fitted, instead of having a purely physical base. The addition of extra parameters makes it more difficult to use, though it is generally more accurate than the Hudson's formula. Thanks to its simplicity however, some people prefer using Hudson's formula instead of Van der Meer's formulas.

Though stability formulas are useful for designing breakwater armour, they do not really give information about the movement of individual blocks. Therefore, more specific information is needed to find out how to translate wave attacks into forces on the units due to rocking, and how these forces lead to breakage of the armour units.

2.3 CUR Reports

The Dutch CUR, 'Civieltechnisch Centrum Uitvoering Research en Regelgeving', or 'Centre for Civil Engineering Research and Codes' in English, has carried out an extensive research in the 1980's about the strength of concrete armour units of breakwaters, CUR (1989, 1990). Multiple cases of newly built breakwaters that failed or were severely damaged, led to the believe that the conventional methods to design breakwaters were not sufficient anymore. Especially because the problems with most of these breakwaters did not just come from a hydraulic background, but from structural strength of the armour units as well. An analysis of the failure cases showed that in all of these cases, a considerable percentage of armour units was broken. The former conventions in breakwater design mainly focussed on hydraulic problems, while the importance of structural strength was not recognized, or underestimated. The hydraulic stability of breakwater amour units underwent a significant improvement by the development of slender interlocking units. The dimensions of these special units increased, until eventually the structural strength of the units started being critical, rather than the hydraulic stability. Since this requires a different point of view for design, the CUR set up this research to investigate whether a new design procedure should be pursued and whether unprecedented research would be needed.

A part of the research was dedicated to finding force-time relations of the impact, CUR (1989 - 1). Theoretically, the area under the force-time curve is equal to the total momentum (mass times velocity). An analysis of experiments shows that the area under the measured force-time curve is indeed approximately equal to the momentum. This is the basis for mathematical determination of the force-time curve. The force-time relation is based on an elasto-plastic model, divided in a rising stage at the start, followed by a more or less flat stage, and a restitution stage, as shown in Figure 2.3: Force-time relation elasto-plastic model, CUR (1990 – 2).

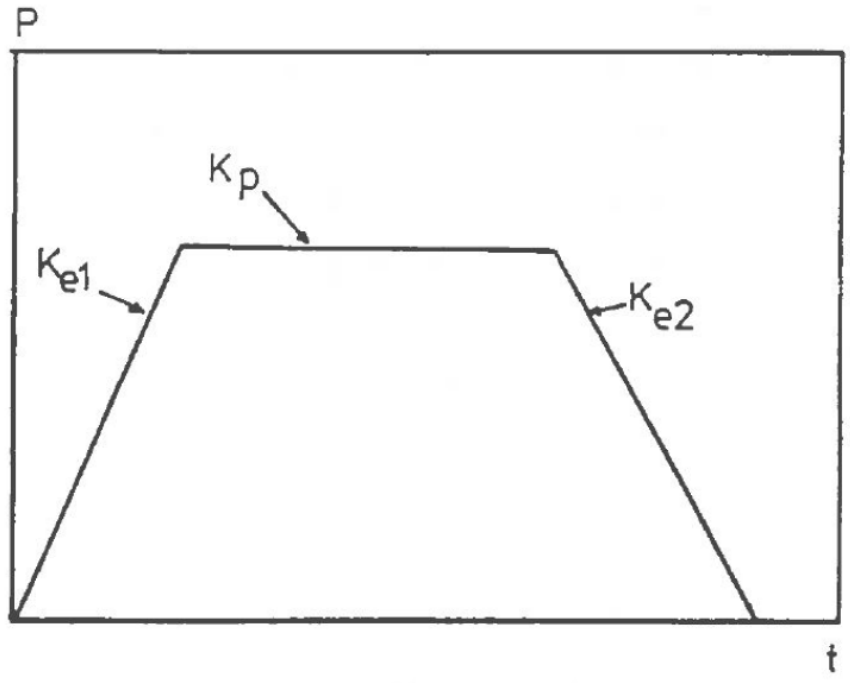

Figure 2.3: Force-time relation elasto-plastic model, CUR (1990 – 2)

The contact stiffnesses in the model are based on Hertz's contact law, that states:

$$P = K\delta^{3/2}$$ Equation 2.13

Where P is a force [kN] , K is a contact stiffness [kN/mm$^{3/2}$], and δ is a deformation [mm].

The first stage has a constant loading rate, characterized by contact stiffness parameter K_{e1}. The procedure for calculating the value of K_{e1} is, to follow the rising segment of the measurements by means of a sine curve. The values of P_{max} and t_{max} that belong to the peak of the sine curve are then used to calculate K_{e1}, using the following formula:

$$\mathrm{K_{e1}} = 1.79\ \frac{P_{max}}{(v \cdot t_{max})^{3/2}}$$ Equation 2.14

Where v is the impact velocity.

The development of the force over time is captured by:

$$P = P_{max} \cdot \sin\frac{t \cdot \frac{\pi}{2}}{t_{max}}$$ Equation 2.15

For the second, plastic stage, a constant load is assumed, characterized by contact stiffness parameter K_p. The value of K_p is based on yielding in the contact zone. Tests were carried out by the CUR to determine contact stress during failure. Another method to verify the contact stress is by means of Meijer's contact law, instead of Hertz's law. Calculations were performed using Meijer's law, which showed that the contact stress was as expected in the order of three times the cube compressive strength of the concrete.

The third stage, the restitution stage, is governed by elastic recovery of the material under and around the contact zone. This elastic behaviour can also be described by means of Hertz's contact law. It was found that the value of K_{e2} is approximately equal to 70% of K_{e1}. The restitution in the force-time relation can be described well by this value.

The starting point of composing the force-time relation is to set the area under the force-time diagram equal to the total momentum. Due to spalling of concrete or energy losses, the measurement could be off a little. However, the deviations of the theoretical values will generally be small. The rising stage of the force-time relation is based on the value of K_{e1}. The sinusoidal shape of Equation 2.15 will be captured by the following formulas:

$$P_{max} = \left(1.25 \cdot \alpha \cdot v^2 \cdot K^{2/3}\right)^{3/5}$$ Equation 2.16

$$t_{max} = 1.47 \cdot \left(1.25 \cdot \frac{\alpha}{v^{\frac{1}{2}} * K}\right)^{2/5}$$ Equation 2.17

Where α is the effective mass, which is defined as:

$$\alpha = \frac{m_1 \cdot m_2}{m_1 + m_2}$$ Equation 2.18

With m_1 = mass of moving element, m_2 = mass of stricken element.

The maximum force for which the element fails determines the horizontal level in the force-time relation, given by the value K_p. This level is governed by the yield stress of the concrete in the contact area during failure.

The restitution is captured by the value of K_{e2}, for which $K_{e2} = 70\% \cdot K_{e1}$ is determined. The restitution will also be approximated by a sinusoidal curve.

The CUR also investigated possible modification to the concrete surface, to help reduce the vulnerability against rocking, CUR (1990 - 1). One way to do this is by shape modifications of the concrete armour units. More specifically, adding 'saw tooth' ridges to the surface, without changing the actual shape of the concrete armour unit. After a few impacts due to rocking, some ridges will be damaged, which is supposed to have a neutralizing effect. The CUR tested this for the case of tetrapods, but it will have a similar effect on other interlocking armour units.

Another option is to create a 'softer' surface. This would help to dampen the rocking and reduce the contact stiffness. Several possibilities are opted to create a 'soft' surface by adding a different material on the concrete surface. The most promising of these possibilities are: adding a layer of an asphalt like product or adding wooden strips or plastic strips. The idea is to reduce the contact parameter, such that a relatively large amount of energy will be dissipated during rocking.

The investigation of force-time relations of concrete on concrete impact have shown that adding the 'saw tooth' ridges has a beneficial effect on the impact force. The contact parameter of the test sample reduced to 5 to 10 $kN/mm^{3/2}$, which strongly reduces the impact force. However, when the number of collisions increases, the contact parameter will also increase, provided that the collision takes place at the same spot. During the first impacts, the ridges will be damaged, reducing their effectiveness. Damage to the ridges is allowed though, it is mainly important that breakage of the armour units is prevented. The tests for the breakage behaviour have shown that the addition of ridges gives a significant reduction in the percentage of broken units. The other option of surface modification, by adding wooden or plastic strips, turned out to be even more effective in reducing the breakage percentage. It is again noted that the contact parameter is of great importance. Adding strips of a material with a very low contact parameter would therefore be highly effective.

3. Impact velocity

When a rubble mound breakwater is under heavy wave attack, the waves can induce motion of the breakwater armour units. The moving armour unit may then collide with another armour unit. The goal of this chapter is to find an expression for the velocity of the moving breakwater armour unit, at the moment of collision with a surrounding armour unit. The route to finding this impact velocity will be described here shortly. The starting point is to schematize all acting forces on an armour unit under wave attack. Based on these forces, the acceleration of the armour unit can be determined via Newton's 2nd law, although via a rotation rather than translation. Taking into account the available movement space, it can be determined how much the armour unit has accelerated at the moment of impact, leading to an expression for the impact velocity. To fill in the expression, several parameters and variables have to be determined, which will be done for cubes and for Xbloc®s. A small scale lab test will be performed to estimate several geometrical variables for Xbloc®. Once the impact velocity is determined, it will be validated by means of the results from physical model tests. The whole process covered in this chapter is visualised by a flow chart in Figure 3.1.

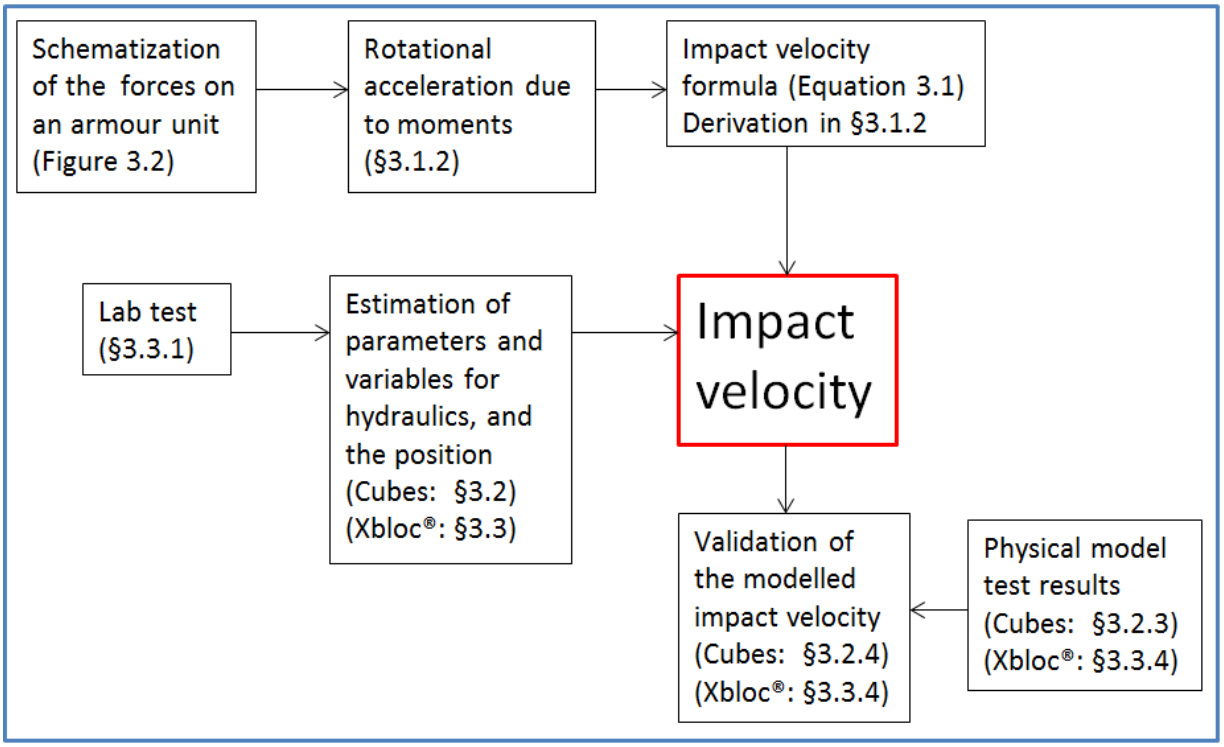

Figure 3.1: Flowchart chapter 3. Impact velocity

3.1 Theoretical determination of impact velocity

This paragraph gives the analytical expression to determine the impact velocity, a quick overview of all required parameters, and the assumptions that lead to the derived equation. Subsequently, the full derivation of this impact velocity equation will be given.

3.1.1 Equation, model and assumptions

The equation of the impact velocity is based on the forces acting on a breakwater armour unit under wave attack, illustrated in Figure 3.2. There is a force from the wave itself, a downward force in the form of the own weight of the block, an upward force in the form of a lift force or buoyancy, a friction force that resists the movement, and a contact force from the underground, as the block will not be able to push through the underground. Note that these forces are not necessarily drawn to scale.

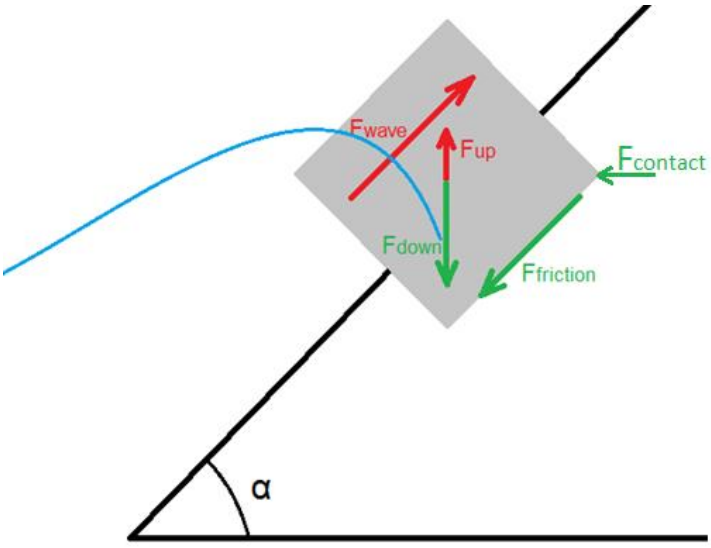

Figure 3.2: Considered forces on an armour unit

Alongside these considered forces, there are a few important assumptions and simplifications:

- Only armour units around the water line will be considered in this MSc thesis (though the run-up fluid velocity could be adjusted when looking at units higher on the slope).
- The wave force is represented as a drag force, acting on the upper part of the block.
- An upward force is included in the form of buoyancy, which effectively reduces the weight.
- Rotation of the block is more important for rocking than translation, since most translational motion is directly blocked by the surrounding armour units, so the impact velocity will be based on the rotation.
- The friction force and contact force work through the rotation point and have therefore no effect on the sum of moments.
- Wave energy dissipation during the movement of the block is neglected.
- For the derivation of the formula, the acceleration is said to be constant, thus neglecting the decrease of the relative velocity, between the fluid and the block, while the fluid decelerates and the block accelerates, as well neglecting the change in the arms of the forces that lead to a different sum of moments. The effect of this assumption is investigated in Appendix B, where a velocity correction factor is determined for the impact velocity of Xbloc®s.
- The situation is treated as a 2D case, so 3D effects are neglected.

From the forces, a sum of moments can be determined, from which an angular acceleration can be determined, which leads to the impact velocity. A full derivation will be given later, in paragraph 3.1.2, but the resulting expression is already given here, in Equation 3.1 and in a dimensionless form in Equation 3.2.

$$v = f_{cor} \cdot \sqrt{2s\left(k_1 \frac{C_D u^2}{(\Delta+1)d_n} - k_2\left[1 - \frac{1}{\Delta+1}\right]g\right)} \qquad \text{Equation 3.1}$$

$$\frac{v}{\sqrt{gH_s}} = f_{cor} \cdot \sqrt{\frac{2s}{H_s}\left(k_1 \frac{C_D u^2}{(\Delta+1)gd_n} - k_2\left[1 - \frac{1}{\Delta+1}\right]\right)} \qquad \text{Equation 3.2}$$

Where:

- f_{cor} is an empirical factor that corrects for the invalid assumption of constant acceleration, established for Xbloc® in Appendix B as: $f_{cor} = 1 - \frac{\sqrt{s}}{4}$.
- s is the available space between the blocks, i.e. the distance a block travels before it hits another block
- C_D is the drag coefficient of the armour unit
- u is the velocity of the water during run-up, determined as: $u = \sqrt{2g(R_u - z_A)}$, with z_A the location on the slope relative to still water level, so $z_A = 0$ around the waterline, and run-up level R_u determined by $\frac{R_{u2\%}}{H_{m0}} = 1.75 \cdot \gamma_b \cdot \gamma_f \cdot \gamma_\beta \cdot \xi_{m-1,0}$
- d_n is the nominal diameter of the armour unit
- H_s is the significant wave height
- Δ is the relative density, $\Delta = \frac{\rho_s - \rho_w}{\rho_w}$, here: $\rho_s = 2400\ kg/m^3$, $\rho_w = 1025\ kg/m^3$
- g is the gravitational acceleration of 9.81 m/s²
- k_1 and k_2 are dimensionless variables, included to consider all the dimensionless parameters that are taken into account in the model.

These dimensionless factors are defined as:

$$k_1 = \frac{\frac{1}{2} \cdot f_{area} \cdot f_{rF} \cdot f_{hit}}{f_{inertia}} \quad \text{and} \quad k_2 = \frac{f_{rW} \cdot f_{hit}}{f_{inertia}}$$

Where:

- f_{area} is the fraction of the area that is subjected to the drag force, a fraction of d_n^2. For example if the affected area is $0.5d_n^2$, then $f_{area} = 0.5$
- f_{rF} is the arm of the wave force to the rotation point, as a fraction of d_n.
- f_{hit} is the distance of the hit point/collision point C to the rotation point R, as a fraction of d_n. For example for the upper corner of a cube as the point of impact, $f_{hit} = 1.0$
- $f_{inertia}$ is the dimensionless part of the mass moment of inertia, as $I = f_{inertia} \cdot m \cdot {d_n}^2$, where $f_{inertia}$ is then dependent on the type of armour unit and the rotation point
- f_{rW} is the arm of the weight to the rotation point, as a fraction of d_n.

The main variables are therefore: the area subjected to the wave, described by f_{area}, the initial orientation angle of the block, θ, the location of the rotation point, R, the location of the collision point, C, and the travel distance of the block before it collides, s, depending on the space between the blocks. Everything else is either a constant that has to be determined once, like the C_D-value and slope angle α, or can be determined from these main variables, like the arms of the forces, f_{rF} and f_{rW}. The main variables are illustrated in Figure 3.3, and since these are different for each block, they will be stochastic variables for the probabilistic method.

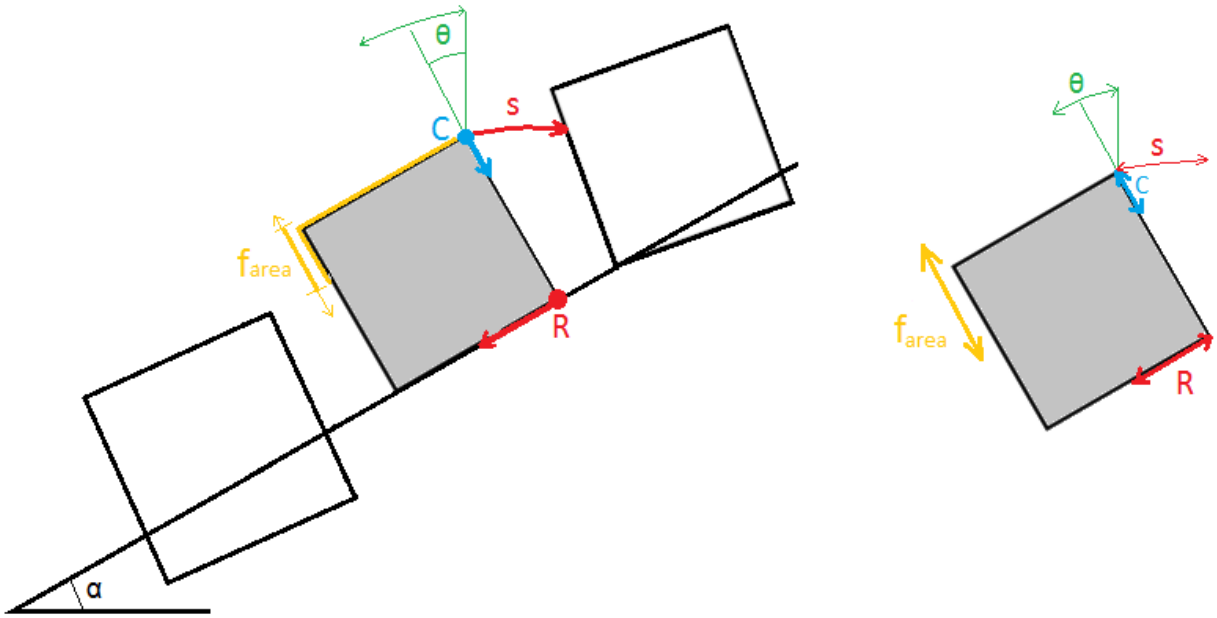

Figure 3.3: Schematic of the main variables

An overview of the required parameters and variables to calculate the impact velocity is given in Table 3.1. An elaboration of how these variables are obtained is given in paragraph 3.2 for cubes, and in paragraph 3.3 for Xbloc®s. Some can be given as a single value, while some others are determined from an expression, and there are some stochastic variables for which the estimated distribution will be given.

	Value for cubes	**Value for Xbloc®**
Constants		
Mass density water, $\rho_w [kg/m^3]$	1025	1025
Mass density concrete, $\rho_s\ [kg/m^3]$	2400	2400
Slope angle, α	$2V:3H$	$2V:3H$
Berm coefficient, γ_b	1.0	1.0
Roughness coefficient, γ_f	0.50	0.45
Oblique wave coefficient, γ_β	1.0	1.0
Drag coefficient, C_D	1.05	1.20
Variables		
Arm of the wave force, f_{rF}	$\frac{0.75}{\cos(\theta-\alpha)} - (0.5 - R) \cdot \sin(\lvert\theta - \alpha\rvert)$	$0.96 + \sin(\alpha) \cdot R$
Arm of the weight, f_{rW}	$R \cdot \cos\theta + 0.5 \cdot \sin\theta$	R
Inertia factor, $f_{inertia}$	$5/12 + R^2$	$0.7783 + R^2$
Stochastic variables		
Rotation point, R	Uniform distribution: $U(\min = 0\,;\max = 0.5)$	Normal distribution: $N(\mu = 0\,;\sigma = 0.144)$
Initial orientation angle, θ	$N(\mu = 33.69\,;\sigma = 10)$	Not relevant for Xbloc®
Movement space, s	Exponential distribution: $Exp(\lambda = 0.4)$	Special distribution: 0 $for\ 50\%\ of\ the\ cases$ $Exp(0.0408)\ for\ 50\%\ of\ the\ cases$
Collision point, f_{hit}	Special distribution: $U(0.75\,;1.0)\ \ for\ 50\%\ of\ the\ cases$ $1.0\ for\ the\ other\ 50\%\ of\ the\ cases$	Uniform distribution: $U(\min = 0.58\,;\max = 1.44)$
Area subjected to wave, f_{area}	Uniform distribution: $U(\min = 0.2\,;\max = 0.4)$	Normal distribution: $N(\mu = 0.381\,;\sigma = 0.083)$
Individual wave height, $H\ [m]$	Rayleigh distribution: $\sqrt{-\frac{1}{2}\ln\left(p(\underline{H} > H)\right)} \cdot H_s$	Rayleigh distribution: $\sqrt{-\frac{1}{2}\ln\left(p(\underline{H} > H)\right)} \cdot H_s$
Spectral wave period, $T_{m-1,0}[s]$	$\sqrt{5 \cdot H} + (H + 3) \cdot U(0,1)$	$\sqrt{5 \cdot H} + (H + 3) \cdot U(0,1)$

Table 3.1: Parameters and variables in the impact velocity formula

3.1.2 Derivation of the impact velocity formula

For the derivation of the formula, the acceleration of the armour unit due to the wave attack is assumed to be constant, such that it can be considered a uniformly accelerated motion, for which:

$$v = a \cdot t$$
$$s = \frac{1}{2} a \cdot t^2 \rightarrow t = \sqrt{\frac{2 \cdot s}{a}}$$
$$v = a \cdot \sqrt{\frac{2 \cdot s}{a}} = \sqrt{2 \cdot s \cdot a}$$

The acceleration a is based on the rotation of the block. a [m/s²] is related to the angular acceleration a_R [rad/s²] via the distance of the observed point to the rotation point. The observed point is the point of the armour unit that collides with another unit, called the collision point, C. The distance of this point to the rotation point, R, can be expressed as a factor times the diameter, say $f_{hit} \cdot d_n$, such that: $a = a_R \cdot f_{hit} \cdot d_n$

The angular acceleration a_R can be determined as the sum of moments divided by the mass moment of inertia: $a_R = \frac{\sum M}{I}$

The mass moment of inertia can be written in the form of: $I = f_{inertia} \cdot m \cdot {d_n}^2$. Where $f_{inertia}$ is a dimensionless factor that depends on the shape of the armour unit and the rotation point. The mass m can be calculated as: $m = \rho_s \cdot {d_n}^3$. Therefore: $I = f_{inertia} \cdot \rho_s \cdot d_n^5$

The sum of moments can be determined from the forces acting on the block. The relevant forces are the wave force, F_{wave}, and the effective weight, W, which is the weight of the block minus the upward force from buoyancy. The forces and their arms to the rotation point are schematized in Figure 3.4.

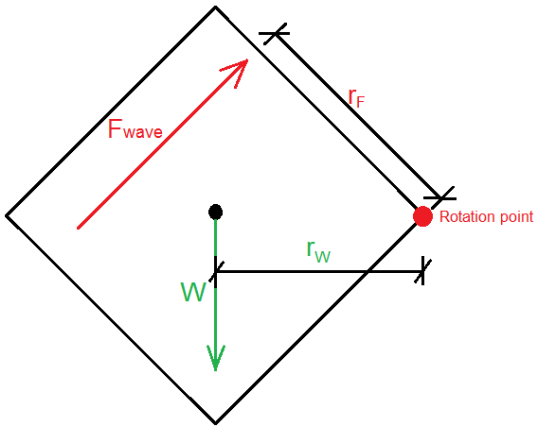

Figure 3.4: Schematization forces for rotation

The sum of moments can be calculated as: $\sum M = F_{wave} \cdot r_F - W \cdot r_W$

Where: $F_{wave} = \frac{1}{2} \rho_w C_D A\, u^2 = \frac{1}{2} \rho_w C_D\, f_{area} \cdot d_n^2 \cdot u^2$, and: $r_F = f_{rF} \cdot d_n$

$W = (\rho_s - \rho_w) g \cdot {d_n}^3$, and: $r_W = f_{rW} \cdot d_n$

Resulting in: $\sum M = \frac{1}{2} \rho_w C_D\, f_{area} \cdot d_n^2 \cdot u^2 \cdot f_{rF} \cdot d_n - (\rho_s - \rho_w) g \cdot d_n^3 \cdot f_{rW} \cdot d_n$

$$= \frac{1}{2} \rho_w C_D\, f_{area} \cdot d_n^3 \cdot u^2 \cdot f_{rF} - (\rho_s - \rho_w) g \cdot d_n^4 \cdot f_{rW}$$

The angular acceleration is then:

$$a_R = \frac{\sum M}{I} = \frac{\frac{1}{2}\rho_w C_D\, f_{area} \cdot d_n^3 \cdot u^2 \cdot f_{rF} - (\rho_s - \rho_w) g \cdot d_n^4 \cdot f_{rW}}{f_{inertia} \cdot \rho_s \cdot d_n^5}$$

Then from $a = a_R \cdot f_{hit} \cdot d_n$ follows:

$$a = \frac{\frac{1}{2}\rho_w C_D\, f_{area} \cdot d_n^3 \cdot u^2 \cdot f_{rF} - (\rho_s - \rho_w) g \cdot d_n^4 \cdot f_{rW}}{f_{inertia} \cdot \rho_s \cdot d_n^5} \cdot f_{hit} \cdot d_n$$

$$= \frac{\frac{1}{2}\rho_w C_D\, f_{area} \cdot d_n^4 \cdot u^2 \cdot f_{rF} \cdot f_{hit} - (\rho_s - \rho_w) g \cdot d_n^5 \cdot f_{rW} \cdot f_{hit}}{f_{inertia} \cdot \rho_s \cdot d_n^5}$$

$$= \frac{\frac{1}{2} f_{area} \cdot f_{rF} \cdot f_{hit} \cdot \rho_w C_D\, u^2}{f_{inertia} \cdot \rho_s \cdot d_n} - \frac{f_{rW} \cdot f_{hit} \cdot (\rho_s - \rho_w) g}{f_{inertia} \cdot \rho_s}$$

Which can be rewritten to: $a = k_1 \cdot \frac{\rho_w C_D u^2}{\rho_s d_n} - k_2 \cdot \frac{\rho_s - \rho_w}{\rho_s} \cdot g$

With: $k_1 = \frac{\frac{1}{2} \cdot f_{area} \cdot f_{rF} \cdot f_{hit}}{f_{inertia}}$, and: $k_2 = \frac{f_{rW} \cdot f_{hit}}{f_{inertia}}$

Then, from $v = \sqrt{2 \cdot s \cdot a}$ follows that: $v = \sqrt{2 \cdot s \cdot \left(k_1 \cdot \frac{\rho_w \cdot C_D \cdot u^2}{\rho_s \cdot d_n} - k_2 \cdot \frac{\rho_s - \rho_w}{\rho_s} \cdot g\right)}$

It is perhaps more convenient to replace ρ_s and ρ_w by the relative density Δ, defined as $\Delta = \frac{\rho_s - \rho_w}{\rho_w} = \frac{\rho_s}{\rho_w} - 1$. Therefore, $\frac{\rho_w}{\rho_s} = \frac{1}{\Delta+1}$, which can be inserted in the above formula for v, resulting in:

$$v = \sqrt{2s\left(k_1 \frac{C_D u^2}{(\Delta+1) d_n} - k_2 \left[1 - \frac{1}{\Delta+1}\right] g\right)}$$

Finally, include a dimensionless correction factor for the invalid assumption that the acceleration is constant. This factor, f_{cor}, is established for Xbloc® in Appendix B. The final formula then becomes:

$$v = f_{cor} \cdot \sqrt{2s\left(k_1 \frac{C_D u^2}{(\Delta+1) d_n} - k_2 \left[1 - \frac{1}{\Delta+1}\right] g\right)}$$

It is sometimes preferred to have a formula in a dimensionless form, which can be achieved by dividing the left- and right-hand side of the formula by $\sqrt{g \cdot H_s}$, such that:

$$\frac{v}{\sqrt{g \cdot H_s}} = \frac{\left[\frac{m}{s}\right]}{\left[\sqrt{\frac{m}{s^2}} \cdot \sqrt{m}\right]} = \frac{\left[\frac{m}{s}\right]}{\left[\frac{m}{s}\right]} = [-]$$

The dimensionless form of the formula then becomes:

$$\frac{v}{\sqrt{g H_s}} = \sqrt{\frac{2s}{H_s}\left(k_1 \frac{C_D u^2}{(\Delta+1) g d_n} - k_2 \left[1 - \frac{1}{\Delta+1}\right]\right)}$$

3.2 Impact velocity of cubes

In order to validate the derived impact velocity expression, the impact velocity will be determined for cubes, and will be compared to the model test results obtained by the CUR (1989 – 2). All parameters and variables required to fill in the analytical expression must be estimated, and in order to get a probabilistic distribution of the impact velocity, a probabilistic distribution must be estimated for several parameters. Once all parameters and variables are available, a Monte Carlo simulation can be performed to obtain the distribution of the impact velocity, which can be compared to the distribution that was obtained by the CUR.

3.2.1 Parameter estimation cubes

A full elaboration of all variables and parameters will be given here for the simple cubes.

Arm of the wave force, f_{rF}, and arm of the weight, f_{rW}

The arms of the forces, f_{rF} and f_{rW}, depend on the orientation angle of the block θ, and f_{rF} also depends on the slope angle α. The location of the rotation point is also needed. This will be called R here, and is defined as a value from 0 to 0.5, with 0 being in the middle and 0.5 at the corner, illustrated in Figure 3.5. In this illustration, imagine a wave going from left to right, causing a clockwise rotation of the block. It is then assumed, that the rotation point may vary from the middle of the block to the corner.

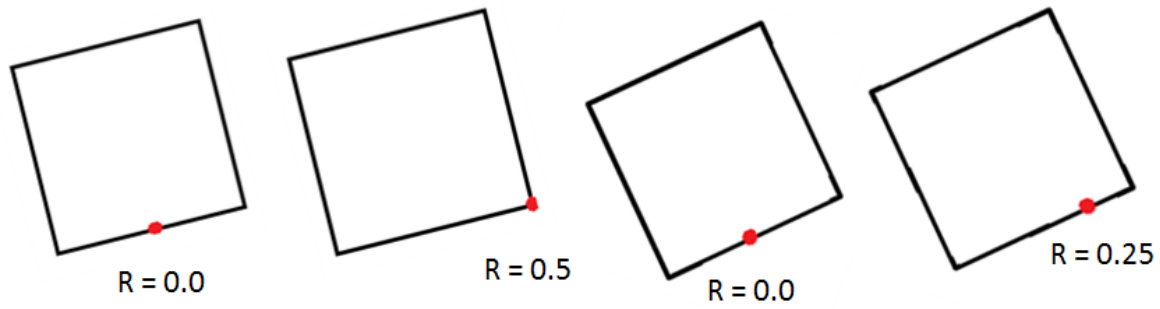

Figure 3.5: Location rotation point

The arms of the forces are calculated with the following formulas:

$$f_{rF} = \frac{0.75}{\cos(\theta-\alpha)} - (0.5 - R) \cdot \sin(|\theta - \alpha|) \qquad \text{Equation 3.3}$$

$$f_{rW} = R \cdot \cos\theta + 0.5 \cdot \sin\theta \qquad \text{Equation 3.4}$$

These equations may seem complicated, so an explanation of the derivation will be given below. The main idea and purpose is to take the orientation angle and rotation point into account when determining the arm of the forces. For a single case, they can be estimated or assumed, but for the probabilistic approach, an equation is required, such that the arms will also be varying with the stochastic variables.

For the determination of the arm of the wave force, Equation 3.3, it was assumed that the arm of the wave force is $0.75d_n$ when the block lays parallel to the slope, because the wave force is working on the upper part of the block. Furthermore, the wave force is assumed to work along the slope. When the block is at an initial orientation θ, that deviates from slope angle α, the arm will increase. This will be accounted for by dividing by cos(θ-α). Since cos(0) = 1, the arm will stay equal to 0.75 while θ = α. Additionally, when the rotation point is not at the corner, the arm is reduced. This will be accounted for by subtracting $(0.5-R)\cdot\sin(|\theta-\alpha|)$, such that there will be no subtraction when $R = 0.5$ (at the corner), nor when θ = α, since sin(0) = 0. Note that the sine is anti-symmetric, while the cosine is symmetric, so the angle difference has to be taken as an absolute value for the sine, as the sine could become negative otherwise. The method to determine the arm of the wave force is illustrated in Figure 3.6, to clarify how it is done. The red dot indicates the rotation point again. The green dots in the far right image indicate where the angle |θ-α| returns, to calculate the sine and cosine with. The arm can then be calculated from the two triangles as the red line minus the blue line.

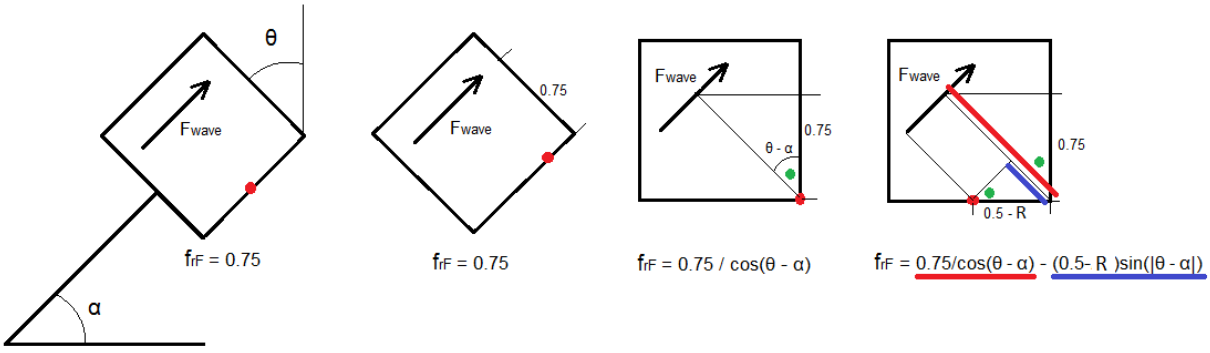

Figure 3.6: Arm between wave force and rotation point

The determination of the arm of the weight, Equation 3.4, is illustrated in Figure 3.7. For the simple cases, it can easily be checked if the formula is correct. When θ = 0, sinθ = 0 and cosθ = 1, so the arm is simply equal to the deviation of the rotation point, defined as R. When the block is under an angle, and with the rotation point at the middle of the block, $R = 0$, the arm will be equal to $0.5d_n\cdot\sin\theta$, but since f_{rW} is defined as a fraction of d_n, $f_{rW} = 0.5\cdot\sin\theta$. The last block shows the full formula, with the block under an angle and a deviation of the rotation point. The green dots indicate where the angle θ returns, such that the arm can be calculated from the two triangles, with the hypotenuse being $0.5\cdot d_n$ and $R\cdot d_n$ respectively.

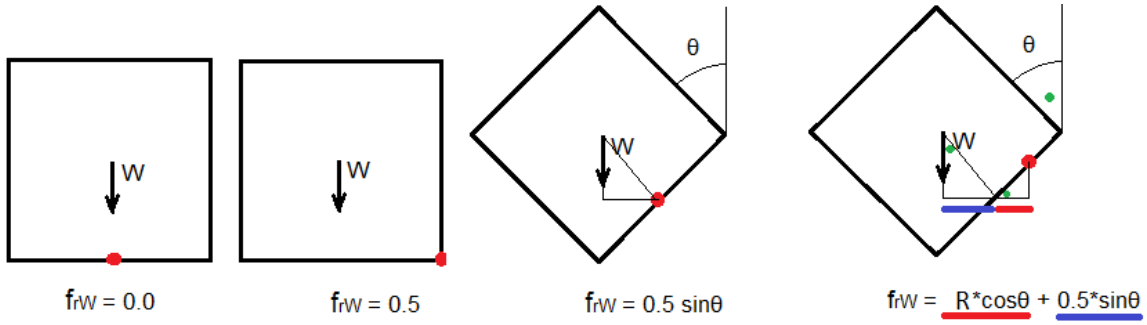

Figure 3.7: Arm between weight and rotation point

Mass moment of inertia

The mass moment of inertia of a cube around its centre of gravity can be calculated as: $I_{G\_cube} = 1/6\ md_n{}^2$. With a rotation point at the edge of the cube, there is additional contribution to the mass moment of inertia, determined with Steiner's rule: $I = I_G + m \cdot d^2$, with *d* as the distance between the centre of gravity and the rotation point, which thus depends on the location of the rotation point. This distance *d* can be determined as: $d = \sqrt{\left(\frac{1}{2}\right)^2 + R^2}\ \cdot d_n$, where *R* is the location of the rotation point, 0 ≤ *R* ≤ 0.5, where 0 is the middle and 0.5 is the corner of the cube. The determination of distance *d* is further illustrated in Figure 3.8, for the two extreme cases R = 0 and *R* = 0.5.

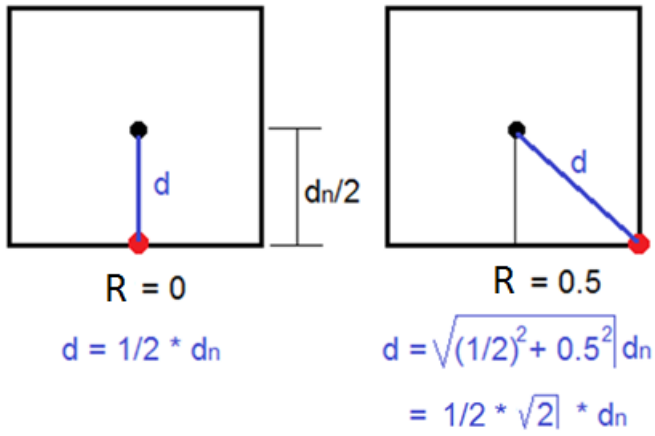

Figure 3.8: Determination distance *d* for Steiner's rule

Ultimately, filling the values in into Steiner's rule leads to a mass moment of inertia of:

$$I_{cube} = \frac{1}{6} m d_n{}^2 + m\left(\sqrt{\left(\frac{1}{2}\right)^2 + R^2}\right)^2 d_n{}^2 = \left(\frac{1}{6} + \left(\frac{1}{2}\right)^2 + R^2\right) m\, d_n{}^2 = \left(\frac{5}{12} + R^2\right) m d_n{}^2$$

If written as: $I_{cube} = f_{inertia}\ m\ d_n{}^2$, then $f_{inertia} = \frac{5}{12} + R^2$

Parameters wave drag force

As discussed before, the wave force acting on the armour unit is treated as a drag force. The equation to determine the wave force can be written as: $F_{wave} = \frac{1}{2}\rho_w C_D A(\Delta u)^2$.

The drag coefficient C_D depends on the shape of the armour unit, but C_D also depends on the Reynolds number ($Re = \frac{u \cdot L}{\nu}$), as described in the book Engineering Fluid Mechanics by Elger et al. (2014). Though, for high Reynolds numbers, Re > 10^4, the drag coefficients tends to become more or less constant and a value for C_D can be attached to the shape of an object. The kinematic viscosity of water is in the order of $\nu \sim 1 \cdot 10^{-6}\ m^2/s$, and in the observed case, the velocity is in the order of $u \sim 10\ m/s$, and the length scale is in the order of $L \sim 1\ m$. The Reynolds number will therefore be in the region Re > 10^4 in the observed case.

The book Engineering Fluid Mechanics, by Elger et al. (2014) also gives a table for various shapes in the case of Re > 10^4. Some relevant cases are given in Figure 3.9.

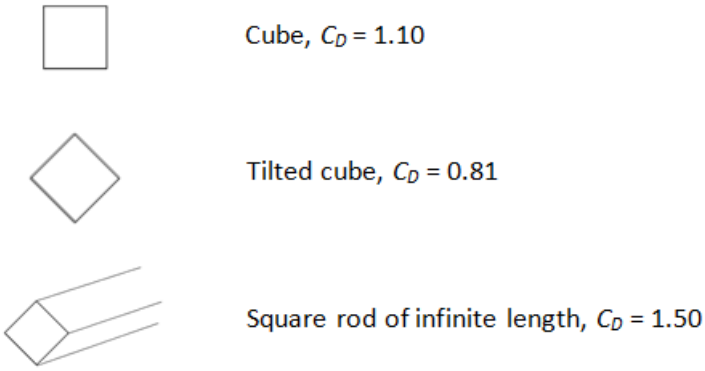

Figure 3.9: C_D-values for a few shapes

Note that the position of the cube is of importance for the C_D-value. For randomly placed cubes, the position varies and so does the C_D-value. A value of C_D = 1.05 will be used for the cubes, though it could be opted to include it as a stochastic variable in the probabilistic calculations.

The affected area *A* will be treated as a frontal area, and has to be estimated based on the positioning of the blocks. The lower part of the armour unit is sheltered by the surrounding armour units. The upper part is subject to the drag force from the wave. Since all blocks are positioned slightly differently, there is not a single value valid for all cases. Therefore, a stochastic variable will granted to the affected area, with an assumed distribution ranging from $0.2d_n^2$ to $0.4d_n^2$.

Furthermore, $\Delta u = u - v$, the difference between the fluid velocity u and the velocity of the armour unit v, has to be determined. The velocity of the armour unit v is increasing during the acceleration of the unit, though this is neglected in the probabilistic approach treated in paragraph 3.1.4. It is an option to repeat the calculation for a number of time steps, updating the armour unit velocity during each time step, such that a more correct velocity difference between fluid and block will be used, but it is left out of the probabilistic determination. The fluid velocity u will be determined from the incoming wave. This velocity will be based on the run-up velocity.

The run-up velocity can be determined based on a balance between kinetic and potential energy, as described in a paper by Van der Meer (2011). The following is considered:

$$E_{kin} = E_{pot}$$

$$E_{kin} = 0.5 \cdot m \cdot u_d^2 \qquad E_{pot} = m \cdot g \cdot (R_u - z_A)$$

Where:

- m = mass of water
- u_d = run-down velocity
- g = gravitational acceleration, 9.81 m/s²
- R_u = maximum wave run-up level relative to still water level
- z_A = location on the slope relative to still water level

Elaboration of the energy formulas gives:

$$u_d = \sqrt{2g(R_u - z_A)} \qquad \text{Equation 3.5}$$

A similar equation is valid for the run-up velocity, written as:

$$u = c_u\sqrt{g(R_u - z_A)} \qquad \text{Equation 3.6}$$

Where c_u is a coefficient that has to be determined by research, though a first estimation of $c_u = \sqrt{2}$ is generally a good approximation. Values of $c_u = 1.4 - 1.5$ are also suggested in the Overtopping Manual, EurOtop (2018).

When looking at rocking around the waterline, z_A can simply be set to zero, resulting in the largest run-up velocity, which is the most interesting value.

Then there is still one unknown left, namely the maximum run-up level R_u. A formula for determination of $R_{u2\%}$, the run-up level exceeded by 2% of the waves, is given in the Overtopping Manual, EurOtop (2018):

$$\frac{R_{u2\%}}{H_{m0}} = 1.75 \cdot \gamma_b \cdot \gamma_f \cdot \gamma_\beta \cdot \xi_{m-1,0} \qquad \text{Equation 3.7}$$

Where γ_b, γ_f and γ_β are influence factors for a berm, roughness of the slope, and oblique wave attack respectively. H_{m0} is the significant wave height (from the wave spectrum), and $\xi_{m-1,0}$ is the breaker parameter:

$\xi_{m-1,0} = \frac{\tan\alpha}{\sqrt{s_{0m-1,0}}}$, with $s_{0m-1,0} = \frac{2\pi H_s}{gT_{m-1,0}^2}$, where α is the slope angle, H_s the significant wave height, and $T_{m-1,0}$ is a spectral wave period.

Note that the coefficient 1.75 is a stochastic variable where 1.65 is the mean value, with a standard deviation of 0.10. For a design and assessment approach, the Overtopping Manual suggests to use a value of 1.75 instead of 1.65. This MSc thesis can be considered as an assessment approach, so the value of 1.75 will be used.

The influence factors γ_b and γ_β are set to 1.0, since no berm reduction is considered, and no oblique waves are considered (wave angle β = 0°). These two factors can therefore be left out of the formula during the calculations. A table with values for γ_f is given in the Breakwater design lecture notes, by Van den Bos and Verhagen (2018). This table gives for a single layer of cubes: $\gamma_f = 0.50$.

Note that this method to determine the fluid velocity near the armour units is based on the assumption that this fluid velocity is comparable to the run-up velocity during wave run-up, which is determined by several formulas that also have underlying assumptions. Therefore, there is some uncertainty in the determined fluid velocities, so if more accurate information about the fluid velocity near the armour units is known, for example from physical model tests, it would be better to use that data instead of this theoretical velocity.

Collision point

The location of the collision point is one of the main variables, that differ for each block. The parameter f_{hit}, defined the distance between the collision point and the rotation point, is directly related to the location of the collision point. The moving block may hit another block with its upper corner, but it may also be somewhere below the upper corner. Therefore, the location of the collision point (and thus f_{hit}) will be included in the probabilistic method as a stochastic variable, with a certain distribution.

Travel distance/space between armour units

The travel distance is one of the main variables, that differ for each block. The travel distance depends on the available space between the armour units, and some blocks have more space to move than other blocks. There is not a single valid value, but an estimation has to be made for a distribution of the travel distance.

3.2.2 Stochastic variable distributions of cubes

The earlier derived formula can be used in a probabilistic approach, by giving distributions to the stochastic variables of the armour unit, which are illustrated in Figure 3.10.

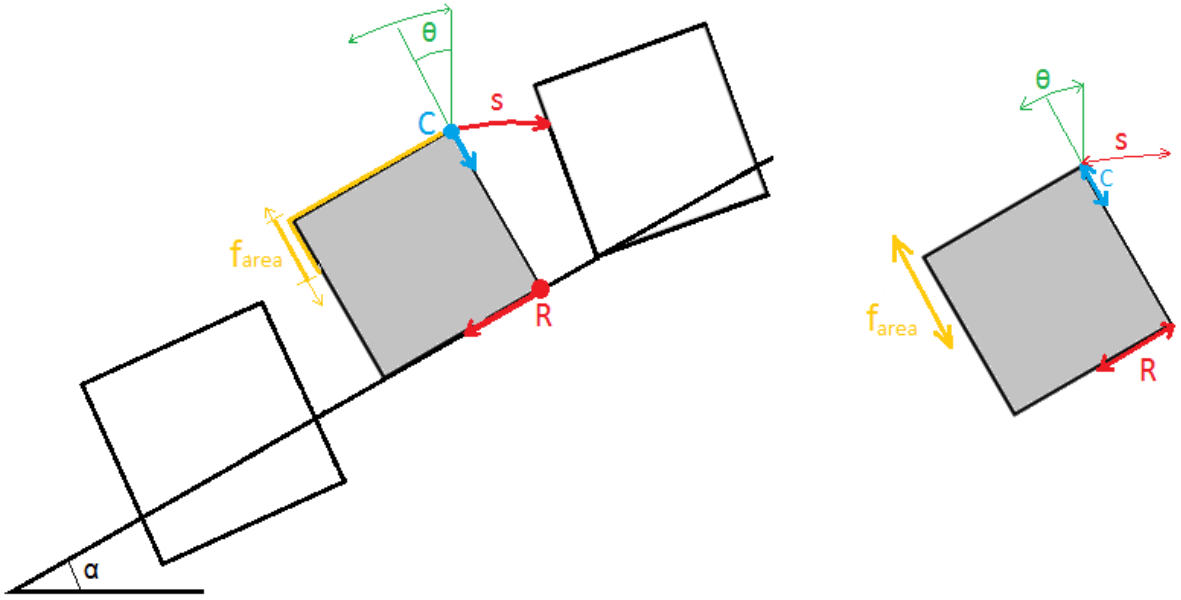

Figure 3.10: Schematic of the main variables

1. The initial orientation angle of the moving block, θ
2. The travel distance of the block, s
3. The location of the rotation point, R
4. The location of the collision point, C
5. The fraction of the area that is subjected to the wave drag force, f_{area}

However, there is one more variable that can be included as a stochastic variable, namely:

6. The wave height, H

The type of distribution given to each parameter will be explained below. An elaboration is given here for the case of cubes. Note that the values of the distributions will likely change when viewing another type of armour unit.

1. The initial orientation angle of the moving block is given a normal distribution around slope angle α. With a random placement, the orientation angle will vary, so it is given a standard deviation of 10°, to account for this variation. This value is not investigated in detail, but just chosen to obtain reasonable values. For a slope of 1:1.5, corresponding to an angle of 33.69°, the normal distribution $N(\mu = 33.69; \sigma = 10)$ is given in Figure 3.11.

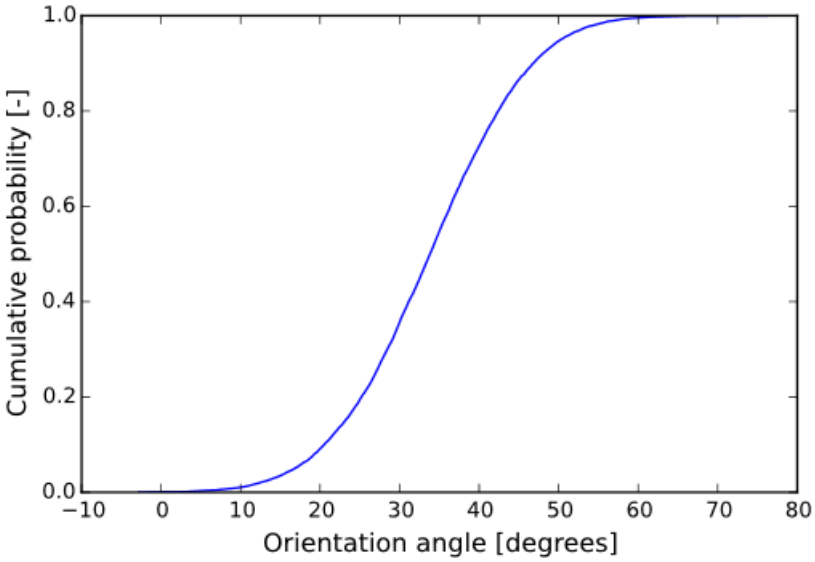

Figure 3.11: Distribution orientation angle

2. The travel distance of the block, i.e. the space in between blocks, is given an exponential distribution. Most blocks do not have much space for movement, but occasionally there is a larger gap between the blocks. The distribution of the travel distance is given as a fraction of d_n, so the actual distance is then $s \cdot d_n$. The exponential distribution is given a value of $\lambda = 0.4$, which would be the maximum value that can be obtained. The distribution $Exp(\lambda = 0.4)$ is given in Figure 3.12.

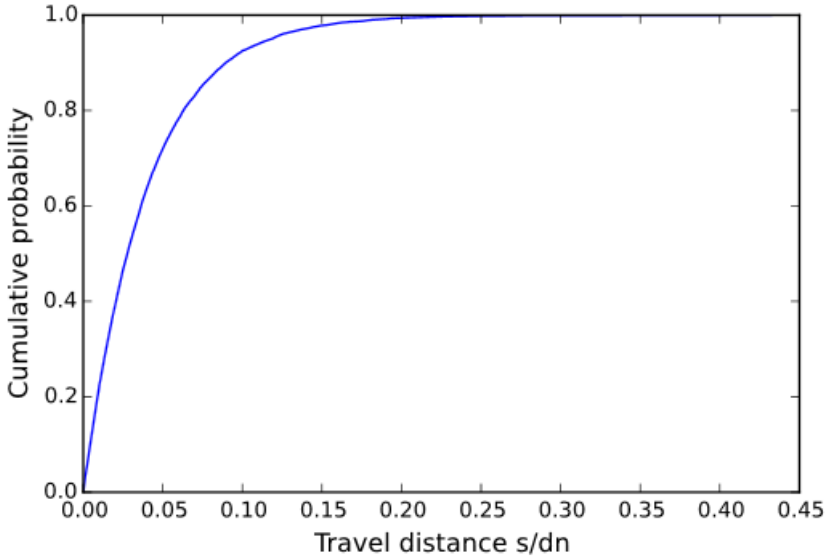

Figure 3.12: Distribution travel distance as a fraction of d_n

3. The location of the rotation point is given a uniform distribution. The point around which the block can rotate depends on the surroundings, mainly the underlayer. It is assumed that there is no difference in probability between the possible rotation points, so the rotation point is uniformly distributed. The rotation point is assumed to be always at the bottom of the block, somewhere between the corner and the middle. The distribution U(min =0 ; max = 0.5) is used, where the location of the rotation point is given as a fraction of d_n. 0.5 is at the corner, while 0 is at the middle of the block.

4. The location of the collision point is given an adjusted distribution, because it is much more likely that the moving block will hit another block with its upper corner, than with any other point. It is therefore decided to say that there is probability of 50% that the upper corner (at $1.0 \cdot d_n$) of the moving block will hit the other block, while the other 50% is uniformly distributed between the upper corner and a point somewhere below ($0.75 \cdot d_n$). This is an arbitrary choice, but note that this is only used to determine the velocity and is not binding for the eventual determination of the stresses in the blocks. This distribution can be expressed as:

$$f_{hit} = \begin{cases} U(\min = 0.75\,;\max = 1.0) & for\ 50\%\ of\ the\ cases \\ 1.0 & for\ the\ other\ 50\%\ of\ the\ cases \end{cases}$$

The distribution of the location of the collision point as a fraction of d_n will then look like what is given below in Figure 3.13.

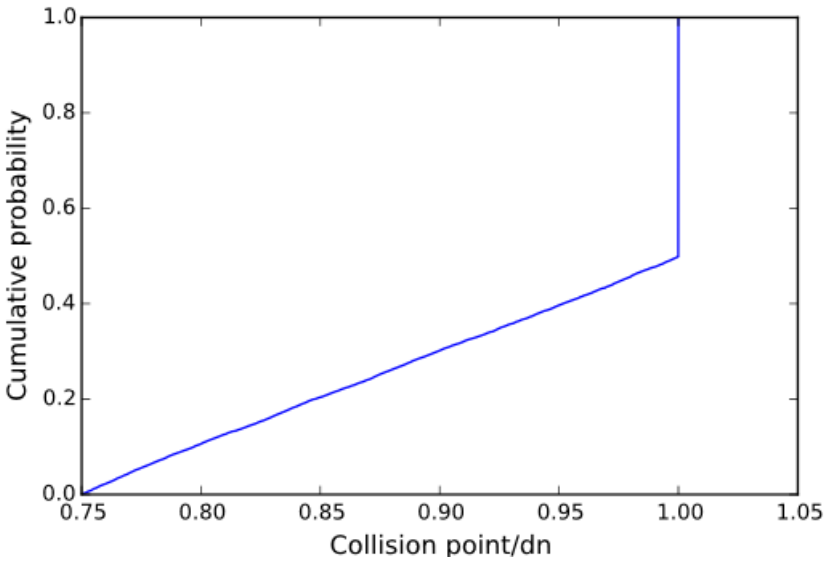

Figure 3.13: Distribution collision point

5. The fraction of the area that is subjected to the wave drag force is given a uniform distribution. This area is not investigated in detail, but it is clear that a large part of the block is sheltered by the surrounding blocks. The area that is affected by the waves is depending on the position of the block, the slope angle, and the position of the surrounding blocks. Without extensive investigation of the distribution of the affected area, it is decided to use a uniform distribution between 0.2 and 0.4 as a fraction of d_n^2, or denoted as U(min = 0.2 ; max = 0.4).

6. The distribution of the wave height can be described by a Rayleigh distribution, as in Equation 3.8, which is widely used and described for example in the book 'Waves in Oceanic and Coastal Waters' by Holthuijsen (2010). Note that this equation is for the case of deep water, which is assumed to be valid here. In case of shallow water, the wave height distribution by Battjes and Groenendijk can be used, which is similar, but flattens for the higher waves, since the high waves start breaking in shallow water.

$$p(\underline{H} > H) = \exp\left(-2\left(\frac{H}{H_s}\right)^2\right) \qquad \text{Equation 3.8}$$

Alternatively, this equation can be rewritten to determine H for a certain probability:

$$H = \sqrt{-\frac{1}{2}\ln\left(p(\underline{H} > H)\right)} \cdot H_s$$

By filling in a large number of probabilities in the above expression, a distribution of the wave height is obtained, representing a wave field with a certain significant wave height H_s. A random value can be picked from this distribution, i.e. one wave out of the wave field.

The distribution depends on the significant wave height, H_s, and is thus not constant. An example of the cumulative wave height distribution is given in Figure 3.14, for significant wave height H_s = 5.0 m.

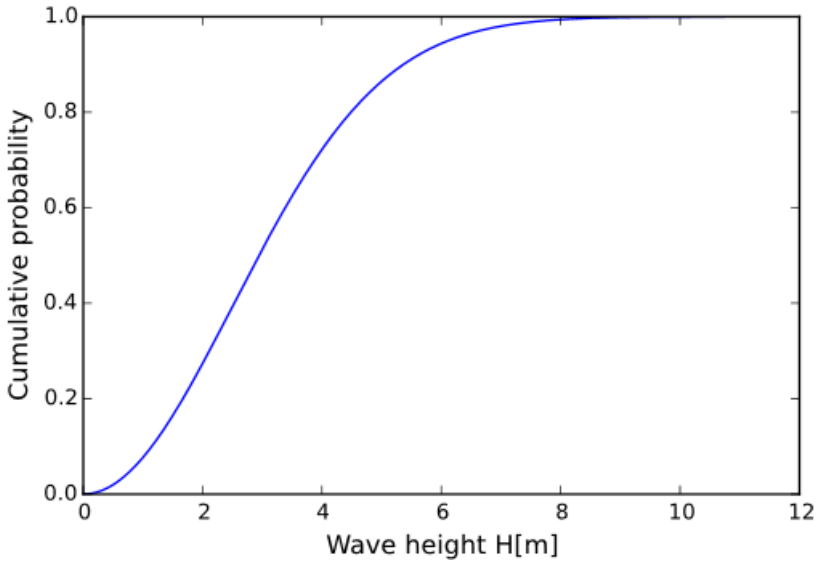

Figure 3.14: Cumulative wave height distribution for H_s = 5.0 m

When varying the wave height, it is important to also vary the wave period, as those two are correlated, so it would not make much sense to use only a single value for the wave period. Sadly, there is no clear expression to link the wave height to the wave period, since there tends to be a large scatter, and it usually differs for each individual case. Still, the wave period has to be determined in some way here, in order to be able to use it for determining the impact velocity, which is why the following expression is created, to try to get realistic values:

$$T_{m-1,0} = \sqrt{5 \cdot H} + (H + 3) \cdot U(\min = 0, \max = 1)$$

Where H is simply the wave height, and the uniform distribution of U(min = 0, max = 1) indicates a random number between zero and one, incorporated to create some scatter in the wave period versus wave height.

This artificial relation between wave height and wave period is plotted in Figure 3.15. This is by no means meant as an accurate way to link the wave height and wave period, but is solely meant as a tool to be able to incorporate a variation in the wave period, linked to the wave height, thus trying to approximate a real situation. If any wave data is available, that should be always be used instead of this method.

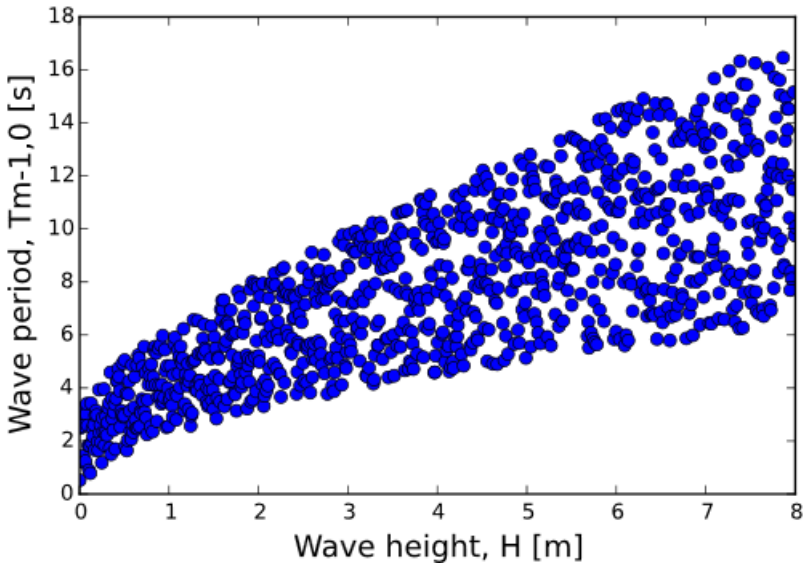

Figure 3.15: Artificial wave height vs wave period

Once all probabilistic distributions are defined, a Monte Carlo simulation can be performed to determine the impact velocity for a certain exceedance probability, for example by means of a Python script. A random value is picked for each stochastic variable, with which the calculation is then performed. This procedure is repeated N times, for example N = 100,000 times, picking new random values every time.

3.2.3 Empirical determination of impact velocity of cubes, CUR research

This paragraph treats the formulas for the impact velocity as the determined in the research by the CUR.

In the tests in the wave flume, performed by the CUR (1989 – 2), the accelerations during impact were measured inside armour elements. The impact velocity is obtained by integrating the accelerations over time. The measured elements were placed at several locations, giving some variation in space. The wave conditions are varied as well, giving a variation in time. There is thus variation in time and in space, though the variation in time (many different waves) is prevalent, since only a few different locations are measured.

The research by the CUR (1989 – 2) resulted in formulas for the distribution of impact velocities. It is defined such that the impact velocity can be calculated for a certain probability of exceedance $p\left(\frac{v}{\sqrt{gd_n}}\right)$. The formula for the impact velocity of cubes is given as:

$$p\left(\frac{v}{\sqrt{gd_n}}\right) = \exp\left(-\frac{\frac{v}{\sqrt{gd_n}} - c}{B}\right)$$ Equation 3.9

with: $c = 0.049 \cdot \exp\left(-0.4 \cdot \left|\frac{y}{d_n}\right|\right)$

and $B = 0.025 \cdot \exp\left(-0.4 \cdot \left|\frac{y}{d_n}\right|\right) \cdot \frac{H_s}{\Delta d_n}$

Where *y* is the vertical distance relative to the still water level. When looking at the impact velocities at the waterline, *y* = 0 m, which essentially reduces *c* and *B* to $c = 0.049$, and $B = 0.025\frac{H_s}{\Delta d_n}$.

The formula can be rewritten to directly calculate the impact velocity:

$$v_{cubes} = \sqrt{gd_n} \cdot \left(-B \cdot \ln\left(p\left(\frac{v}{\sqrt{gd_n}}\right)\right) + c\right)$$ Equation 3.10

The values for the nominal diameter d_n, specific weight Δ, and significant wave height H_s can be defined, so the impact velocity can be calculated for a range of exceedance probabilities.

3.2.4 Comparison theoretical and empirical impact velocity of cubes

Now, the previously determined theoretical impact velocity and the empirical impact velocity will be compared, to see if the derived theoretical expression gives reasonable values for the impact velocity. Both methods give a probabilistic distribution of the impact velocity, which can be plotted in the same figure to be able to compare them easily.

Up front, there is already a notable difference between the theoretical and empirical formulas, namely the wave period, which is included in the theoretical impact velocity formula as derived in this MSc thesis, but is not included in the empirical formula from the CUR report

Furthermore, in the theoretical method in this MSc thesis, the blocks will not move at all for a favourable set of stochastic variables, thus give a value of zero for the impact velocity. This differs from the formula from the CUR report, which never gives values of zero, probably because non-moving blocks were already excluded when the curve was fitted. To be able to make a better comparison, all zero values are removed from the theoretically determined impact velocities.

A Python script is written, where the formulas from the CUR report are added, and the whole probabilistic method as established in this MSc thesis is implemented, carrying out a Monte Carlo simulation for N = 100,000, in order to have sufficient moving blocks. Again, note that non-moving blocks are removed for the plots, in order to obtain a useful comparison. Both are then plotted in the same graph, to make the comparison easier. Figure 3.16 shows a plots for a relatively small significant wave height, with corresponding d_n, loosely based on the Hudson formula to have a realistic situation, with blocks near their stability limit. Figure 3.17 then shows the plot for a relatively high significant wave height, in order to assess the validity for various cases. Several wave heights in between have been checked as well, and it is observed that the results follow a trend, with a decreasing deviation between the two formulas for increasing wave height and unit diameter.

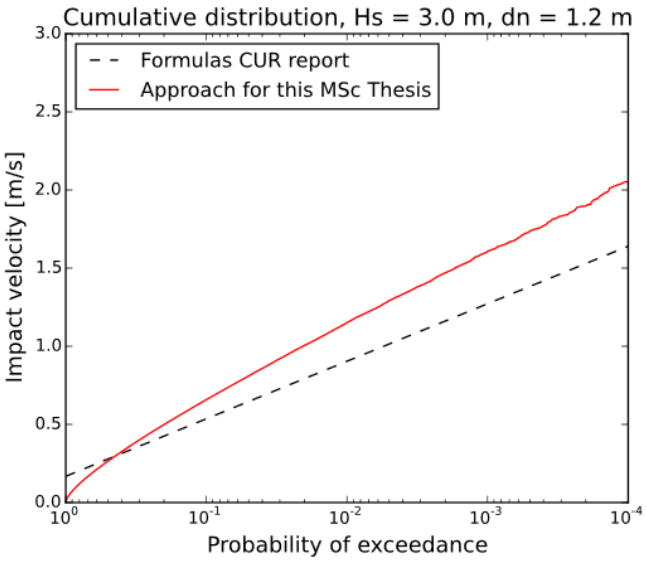

Figure 3.16: Comparison formulas for cubes, Hs = 3.0 m, dn = 1.2 m

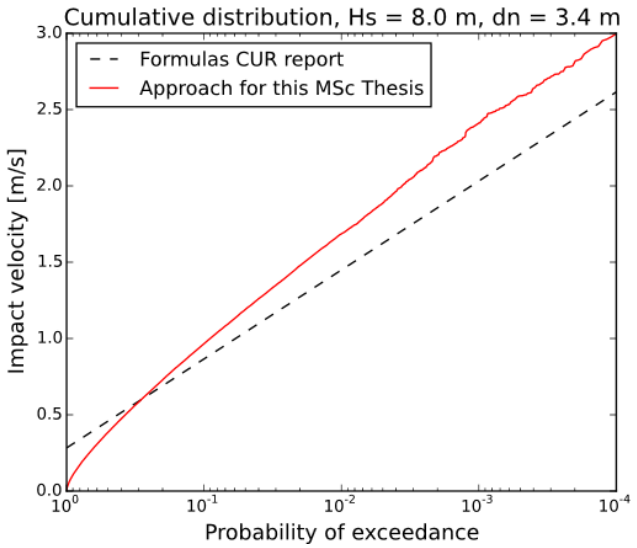

Figure 3.17: Comparison formulas for cubes, Hs = 8.0 m, dn = 3.4 m

Conclusions

Overall, it can be said that the theoretical approach in this MSc thesis is relatively close to the empirical formulas from the CUR report; at least in the same order of magnitude. It is also realised that the CUR formulas are not perfect either, so there is no need to try to approach those values. A notable difference is the deviation at the lower probabilities, because the CUR formulas do not start from an impact velocity of zero. Though, the higher impact velocities are more interesting anyway, as they may cause breakage of the armour units, so it is more important to predict those correctly. Furthermore, the approach for this MSc thesis seems to work slightly better for higher waves, but it is difficult to link that to a range of viability.

All in all, the results are good enough to use this method of determining the impact velocity in the remainder of this MSc thesis.

3.3 Impact velocity Xbloc®

The previous paragraph determined the impact velocity of cubes. Now, this procedure will be repeated for Xbloc®. In order to get a reasonably accurate estimate of the parameters and their distributions, a laboratory measurement is performed on a small scale breakwater. The data from this measurement will be converted to distributions that can be used as input to eventually determine a distribution of the impact velocity.

3.3.1 Laboratory measurements of Xbloc® parameters

For the determination of the parameters of the Xbloc®, a breakwater piece is recreated in the laboratory of the TU Delft. The parameters of a block can then be determined from the position of the block and by moving it slightly. By repeating this for a large number of blocks, a probabilistic distribution of these parameters can be obtained. Note that these distributions also depend on the situation. A different packing density (possibly caused by settlements) leads to slightly different parameter distributions. The obtained distributions are therefore never 100% correct, but they surely will be better approximations than when the distributions would just be assumed.

The test is performed on a slope that happened to be available in the laboratory, as a leftovers from tests in the wave flume. It is a wooden slope of 2V:3H. Gravel of approximately d_{n50} = 1 cm is glued on the wooden surface, to function as an underlayer. A picture of this slope is given in Figure 3.18.

Figure 3.18: Slope with glued underlayer

The main dimension of the Xbloc®s that were used is $D = 5.64\ cm$, which translates to $d_n = 3.9\ cm$. The first layer of Xbloc®s is placed regularly, with their cubical leg on the base, to create a stable first layer. In all other layers, the blocks are placed randomly, while making sure that they touch two blocks below to secure them, which is the normal placing procedure. For the placing density, a centre-to-centre distance is kept of $D_x = 1.32 \cdot D$ in horizontal direction, and $D_y = 0.63 \cdot D$ upward along the slope, in accordance with the guidelines provided by Delta Marine Consultants (2018). All odd rows consist of 11 blocks, while the even rows consist of 10 blocks. To prevent inaccuracies from the edge blocks, only the inner blocks are included in the determination of the parameters. The first two rows and last two rows are excluded, as well as the outer blocks of each row. An overview of all blocks on the slope is given in Figure 3.19.

Figure 3.19: Overview of the Xbloc®s on the slope

The following parameters will be determined for each block:

- The fraction of the area that is not sheltered, thus the fraction of the area that will be subjected to the wave, f_{area}. It is estimated as a fraction of D^2.
- The available movement space, thus the travelled distance s when a block hits another block. It will be determined in [cm] and will later be converted to a fraction of d_n.
- The initial orientation angle θ, determined relative to slope angle α, as that is slightly easier to estimate quickly.
- The rotation point R, around which the block rotates, as the distance from the centre, as a fraction of D. Note that R is determined as a horizontal distance. This is slightly easier to determine in the test, and is also convenient later on, when determining the arm of the weight force, which is then equal to R.
- The contact/collision point on the moving block, as a distance to the rotation point, as a fraction of D.
- The contact/collision point on the stricken block. It is noted as the location on the stricken leg of the armour unit, between 0 and 1, with 0 being the top of the leg, and 1 being the bottom of the leg, where it is attached to the body. It is also noted if a spiky leg or cubical leg is hit, such that a separation can be made if needed.
- The angle of the incoming force θ_F, i.e. the angle under which one block hits the other. The angle is relative to the stricken leg, where 0° is parallel to the leg and 90° is perpendicular to the leg.

In an attempt to clarify the measured parameters, they are added in a picture of an Xbloc® on the slope, given in Figure 3.20. The block rotates around R, until $C1$ hits $C2$, after travelling over distance s Note that the angle of in the incoming force θ_F is actually lower than 90° in this case, although it looks larger, because of the 3D visualisation.

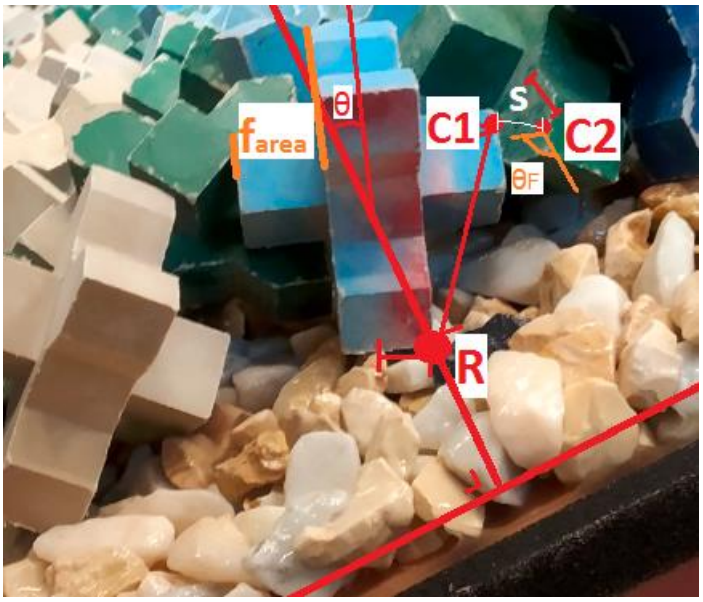

Figure 3.20: Xbloc® position parameters

The parameters are determined by slightly moving the blocks by hand. By starting on the lower rows, some artificial settlements are created, to imitate settlements on a real breakwater slope. The results are therefore for the case of a slightly settled configuration, and not for a breakwater that is still in its original packing density. It is done this way, because that seems most relevant for a real case.

3.3.2 Estimated parameter distributions based on lab measurements

Now, the data obtained from the measurements in the laboratory will be used to determine probabilistic distributions. The 7 parameters are individually estimated for 97 blocks, which is sufficient to get an idea of the parameter distributions. For each parameter, a histogram is plotted for the probability density, and the cumulative distribution is plotted in a separate graph. Then, the probabilistic distribution is estimated, for which the probability density function (pdf) and cumulative distribution function (cdf) are plotted in the corresponding graph in the form of a red line. The distributions of the parameters will individually be treated below. Where needed, the probabilistic distribution obtained from the data will be translated to a function of d_n, such that they are ready to be included in the determination of the impact velocity.

Note that some of the estimated parameters here are not needed to determine the impact velocity, but are important later on when determining the impact force and resulting stresses. It is decided to those in this paragraph as well, to keep all laboratory measurements together.

Fraction of the area subjected to wave attack, f_{area}

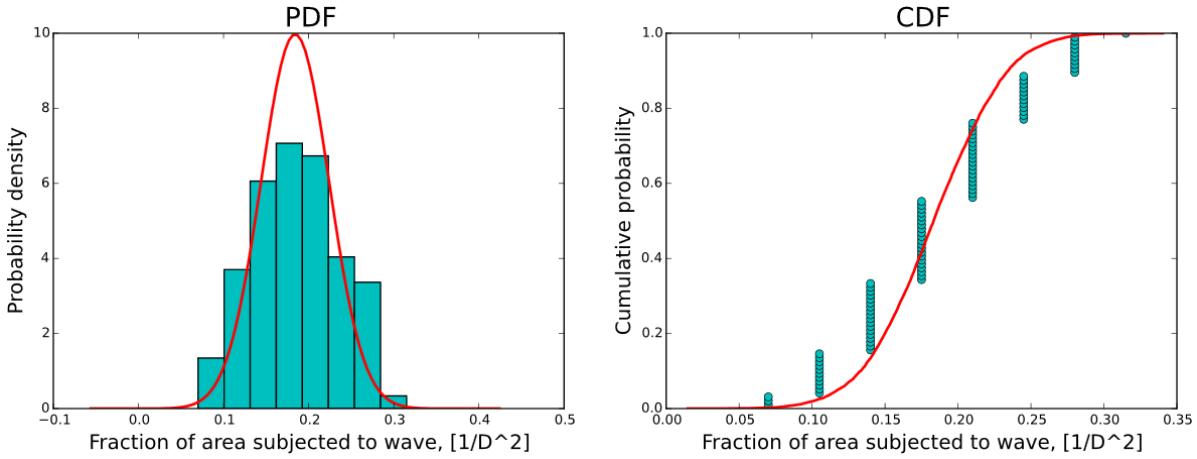

Figure 3.21: Distribution f_{area}

Based on the obtained data, the fraction of the area that is subjected to waves seems normally distributed. The mean and standard deviation can be obtained from the data as: $\mu = 0.184$ and $\sigma = 0.058$. However, it is decided to use a slightly lower standard deviation of $\sigma = 0.04$, which increases the peak around the mean, but secures that the probability of getting impossible negative values, is negligible.

The obtained probabilistic distribution is thus:

$$\frac{f_{area}}{D^2} = N(\mu = 0.184;\ \sigma = 0.04)$$

In order to use this distribution in the impact velocity determination, it will be translated to d_n^2, by $D = 1.443 d_n$, resulting in the distribution as in Figure 3.22, expressed by:

$$\frac{f_{area}}{d_n^2} = N(\mu = 0.381;\ \sigma = 0.083)$$

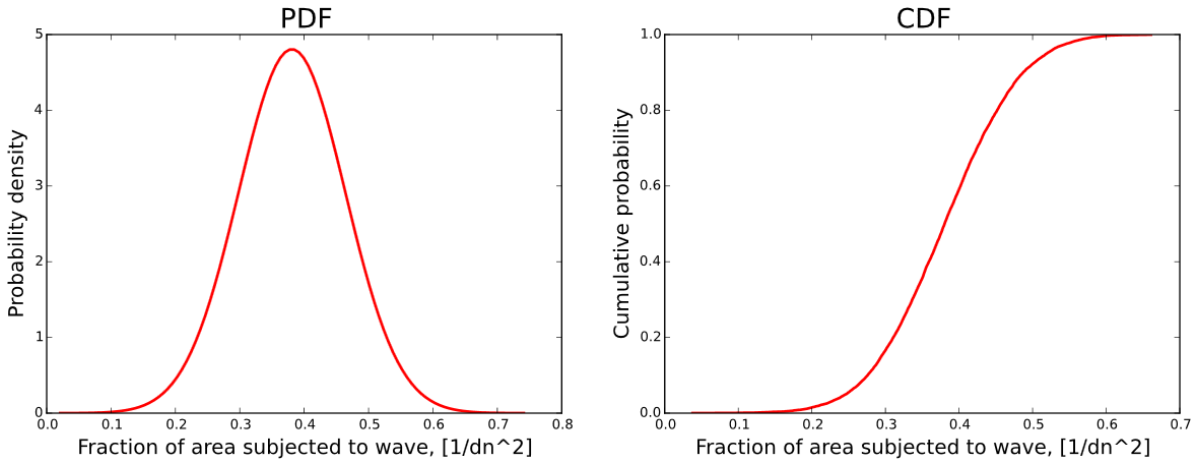

Figure 3.22: Distribution subjected area, as a function of $1/d_n^2$

Travel distance/movement space, s

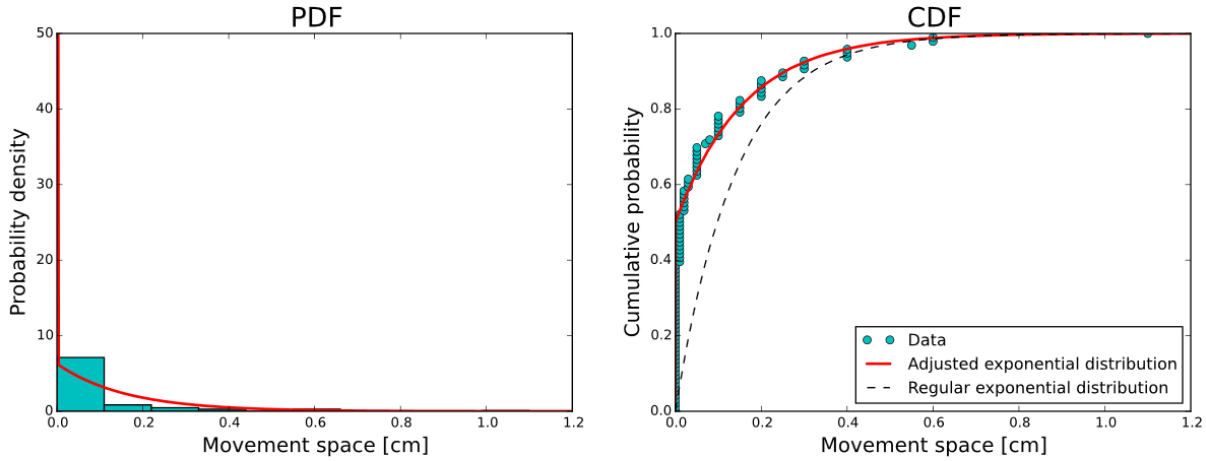

Figure 3.23: Distribution travel distance/movement space, s

Most of the blocks have (almost) no movement space, while there are some blocks that do have significant space. An exponential distribution can approximate this, but will either give a severe overestimation for the lower values, as visualise by the black dashed line in the right graph of Figure 3.23, or will severely underestimate the higher values if a much lower λ-value is chosen. Therefore, a custom exponential distribution is made, where s is set to 0 for 50% of the cases, visualised by the red line in the right graph of Figure 3.23. This is an arbitrary choice, but it does give a better representation of the movement space, because many blocks simply do not have any space to move, because they are directly secured by surrounding blocks. The obtained probabilistic distribution is:

$$s[cm] = \begin{cases} 0 & for\ 50\%\ of\ the\ cases \\ Exp(\lambda = 0.16) & for\ the\ other\ 50\%\ of\ the\ cases \end{cases}$$

The expression obtained from the data of the absolute value of the space, will be rewritten as a fraction of d_n in order to incorporate it in the determination of the impact velocity. For this test, $D = 5.64\ cm$, equal to $d_n = 3.91\ cm$, so the expression becomes:

$$\frac{s}{d_n} = \begin{cases} 0 & for\ 50\%\ of\ the\ cases \\ Exp(\lambda = 0.0408) & for\ the\ other\ 50\%\ of\ the\ cases \end{cases}$$

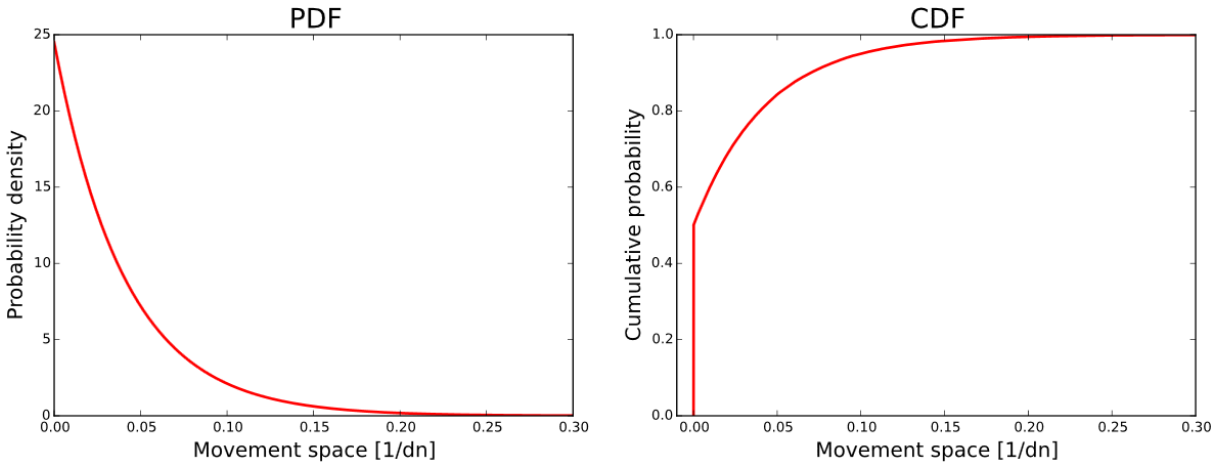

Figure 3.24: Distribution movement space, as a fraction of d_n

Initial orientation angle, θ

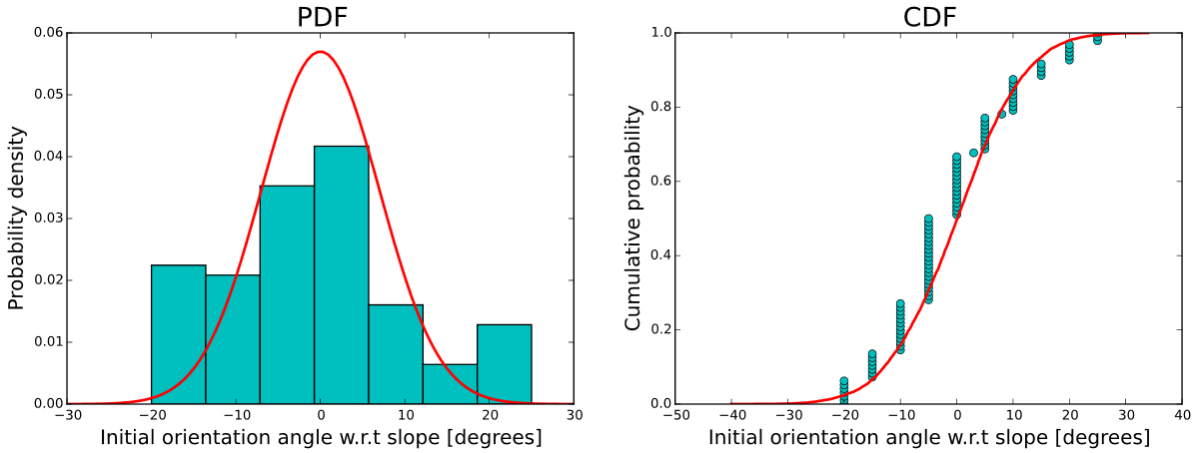

Figure 3.25: Distribution initial orientation angle, θ

The initial orientation is measured relative to the slope angle. Note that the orientation angle is arbitrary, because there are multiple orientations possible, due to the symmetry of the block. This difficulty is further enhanced by the fact that most blocks are slightly twisted. Based on the obtained data, it is not entirely clear whether a normal distribution or a uniform distribution would be most fitting, but since the blocks are supposed to be placed randomly, a normal distribution seems appropriate. The mean of the data is slightly below 0, but $\mu = 0°$ will be used, as that seems appropriate for random placement. A standard deviation of $\sigma = 10°$ is used.

The obtained probabilistic distribution is then:

$$\theta = N(\mu = 0\,; \sigma = 10)$$

Where θ is defined relative to the slope angle α.

Rotation point, R

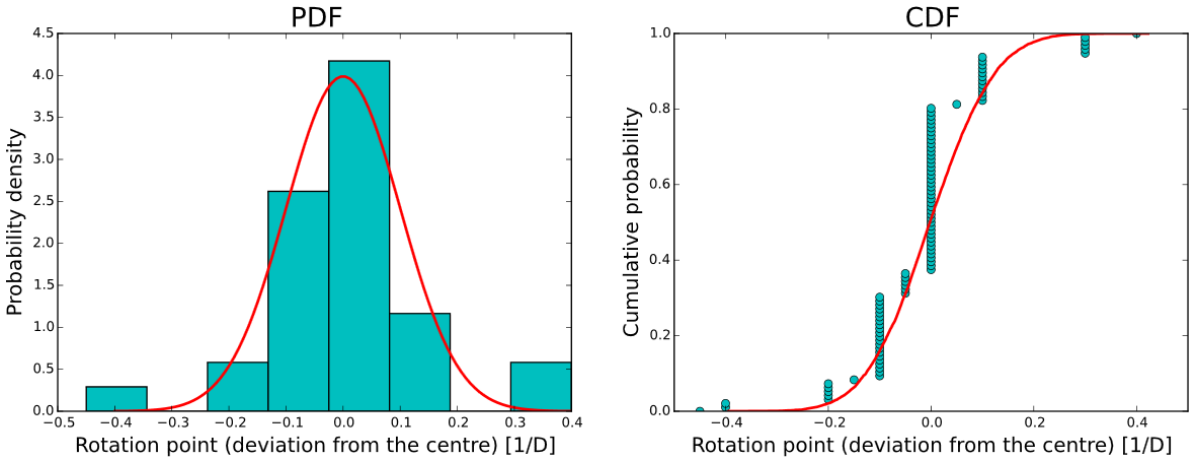

Figure 3.26: Distribution rotation point

From the data it seems that the rotation point is either close to the centre, or close to the edge of the block, and not somewhere in between. Nevertheless, a normal distribution seems appropriate. Mean $\mu = 0$ and standard deviation $\sigma = 0.1$ are used, to obtain the plots as in Figure 3.26, which is acceptable.

The obtained probabilistic distribution is thus:

$$\frac{R}{D} = N(\mu = 0\,; \sigma = 0.1)$$

In order to use this distribution in the impact velocity determination, it will be translated to d_n, by $D = 1.443 d_n$, resulting in the distribution as in Figure 3.27, expressed by:

$$\frac{R}{d_n} = N(\mu = 0\,; \sigma = 0.144)$$

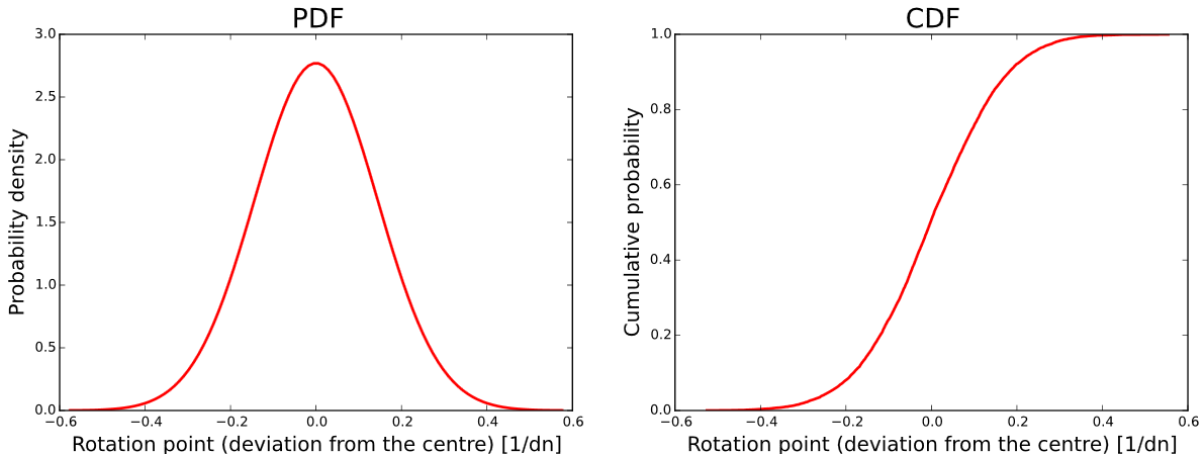

Figure 3.27: Distribution rotation point, as fraction of d_n

Collision point moving block, C1

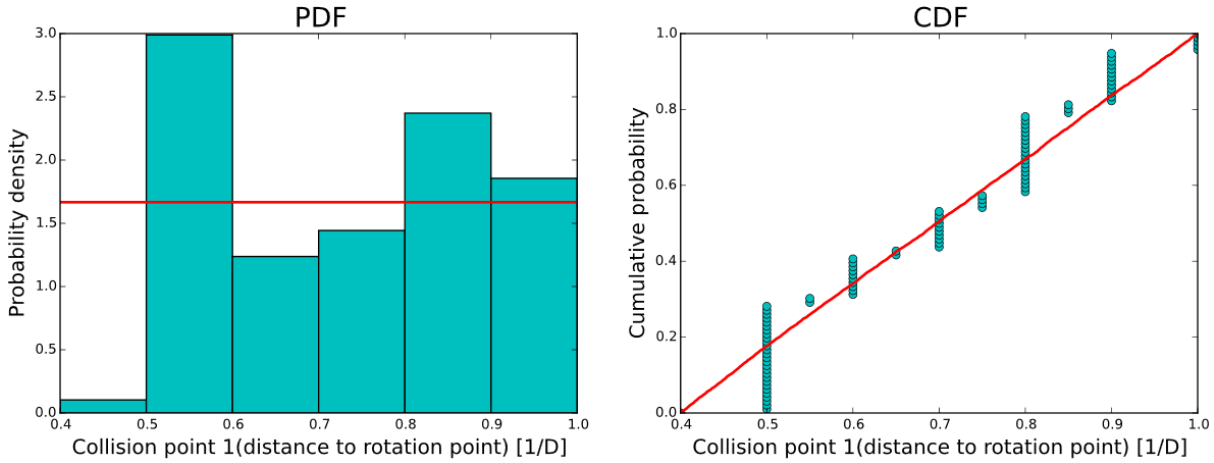

Figure 3.28: Distribution collision point moving block, C1

The point of the moving block that hits another block is estimated as the distance to the rotation point, as a fraction of block size D. The data is not entirely clear, but there seems to be a uniform distribution from roughly 0.4 to 1.0. Many blocks are estimated at 0.5, so it could be opted to give a higher probability of occurrence to 0.5, but that may as well be a measuring error.

The obtained probabilistic distribution is:

$$\frac{C1}{D} = U(\min = 0.4\,;\max = 1.0)$$

In order to use this distribution in the impact velocity determination, it will be translated to d_n, resulting in the distribution as in Figure 3.29, expressed by:

$$\frac{C1}{d_n} = U(\min = 0.58\,;\max = 1.44)$$

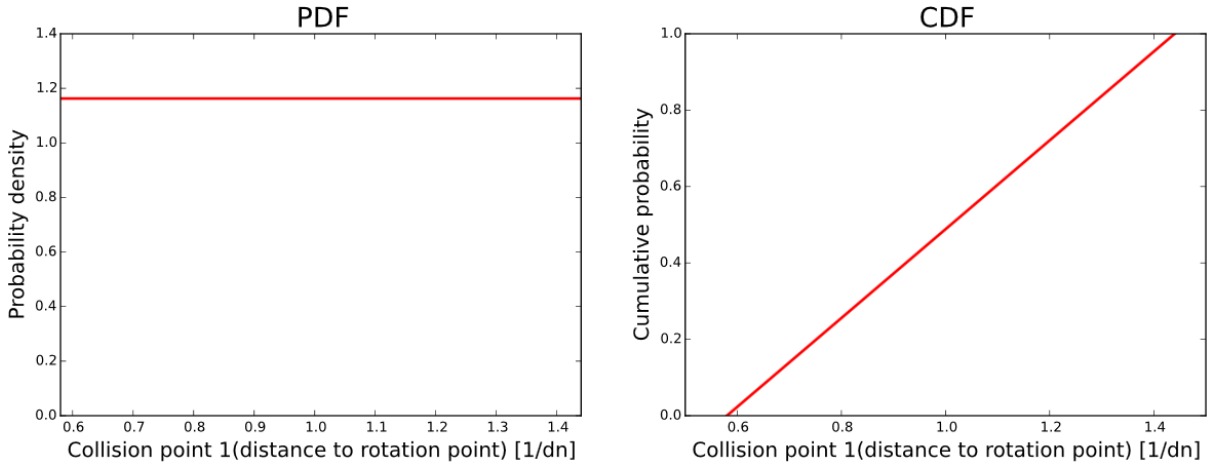

Figure 3.29: Distribution collision point moving block, as a fraction of d_n

Collision point stricken block, C2

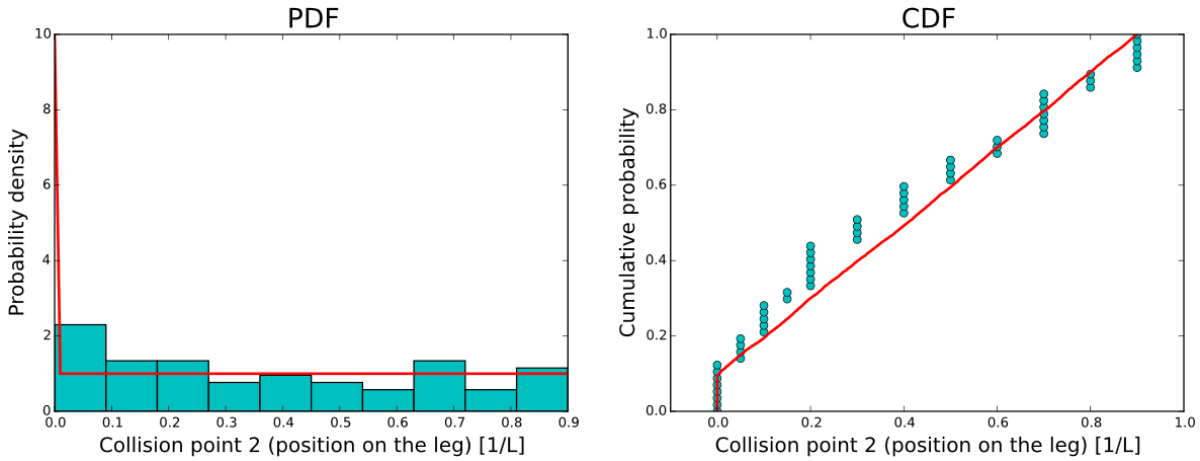

Figure 3.30: Distribution collision point stricken block, spiky leg, C2s

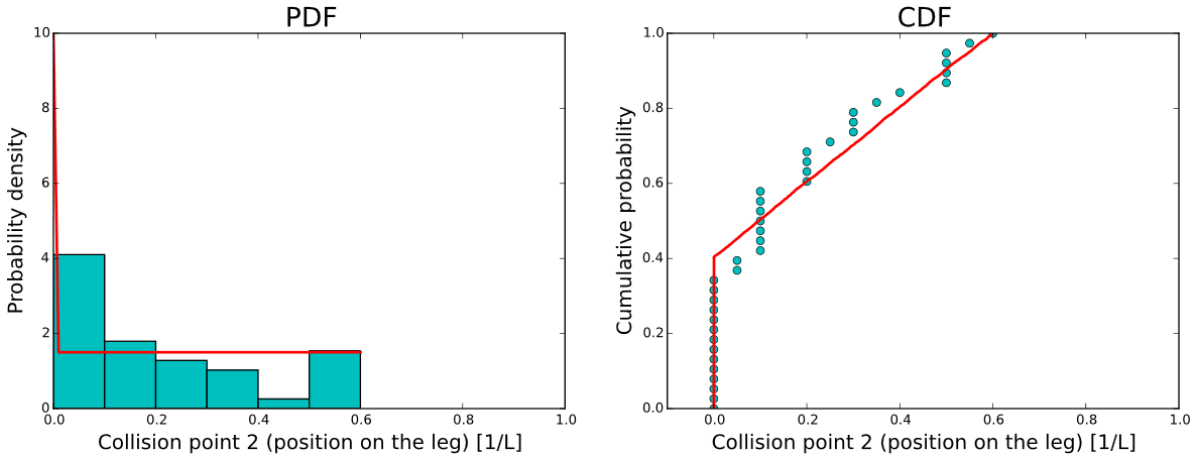

Figure 3.31: Distribution collision point stricken block, cubical leg, C2c

The distribution of the collision point of the stricken block is divided in two parts: the spiky leg, given in Figure 3.30, and the cubical leg, given in Figure 3.31. It was necessary to split the two different legs, because there is a significant deviation, namely that the spiky legs can get hit lower on the leg (i.e. closer to the body) than the cubical legs. Also, the cubical legs are way more likely to get hit on the top than the spiky legs.

The collision point is defined as the location on the leg, where the collision takes place, as a fraction of the length of the leg, with 0 at the top of the leg, and 1 at the bottom of the leg, where it is connected to the body. Both of the distributions have a higher density at 0 (the top of the leg), while the rest of locations are more or less uniformly distributed. For the spiky legs, the estimated distribution goes up to 0.9 (close to the body), while 10% of the hits are said to be at 0. For the cubical legs, the estimated distribution goes up to 0.6, while 40% of the hits are said to be at 0.

These are not standard applied distributions, but they can be obtained from a uniform distribution relatively easily when programming in e.g. Python. Just start the uniform distribution below 0, then make a loop to set any negative values to zero.

The obtained distributions are then:

$\frac{C2_{spiky\ leg}}{L_{spiky}} = U(\min = -0.1\ ; \max = 0.9)$, but set any negative values to zero

$\frac{C2_{cubical\ leg}}{L_{cubical}} = U(\min = -0.4\ ; \max = 0.6)$, but set any negative values to zero

Angle of incoming force, θ_F

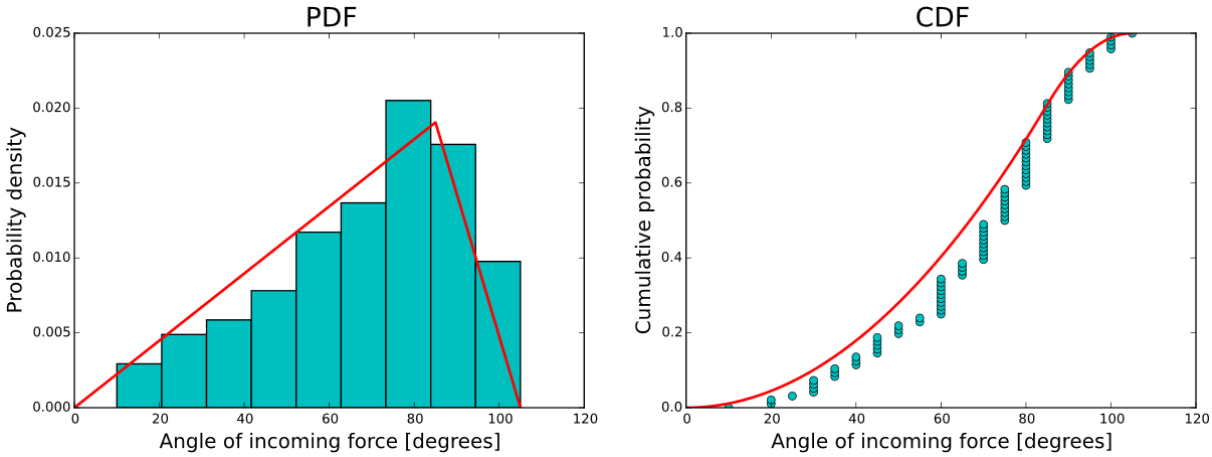

Figure 3.32: Distribution of the angle of the incoming force, θ_F

The distribution of the angle of the incoming force is not split in separate distributions for spiky legs and cubical legs, because there did not seem to be a significant difference between the different legs. The probability density of the angle of the incoming force has a sort of triangular shape, which can be approximated by two linear lines. The cdf can be calculated as the integral of the pdf, so a squared function is obtained from the linear lines.

To create the pdf, keep in mind that the integral over the pdf should equal 1, so the area of the triangle $A = \frac{1}{2} \cdot base \cdot height = 1$. With a base of 0° to 105°, the height should thus be $2.0/105$. Therefore the first line is described by:

$pdf_1(\theta_F) = \frac{2.0}{105} \cdot \frac{\theta_F}{p}, interval\ [0\ ;\ p]$ where p is the peak angle, the top of the triangle

The ascending line is then described by:

$$pdf_2(\theta_F) = \frac{2.0}{105} - \frac{\theta_F - p}{105 - p} \cdot \frac{2.0}{105} = \frac{2.0}{105} + \frac{2p}{105^2 - 105p} - \frac{2\theta_F}{105^2 - 105p}\ ,\ interval\ \langle p\ ;\ 105]$$

Then, the cdf is the integral of the pdf, so:

$$cdf_1(\theta_F) = \int pdf_1 = \int_0^p \frac{2.0}{105} \cdot \frac{\theta_F}{p}\ d\theta_F\ = \frac{\theta_F^2}{105p}\ ,\ interval\ [0\ ;\ p]$$

$$cdf_2(\theta_F) = \int pdf_2 = \int_p^{105} \frac{2.0}{105} + \frac{2p}{105^2 - 105p} - \frac{2\theta_F}{105^2 - 105p}\ d\theta_F\ =$$

$$\left(\frac{2.0}{105} + \frac{2p}{105^2 - 105p}\right) \cdot \theta_F - \frac{\theta_F^2}{105^2 - 105p}\ ,\ interval\ \langle p\ ;\ 105]$$

For the plot in Figure 3.32, $p = 85°$ is used as the turning point, i.e. the top of the triangle.

The obtained probabilistic distribution is then:

$$cdf = \begin{cases} \frac{\theta_F^2}{8925}, & for\ 0 \leq \theta_F \leq p \\ 0.1 \cdot \theta_F - \frac{\theta_F^2}{2100}, & for\ p < \theta_F \leq 105 \end{cases}$$

3.3.3 Other Xbloc® parameters

There are still a few parameters left that were not determined by the laboratory measurements, so they will be treated here.

Drag force

The wave drag force depends on the drag coefficient ($F_{wave} = \frac{1}{2}\rho_w C_D A(\Delta u)^2$) . This C_D-value is based on the values given in Figure 3.33, obtained from .

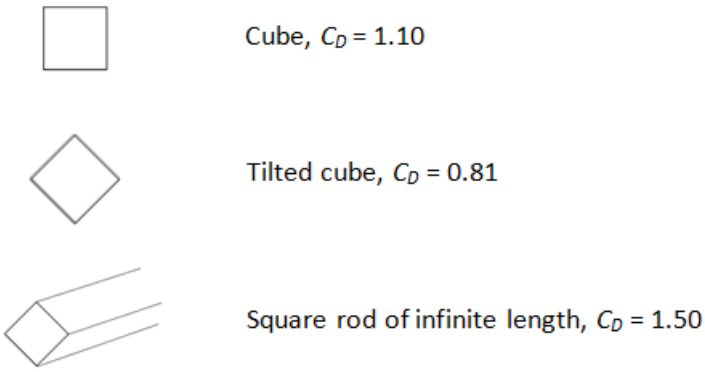

Figure 3.33: C_D-values for a few shapes

Xbloc®s have a more complicated shape than cubes, where the arms could be considered as square rods, though definitely not infinite, so the drag coefficient will be slightly higher than for cubes, but not up to C_D = 1.50. This idea is supported by a value found by Ten Oever (2006), who performed a study on Xbloc®s and found a value for the drag coefficient of C_D = 1.20, by comparing numerical calculations to model test results.

Roughness coefficient

The roughness coefficient is used to determine the run-up velocity, that is used to determine the wave drag force. The determination of the run-up velocity is treated in the determination of the parameters of cubes. Only the roughness coefficient γ_f differs in the case of Xbloc®s. A table with values for γ_f is given in the Breakwater design lecture notes, by Van den Bos and Verhagen (2018). This table gives for a single layer of Xbloc®s: γ_f = 0.45.

Arm of the wave force, f_{rF}, and arm of the weight, f_{rW}

For the cubes, the arms where estimated as being dependent on the initial orientation angle of the cube on the slope. Due to all the possible orientations of an Xbloc®, with twists in multiple planes, it would be very complicated to define the arms of the forces in a similar way. Therefore, the initial orientation angle of the block is not used, as it would be unreliable, since there is not a single angle that defines the position of the block. Instead, the arm of the weight is estimated directly in the laboratory measurements, since the rotation point R is determined as the horizontal distance from the centre of the block, which is exactly equal to the arm of the weight, thus:

$$f_{rW} = R$$

The arm of the wave force is not easily determined, since it really depends on which parts of the block are exposed to wave attack, and there is not a solid area, with the legs sticking out of the body. Therefore, it is decided to say that the wave force works mostly on the upper part of the block, with the resultant force acting at distance of 2/3 D to the rotation point.

$$f_{rF} = \frac{2}{3}D = 0.96\ d_n$$

Mass moment of inertia

This is elaborated in Appendix A, where the mass moment of inertia of an Xbloc® around its centre of gravity was found to be:

$$I_{cg_{Xbloc}} = 0.25988\ \rho d_n^5$$

Though, for a rotation around a point that is not the centre of gravity, there is an additional contribution from Steiner's rule:

$$I_{Xbloc} = I_{cg_{Xbloc}} + md^2 = 0.25988\ \rho d_n^5 + \rho d_n^3 \cdot d^2$$

Where d is the distance from the centre of gravity to the rotation point, visualised in Figure 3.34. From Pythagoras' theorem follows that:

$$d = \sqrt{\left(\frac{1}{2}D\right)^2 + r^2}$$

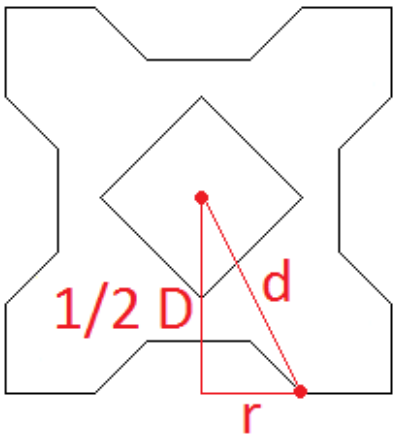

Figure 3.34: Distance of centre of gravity to rotation point

Now, D = 1.443 d_n, and using $r = R$, the earlier estimated horizontal distance between the rotation point and the centre as a fraction of d_n, it follows that:

$$d = \sqrt{0.72^2 + R^2} \cdot d_n$$

Inserting this into the equation for the mass moment of inertia:

$$I_{Xbloc} = I_{cg_{Xbloc}} + md^2 = 0.25988\,\rho d_n^5 + \rho d_n^3 \cdot \left(\sqrt{0.72^2 + R^2} \cdot d_n\right)^2$$

$$I_{Xbloc} = (0.25988 + \ 0.72^2 + R^2)\rho d_n^5$$

$$I_{Xbloc} = (0.7783 + \ R^2)\rho d_n^5$$

Finally, the mass moment of inertia as a fraction of ρd_n^5 is then:

$$f_{inertia} = 0.7783 + R^2$$

Velocity correction factor

In the derivation of the impact velocity formula, it was assumed that the acceleration of the armour unit is constant during its movement. However, it is realised, that the acceleration is not really constant. The sum of moments changes due to a decrease of the wave drag force when the armour unit accelerates, and due to a change of the arm of the weight force when the unit rotates. These effects are investigated in Appendix B, where a velocity correction factor is determined for Xbloc®s.

This factor is established as:

$$f_{cor} = 1 - \frac{\sqrt{s}}{4}$$

Such that the corrected velocity becomes:

$v_{corrected} = f_{cor} \cdot v$, which is added in Equation 3.1.

3.3.4 Validation impact velocity Xbloc®

All the required parameters and variables are determined in the previous subparagraphs, so the distribution of the impact velocity of Xbloc®s can now be determined for various wave heights and armour unit diameters. In fact, even for small scale waves and units, such as the ones used in laboratory tests. Caldera (2019) performed such tests on Xbloc®s with a size of D = 5.64 cm, corresponding to d_n = 3.91 cm. She used significant wave height of the wave field of H_s = 11.5 cm during one of the tests, leading to the results in Figure 3.35. These values of H_s and d_n are used as input for the model that is developed in this MSc thesis, for which the results are given in Figure 3.36. Note that it is now plotted without a log scale, to resemble the graphs made by Ganga Caldera.

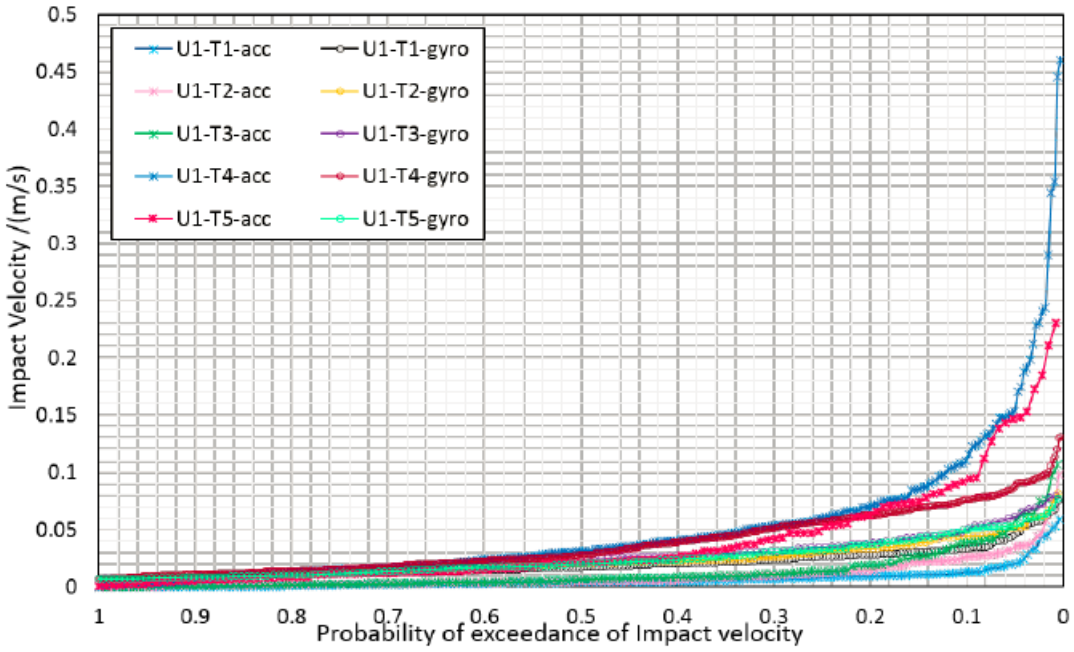

Figure 3.35: Probability of exceedance of impact velocity, measured by Ganga Caldera (2019)

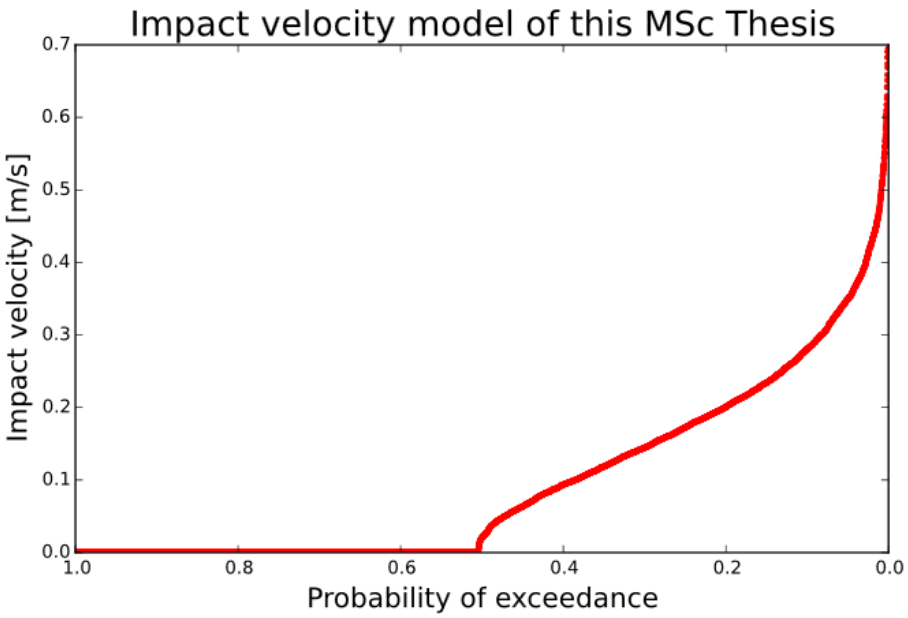

Figure 3.36: Probability of exceedance impact velocity, Hs = 11.5 cm, dn = 3.91 cm

For the comparison, it is important to know that the test results of Caldera (2019) are obtained from a measurement unit that is positioned slightly different for each test, thus having different position parameters per test. However, in the method of this MSc thesis, every single simulation has a completely new set of position parameters, eventually leading to some very unfavourable cases in the number of simulated cases. It is therefore most logical to compare the results of this MSc thesis with the results obtained for the most unfavourable case measured by Caldera (2019), plotted with the blue line.

With this in mind, it is seen that there are two measurements of around $v = 0.45\ m/s$. The model of this MSc thesis gives somewhat higher highest values, with a few values higher than $v = 0.6\ m/s$. However, these are just a few cases out of a simulation of N = 100,000, so logically, there will be some higher values simply because the sample size is so much larger. Therefore, it is opted to make a plot with less simulations, as shown in Figure 3.37, with N = 100. Coincidentally, the highest obtained value is now $v = 0.46\ m/s$. It is therefore concluded that the impact velocity for the very low probabilities of exceedance is decently accurate.

A point of attention is that the shape of the simulated model is somewhat different. The tail is less steep, so while the highest values are perhaps correct, the values around $p = 0.1 - 0.3$ are significantly higher. For example, at $p = 0.1$, the model gives approximately $v = 0.22\ m/s$, while the measurements give approximately $v = 0.13\ m/s$.

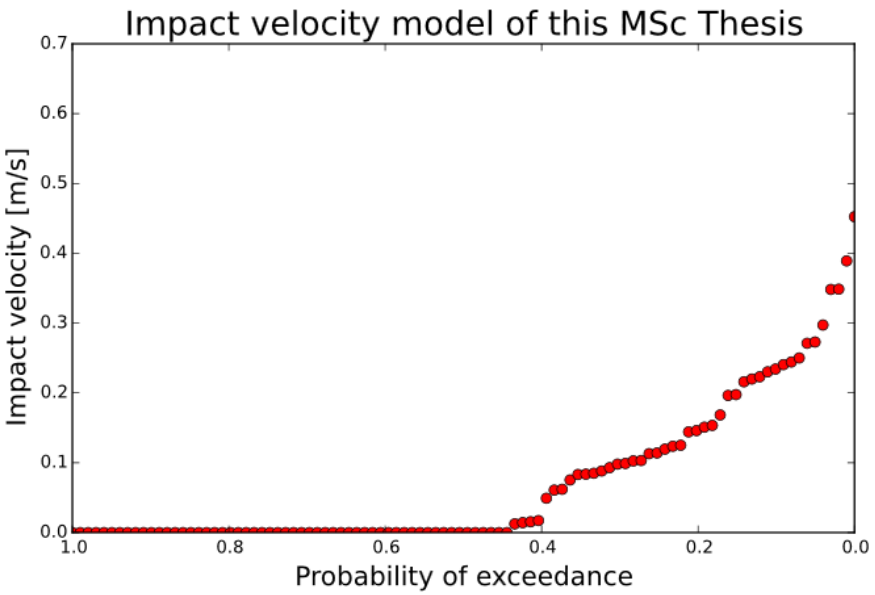

Figure 3.37: Probability of exceedance impact velocity, Hs = 11.5 cm, dn = 3.91 cm, N = 100

4. Impact force

The goal of this chapter is to find an expression to determine the maximum force during a collision between the moving armour unit and another unit. The first step to determining this impact force is to set up an energy balance, containing the kinetic energy of the moving unit (where the impact velocity is used as input) and the potential energy. The force can then be determined by representing this potential energy as a spring energy. Therefore, the system must be schematized as a spring, which must contain the effect of the armour unit and of the breakwater bed. This method to determine the force will then be validated by means of the results of physical model tests. The whole process covered in this chapter is visualised by a flow chart in Figure 4.1.

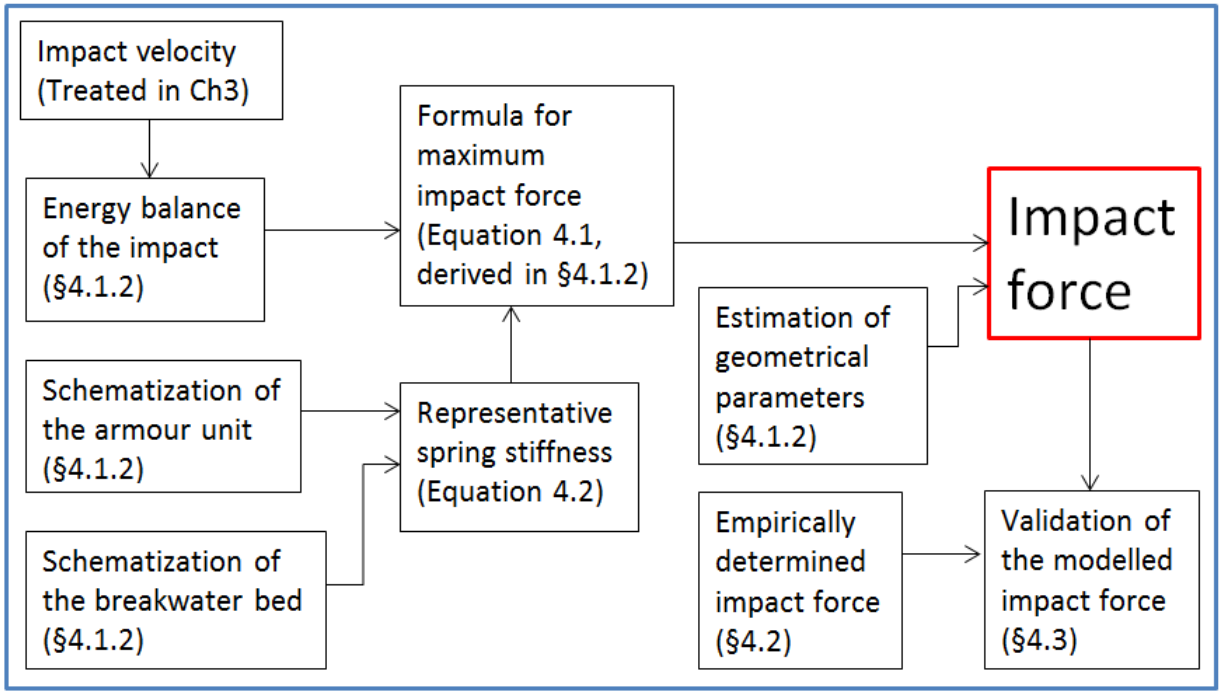

Figure 4.1: Flow chart chapter 4. Impact force

4.1 Forces via energy balance

This paragraph treats the determination of the forces in a theoretical way, via an energy balance. The goal is to determine the forces in an analytical way, such that a probabilistic distribution can be applied to the input variables, in order to incorporate the determination of the force in a probabilistic method. First, the eventual model with analytical equations will be shown, including the main assumptions. Subsequently, the derivation of said equations will be treated.

4.1.1 Equation, model and assumptions

In the observed situation, an armour unit is moved by a wave impact, causing a collision of this armour unit with another armour unit. The kinetic energy of the moving armour unit can be absorbed by elastic or plastic deformation during the impact, or can partially be converted kinetic energy of the stricken armour unit, if the stricken unit is able to move as well. Plastic deformation is undesirable though, as that may quickly lead to breakage of the armour unit. In order to determine if plastic deformation will occur, the stresses in the concrete must eventually be determined, for which first the force during impact will be determined. This can be done by means of an energy balance, as in, including the aforementioned kinetic energy of the moving unit (block 1) and of the stricken unit (block 2), as well as a potential energy, representing elastic stiffness.

Before going to the equations, a list of assumptions will be given, that were necessary to obtain the equations:

- Rupture of the legs is assumed to be the most important failure mechanism
- It is assumed that the critical cross-sections are located at the junctions, where the legs are connected to the main body of the armour unit
- The energy balance consists of the kinetic energy of the moving block, a potential energy, and possibly the kinetic energy of the stricken block, which may move due to the collision
- The potential energy is introduced in the form of elastic/spring energy, which includes a force and a stiffness, which eventually allows the determination of the force
- The stiffness of the system is a combination of the stiffness of the breakwater bed, and the stiffness of the Xbloc® leg, which is represented as springs in series
- The mechanical model of the legs is treated as a beam that is clamped at the connection with the main body, illustrated in Figure 4.2
- This “beam” has an axial stiffness and a bending stiffness, which are modelled in a mass-spring system by a vertical (k_1) and horizontal spring (k_2) for which a combined stiffness (k) will be determined in order to determine the force

The formula to determine the force derived from the energy balance is given by:

$$F = \sqrt{m_1 v_1^2 k - m_2 v_2^2 k}$$ Equation 4.1

Where:

- m_1 is the mass of object 1, the moving armour unit
- v_1 is the velocity of object 1 at the moment of impact
- k is the stiffness of the leg, the resistance to deformations, determined with Equation 4.2
- m_2 is the mass of object 2, the stricken armour unit, and is equal to m_1
- v_2 is the velocity of object 2, which can be left out when it is unknown how much of the energy is converted into kinetic energy, reducing the formula to: $F = \sqrt{m_1 v_1^2 k}$

The stiffness k of the system is determined from:

$$\frac{1}{k} = \frac{1}{k_{bed}} + \frac{1}{k_{leg}}$$ Equation 4.2

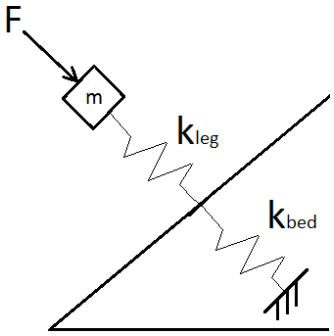

Where the stiffness of the bed is estimated as:

$$k_{bed} = 69.4 \cdot 10^6 \cdot d_n^2$$

The stiffness of the leg can be determined as the combined stiffness of the two springs in the mass-spring system, shown in Figure 4.2, using the following equation:

$$k_{leg} = \frac{1}{\sqrt{\frac{\cos^2 \theta_F}{\left(\frac{EA}{L}\right)^2} + \frac{\sin^2 \theta_F}{\left(\frac{3EI}{L^3}\right)^2}}}$$ Equation 4.3

Where:

- θ_F is the angle of the incoming impact force, see the definition further ahead in Figure 4.5
- E is the Young's modulus of the concrete
- A is the area of the observed cross-section
- I is the area moment of inertia of the observed cross-section
- L is the length of the leg

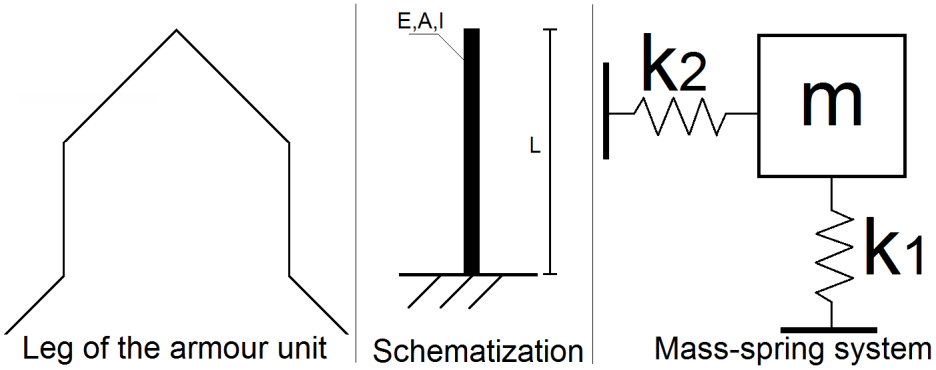

Figure 4.2: Schematization leg armour unit

An overview of the values of the parameters and variables used for determining the impact force is given in Table 4.1.

	Values
Parameters	
Mass density concrete, $\rho_s[kg/m^3]$	2400
Young's modulus of the concrete, $E\ [N/mm^2]$	32837
Variables	
Area of the cross section, $A\ [m^2]$	$0.2297 \cdot d_n^2$
Area moment of inertia of the cross section, $I\ [m^4]$	$0.004461 \cdot d_n^4$
Full length of the leg, $L_{leg}[m]$	Spiky leg: $0.540 \cdot d_n$ Cubical leg: $0.481 \cdot d_n$
Spring stiffness representing the breakwater bed, $k_{bed}[N/m]$	$69.4 \cdot 10^6 \cdot d_n^2$
Stochastic variables	
Incoming angle of the force, θ_F [°]	Special probabilistic distribution: $cdf = \begin{cases} \frac{\theta_F^2}{8925}, & for\ 0 \leq \theta_F \leq 85 \\ 0.1 \cdot \theta_F - \frac{\theta_F^2}{2100}, & for\ 85 < \theta_F \leq 105 \end{cases}$

Table 4.1: Parameters and variables used to determine the impact force

4.1.2 Derivation of the equations

Due to a wave impact, one armour unit starts moving, leading to a collision with another armour unit. Say, the moving armour unit is called 'block 1', and the stricken armour unit is called 'block 2'. An energy balance as in Equation 4.4 can be set up, including the kinetic energy of block 1, a potential energy, and a kinetic energy of block 2, which might also move due to the collision. Although block 2 must first experience an acceleration, the possible movement of this block can still be described by a kinetic energy, since the acceleration will take place during the contact moment between the two blocks, such that block 2 will have a certain velocity once the contact is over.

$$E_{kin,1} = E_{pot} + E_{kin,2} \qquad \text{Equation 4.4}$$

Kinetic energy can be described by:

$$E_{kin} = \frac{1}{2}mv^2 \qquad \text{Equation 4.5}$$

Where m is the mass of the moving object, and v is the velocity of said object.
The impact force can eventually be determined from the potential energy, though some assumptions are required in order to describe the potential energy. The potential energy will be treated in the form of an elastic energy, or also called spring energy, which can be described as:

$$E_{pot,spring} = \frac{1}{2}k\delta^2 \qquad \text{Equation 4.6}$$

Where $k\ [N/m]$ is the spring stiffness, and $\delta\ [m]$ is the deformation.

However, since the force in a spring is $F = k \cdot \delta$, and thus $\delta = \frac{F}{k}$, this can be rewritten to a more convenient expression, that directly includes the force:

$$E_{pot,spring} = \frac{F^2}{2k}$$ Equation 4.7

The energy balance of Equation 4.4 can now be rewritten to determine the force:

$$\frac{1}{2} m_1 {v_1}^2 = \frac{F^2}{2k} + \frac{1}{2} m_2 {v_2}^2$$

$$F = \sqrt{m_1 {v_1}^2 k - m_2 {v_2}^2 k}$$ Equation 4.8

The mass of the armour units can be determined relatively easily. The velocity of the moving armour unit, v_1, is the impact velocity, treated earlier, which can also be determined. It is not yet known how much of the energy that the stricken block receives, will be converted into kinetic energy, so the velocity of that block, v_2, will be neglected for now, but it is good to note that it is possible to include movement of the stricken block in the determination of the force. The stiffness is the last unknown in order to determine the force.

The stiffness will be determined from two springs in series: a spring to represent the stiffness of the bed, and a spring to represent the stiffness of the Xbloc® leg, schematized in Figure 4.3. Note that the stricken leg is not necessarily in contact with the bed, but the force will flow through the body, which transfers the force to the bed.

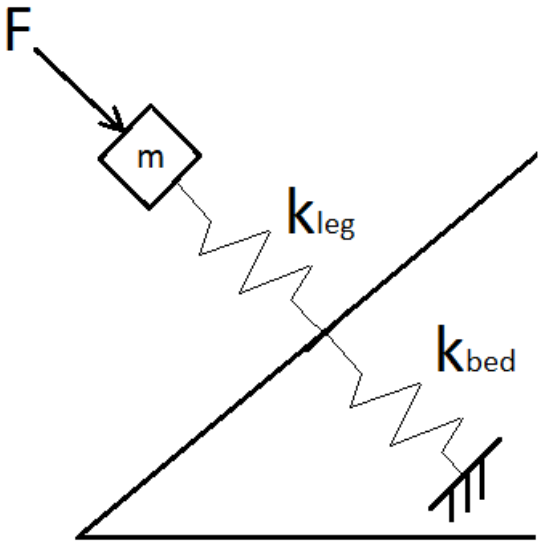

Figure 4.3: Spring system in series

The armour unit is modelled as a relatively simple mass-spring system, containing two springs. A leg of the armour unit can be schematized as a cantilever beam, clamped at the 'bottom', where it is attached to the body of the amour unit. Depending on the direction of the force, the 'beam' will experience axial loading and/or bending, resisting deformations in either direction thanks to a certain stiffness. The model is illustrated in Figure 4.4, where a spiky leg is depicted, but the same model can be applied to the cubical leg of the Xbloc®.

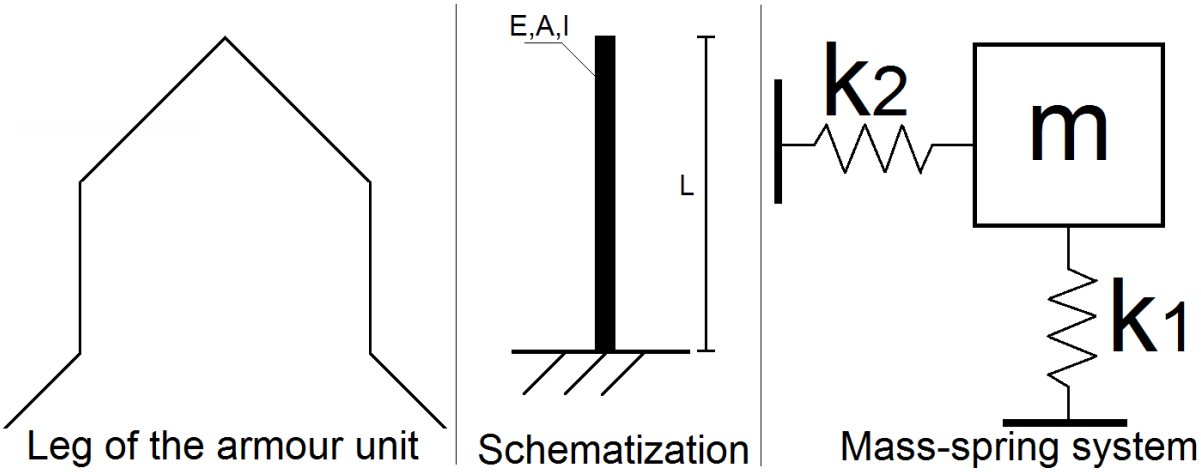

Figure 4.4: Schematization leg armour unit

In this mass-spring system, spring 1 represents the axial stiffness, with $k_1 = EA/L$, and spring 2 represents the bending stiffness, with $k_2 = 3EI/L^3$, which will both be derived below.

For a beam under axial loading, the stress can be determined as the force over the area: $\sigma = \frac{F}{A}$

Furthermore, Hooke's law states that the stress equals the strain multiplied by the Young's modulus: $\sigma = \varepsilon \cdot E$

Therefore: $\frac{F}{A} = \varepsilon \cdot E \quad \rightarrow \quad F = \varepsilon \cdot E \cdot A$

The strain is defined as the deformation over the total length: $\varepsilon = \delta/L$

Then: $F = \frac{\delta}{L} \cdot E \cdot A$

In analogy with the spring force, $F = k \cdot \delta$, it becomes clear that the axial stiffness can be written as:

$$k_1 = \frac{EA}{L} \qquad \text{Equation 4.9}$$

The basic structural mechanics rules give that the deflection of a clamped beam can be determined as:

$$\delta = \frac{FL^3}{3EI} \qquad \text{Equation 4.10}$$

This can be rewritten in accordance with the spring force, $F = k \cdot \delta$, to: $F = \frac{3EI}{L^3} \cdot \delta$

Therefore, the spring that accounts for the bending stiffness will have a stiffness of:

$$k_2 = \frac{3EI}{L^3} \qquad \text{Equation 4.11}$$

Since the stiffness differs for a different direction of the force, this direction must be determined in order to calculate the force. For differing situations, the moving block will hit another block in a slightly different way, and under a different angle. There is thus some variation in the angle of the incoming force. For a probabilistic analysis, it is important to define the incoming angle in order to perform the evaluation systematically. This definition of the incoming angle is depicted in Figure 4.5. An angle of 0° gives a purely axial loading, while an angle of 90° indicates a load perpendicular to the leg, for which the stiffness is determined purely from bending.

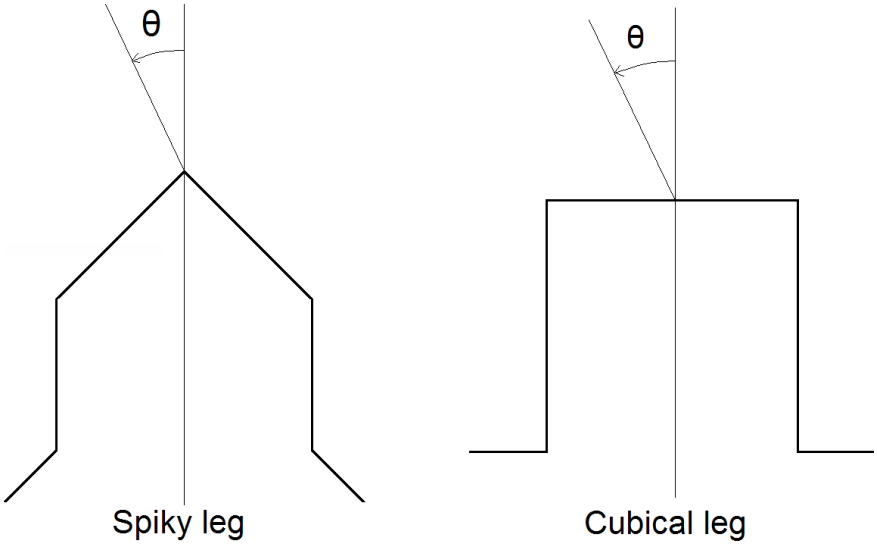

Figure 4.5: Definition incoming angle of the force

As said, the angle of the force varies and may very well be somewhere in between parallel and perpendicular to the leg of the armour unit. The resulting stiffness would then be a combination of the axial stiffness and the bending stiffness. Though, a force can be decomposed into a parallel and perpendicular component, as illustrated in Figure 4.6.

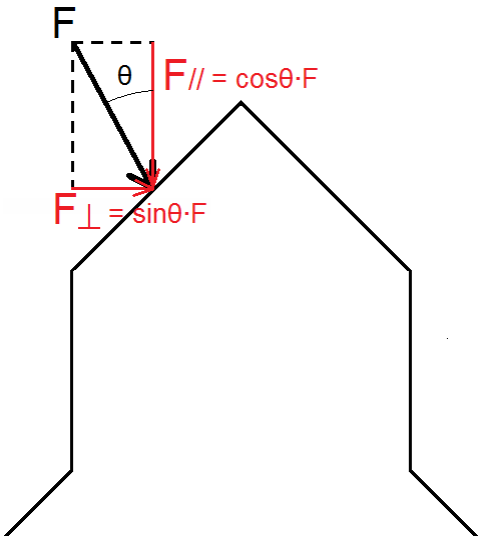

Figure 4.6: Decomposition of the force

This decomposition of the force helps to determine the combined stiffness of the two springs. Based on the decomposed forces, a vertical deformation δ_V and a horizontal deformation δ_H can be determined, using the stiffnesses of the vertical spring and the horizontal spring. The total deformation δ can be determined from δ_V and δ_H via Pythagoras' theorem, which eventually leads to a description of the total stiffness k. The situation is clarified in Figure 4.7, followed by the derivation.

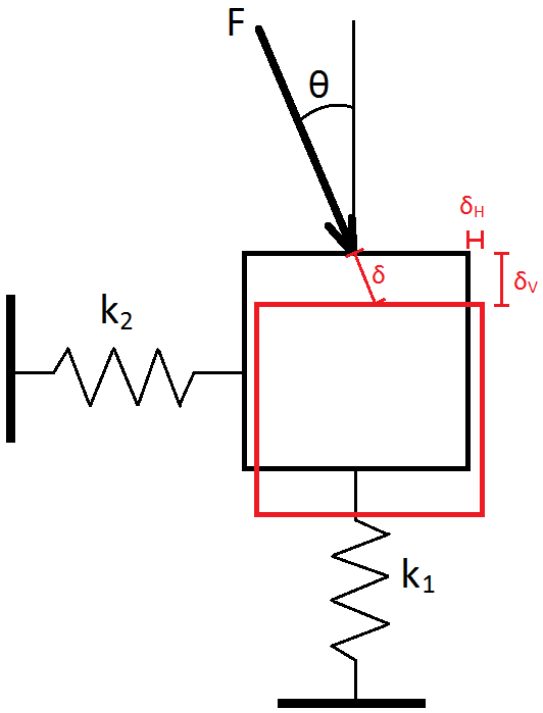

Figure 4.7: Deformations in mass-spring system

From $\delta = \frac{F}{k}$ and the decomposed forces follows that:

$\delta_V = \frac{F \cdot \cos\theta}{k_1}$

$\delta_H = \frac{F \cdot \sin\theta}{k_2}$

From Pythagoras' theorem follows that:

$\delta = \sqrt{\delta_V^2 + \delta_H^2}$

$\delta = \sqrt{\frac{F^2 \cdot \cos^2\theta}{k_1^2} + \frac{F^2 \cdot \sin^2\theta}{k_2^2}} = \sqrt{\left(\frac{\cos^2\theta}{k_1^2} + \frac{\sin^2\theta}{k_2^2}\right) \cdot F^2} = \sqrt{\left(\frac{\cos^2\theta}{k_1^2} + \frac{\sin^2\theta}{k_2^2}\right)} \cdot F$

Now, note again that $\delta = \frac{F}{k}$, so:

$\delta = \sqrt{\left(\frac{\cos^2\theta}{k_1^2} + \frac{\sin^2\theta}{k_2^2}\right)} \cdot F = \frac{F}{k}$

$k = \frac{1}{\sqrt{\frac{\cos^2\theta}{k_1^2} + \frac{\sin^2\theta}{k_2^2}}}$

Filling in the earlier determined axial stiffness $k_1 = \frac{EA}{L}$ and the bending stiffness $k_2 = \frac{3EI}{L^3}$ leads to the following equation for the stiffness k:

$$k = \frac{1}{\sqrt{\frac{\cos^2\theta}{\left(\frac{EA}{L}\right)^2} + \frac{\sin^2\theta}{\left(\frac{3EI}{L^3}\right)^2}}}$$

Equation 4.12

To calculate k, several geometrical properties of the Xbloc® must be determined (area A, area moment of inertia I, and length L), as well as the Young's modulus (E) of the concrete of the Xbloc®.

The behaviour of both the spiky leg and the cubical leg will be investigated, so the geometrical properties will be determined for both of them individually. The dimensions of the Xbloc® are given again, in Figure 4.8.

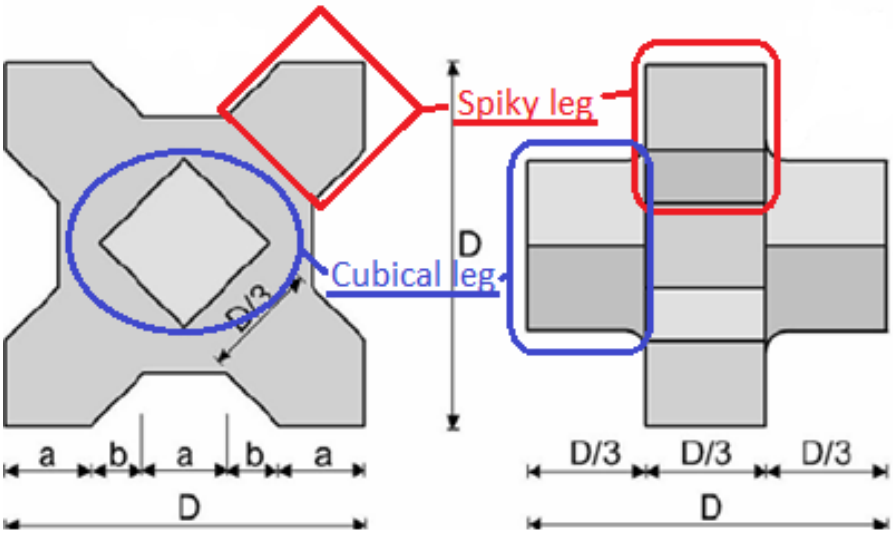

Figure 4.8: Xbloc® legs and dimensions

Cubical leg

The cubical leg has a symmetrical cross-section with width D/3 and height D/3, and the length of the leg is also D/3, which is all shown in Figure 4.9. The area, area moment of inertia, and length will be written as a function of the nominal diameter d_n instead of total length D, since it is more convenient to have all parameters in terms of d_n. As determined in Appendix A, D = 1.443 d_n, so D/3 = 0.481 d_n.

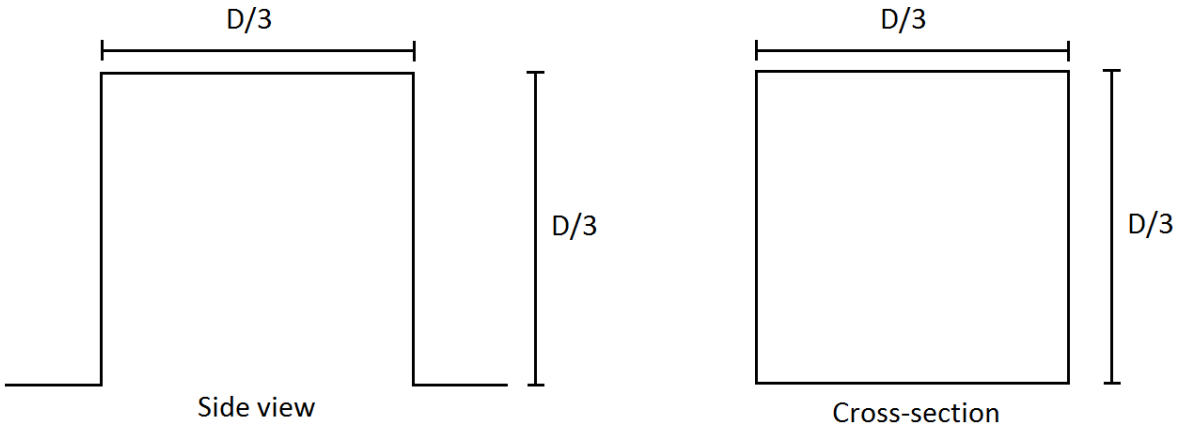

Figure 4.9: Dimensions cubical leg

The full length of the leg is:

$$L_{max} = \frac{D}{3} = 0.481\ d_n$$

The area is simply width times height:

$$A = w \cdot h = \frac{D}{3} \cdot \frac{D}{3} = \frac{D^2}{9} = 0.2297\ d_n^2$$

The area moment of inertia for a rectangle is $I = \frac{1}{12} wh^3$, so:

$$I = \frac{1}{12} wh^3 = \frac{1}{12} \left(\frac{D}{3}\right)^4 = 0.001029\ D^4 = 0.004461\ d_n^4$$

Spiky leg

The dimensions of the spiky leg can be determined from the main dimensions of the Xbloc® as given in Figure 4.8, by using Pythagoras' Theorem. Again, the dimensions will be rewritten in terms of d_n, using $a = 0.2357\ D$, $b = 0.14645\ D$, and $D = 1.443 d_n$. The dimensions of the spiky leg are given in Figure 4.10.

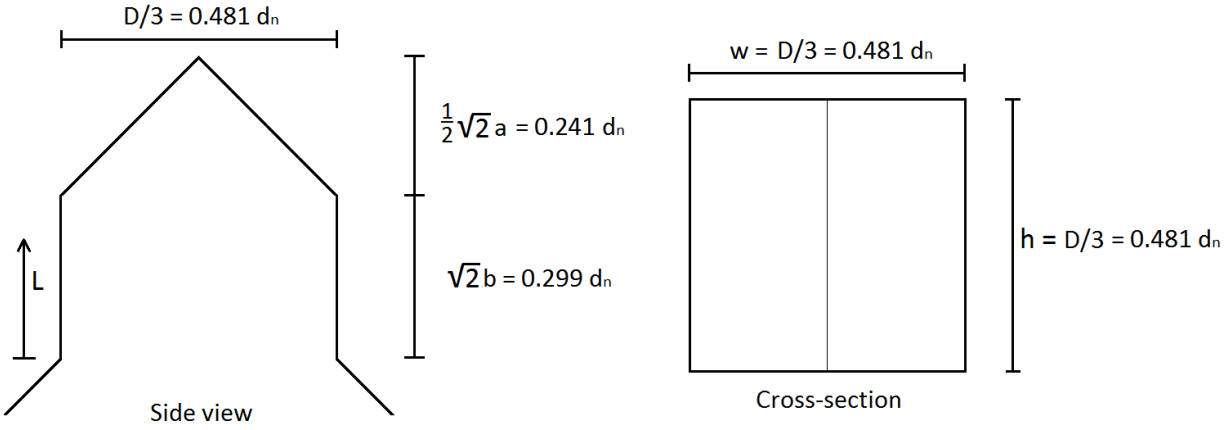

Figure 4.10: Dimensions spiky leg

Note that the spiky leg does not have a constant cross-section. In the upper part, the width declines to zero at the top, while the lower part has a constant width.

The full length of the leg is:

$$L_{max} = \sqrt{2}b + \frac{1}{2}\sqrt{2}a = 0.540\ d_n$$

The lower part of the spiky leg has the same cross section as the cubical leg, so:

$$A = w \cdot h = \frac{D}{3} \cdot \frac{D}{3} = \frac{D^2}{9} = 0.2297\ d_n^2$$

$$I = \frac{1}{12} wh^3 = \frac{1}{12} \left(\frac{D}{3}\right)^4 = 0.001029\ D^4 = 0.004461\ d_n^4$$

The upper part of the spiky leg has a declining width, which can be described as:

$\frac{L_{max} - L}{0.2405\ d_n} \cdot 0.481\ d_n$, which can be rewritten to $1.08\ d_n - 2L$, when filling in L_{max}.

Using the definition of L as in Figure 4.10, going upward starting from the bottom of the leg, the width can be described as:

$$w(L) = \begin{cases} 1.08\, d_n - 2L & for\ \ 0.299\, d_n \leq L \leq\ L_{max} \\ 0.481\, d_n & for\ \ 0\ \leq L \leq 0.299\, d_n \end{cases}$$

This expression for the width can be used to determine the area, and area moment of inertia for each location in the leg, simply via $A = w \cdot h$ and $I = \frac{1}{12} w h^3$

Gravel bed as a spring

Just like the concrete armour unit has a certain stiffness against deformation, the breakwater core, that functions as a bed for the armour units, has a stiffness as well. When a load is applied on the bed, it will experience a certain deformation. The force divided by this deformation could then be interpreted as the spring stiffness of the bed. This spring stiffness is difficult to calculate accurately, but an estimate will be made. This will be done via two methods, to ensure that the determined value is in the right order of magnitude.

Both methods will be elaborated and compared below, resulting in an estimate of the bed spring stiffness of:

$$k_{bed}[N/m] = 69.4 \cdot 10^6 \cdot d_n^2$$

Method 1. Based on Young's modulus

In a similar way as for the compression of a beam, the compressive stiffness of the bed can be estimated as:

$$k_{bed} = \frac{EA}{L}$$

Some information about the Young's modulus of soil is retrieved from Geotechdata.info (2013). The Young's modulus of a gravel bed is dependent on the packing density, so there is not a single valid value. For sand and gravel beds, the Young's modulus varies from 30 MPa to over 300 MPa. Since the breakwater consists or rocks, it is assumed to be comparable to the stiffest gravel soils, so a Young's modulus of E = 300 MPa will be used.

The effective area, over which the force is spread, can be determined based on the friction angle of the gravel, ϕ = 35°. This is illustrated in Figure 4.11.

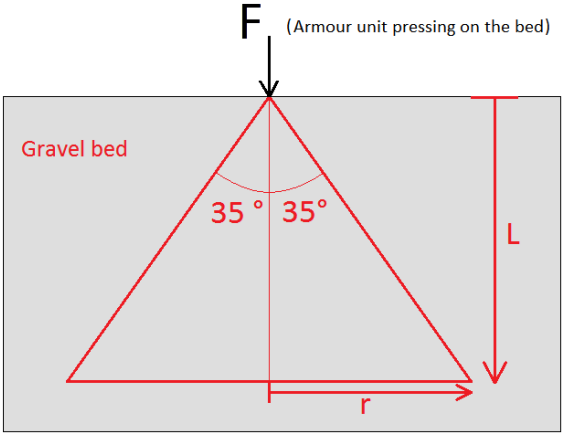

Figure 4.11: Force distribution through the gravel bed

Due to the cone-like shape over which the force is spread, the area will be determined by a circle:

$A = \pi r^2$

where: $r = \tan(35°) \cdot L$

$A = \pi \tan^2(35°) \cdot L^2$

Averaging the area over the length gives:

$A_{avg} = \frac{\pi}{2} \tan^2(35°) \cdot L^2$

The effective length L has to be estimated as well. It seems logical that L will be larger for a larger force. The effective length is therefore correlated with the size of the armour unit, d_n. A precise value of the length cannot be determined without proper investigation, but just to get an idea of the eventual spring stiffness, a value of $L = d_n$ will be used here.

Now, all estimations can be filled in in the formula for the stiffness, leading to:

$k_{bed} = \frac{EA}{L} = E \cdot \frac{\pi}{2} \tan^2(35°) \cdot L = 300 \cdot 10^6 \cdot \frac{\pi}{2} \tan^2(35°) \cdot d_n$

$k_{bed} = 231 \cdot 10^6 \cdot d_n$

Method 2. Based on subgrade modulus

Another possibility to determine a spring stiffness of the soil is to make use of the subgrade modulus, k_s [kN/m³]. This is a parameter that is used in geo-engineering, to determine the deformations and settlements of a soil. Though a breakwater core is different from regular soils, the subgrade modulus may still provide a reasonable estimate of the spring stiffness.

The spring stiffness will then be determined as:

$k_{bed} = k_s \cdot A$

Where the area A can be determined by the contact area between the armour unit and the soil. This can be estimated as the area of a leg of the armour unit:

$A = \frac{D}{3} \cdot \frac{D}{3} = \frac{D^2}{9} = 0.231 \cdot d_n^2$

The subgrade modulus, k_s, will be based on commonly used values. An article from Avci and Gurbuz (2018) provides these values for several types of soil. The subgrade modulus also depends on the packing density etc., so there is not a single valid value. For massive rock, the subgrade modulus can be $k_s > 2{,}000{,}000\ kN/m^3$, while for sand or gravel, values of $k_s = 100{,}000 - 300{,}000\ kN/m^3$ are common. The breakwater core consists of rocks, so values for a massive rock are not appropriate. It is assumed that the rock bed is comparable to the stiffest gravel soils. Therefore, a value of $k_s = 300{,}000\ kN/m^3$ will be used here.

Then, the formula to determine the bed spring stiffness becomes:

$$k_{bed} = 0.231 \cdot d_n^2 \cdot \ 300{,}000 \cdot 10^3$$

$$k_{bed} = 69.4 \cdot 10^6 \cdot d_n^2$$

Comparison method 1 and method 2

The previously described methods will be compared, to check if their estimations of the bed spring stiffness are in the same order of magnitude. In Figure 4.12, both methods are plotted against the size of the armour unit. Due to the fact that method 1 is linearly correlated with d_n and method 2 is correlated to d_n^2, there will naturally be a deviation between the two, but it is observed that both are roughly in the same order of magnitude, for reasonable values of d_n.

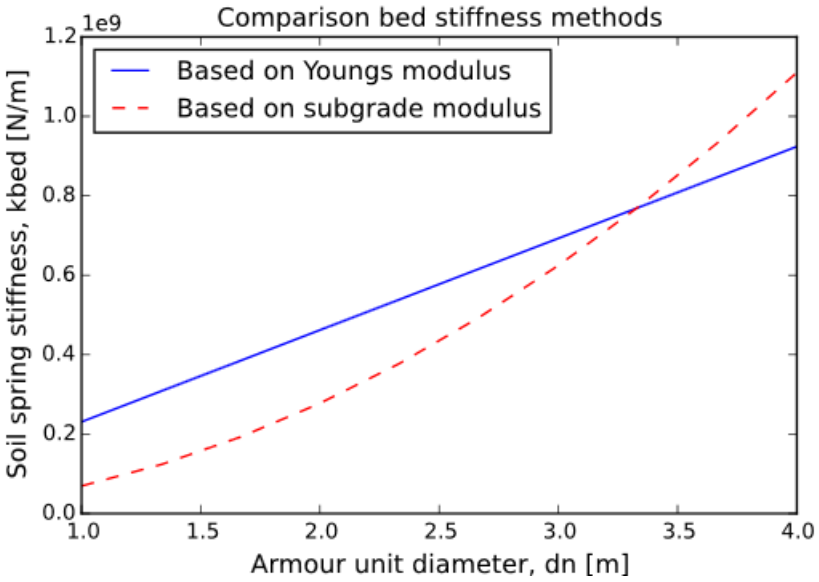

Figure 4.12: Comparison bed stiffness methods

Method 2, based on the subgrade modulus, seems more reliable, since the required assumptions are less arbitrary. It is therefore decided to use the spring stiffness obtained from method 2, so:

$$k_{bed} = 69.4 \cdot 10^6 \cdot d_n^2$$

4.2 Empirical determination of impact force

The CUR (1989 – 1) performed physical model tests to determine the force over time during concrete on concrete impact. They used a test setup as visualised in Figure 4.13. A cube is used as moving element to hit a spherical specimen that is attached to a large concrete pole. The cube is attached to a pendulum that is able to swing in a single direction, while movement in other directions is prevented. The pole is attached to similar pendulums. Measuring devices are placed on both sides of the pole, approximately 1 m away from the start of the pole. A Doppler radar is used to measure the impact velocity of the swinging element.

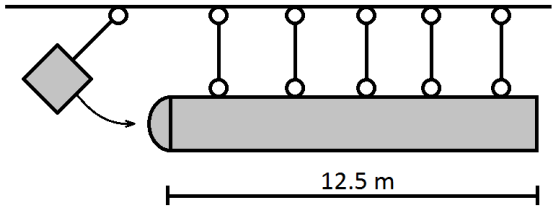

Figure 4.13: Test setup in CUR research

Based on the physical test results, the CUR (1989 – 1) developed a method to determine the force-time relation, based on an elasto-plastic model. The results of this method are found to be in relatively good accordance with the test results. The idea is to make a force-time diagram that looks like the one given in Figure 4.14, with a rising section, a constant section and a restitution section.

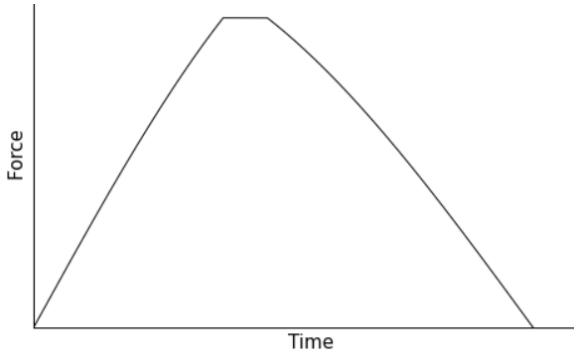

Figure 4.14: Force-time relation

The following formulas are obtained from the CUR report (1989 – 1). Note that the CUR report denotes forces with P, but this is changed to F in this report, to retain coherence and clarity.
The rising section and restitution section are approximated by a sinusoidal curve. This curve is governed by:

$$F(t) = F_{max} \cdot \sin\left(\frac{t \cdot \frac{\pi}{2}}{t_{max}}\right)$$ Equation 4.13

Where F_{max} and t_{max} correspond to the top of this sinusoidal curve, and are calculated with:

$$F_{max} = \left(1.25 \cdot \alpha \cdot v^2 \cdot K^{\frac{2}{3}}\right)^{\frac{3}{5}}$$ Equation 4.14

$$t_{max} = 1.47 \cdot \left(1.25 \cdot \frac{\alpha}{v^{\frac{1}{2}} \cdot K}\right)^{\frac{2}{5}}$$ Equation 4.15

Where K is the contact parameter, K_{e1} for the rising section and K_{e2} for the restitution section, v is the impact velocity, and α is the effective mass, defined as: $\alpha = \frac{m_1 \cdot m_2}{m_1 + m_2}$ with m_1 as the mass of the incoming element, and m_2 as the mass of the stricken element.

m_1 can be determined as the mass of the observed armour unit. m_2 is also dependent on the freedom of movement of the stricken armour unit. If the stricken unit would be free to move, m_2 is just the mass of the unit, though if it were to be fully clamped, m_2 should be set equal to infinity. The two limits are thus $m_2 = m_1$ and $m_2 = \infty$, resulting in respectively $\alpha = \frac{m_1 \cdot m_1}{m_1 + m_1} = \frac{m_1}{2}$ and $\alpha = \frac{m_1 \cdot \infty}{m_1 + \infty} = \frac{m_1 \cdot \infty}{\infty} = m_1$. Therefore: $\frac{m_1}{2} \leq \alpha \leq m_1$ in any case.

The CUR research concluded that the contact parameters for the rising and restitution sections generally are related as: $K_{e2} = 70\% \cdot K_{e1}$.

Since K_{e2} is lower, the restitution section is used as the starting point to capture the force-time relation. The area under the restitution section of the force-time diagram is set equal to 0.5·m·v, so half of the total momentum. This is an arbitrary assumption that is convenient as it helps to fully determine the force-time relation, but the CUR report does not make clear if this assumption is actually based on a clear idea. Anyway, the time interval of the restitution can then be calculated as:

$$t_{e2} = \frac{t_{max}}{\frac{\pi}{2}} \cdot \arccos\left(\frac{\left(F_{max} \cdot t_{max} - 0.5 m v \cdot \frac{\pi}{2}\right)}{F_{max} \cdot t_{max}}\right) \qquad \text{Equation 4.16}$$

Where F_{max} and t_{max} are calculated based on K_{e2}.

The maximum value of the force is then obtained from the sinusoidal curve that was given in Equation 4.13: $F(t_{e2}) = F_{max} \cdot \sin\left(\frac{t_{e2} \cdot \frac{\pi}{2}}{t_{max}}\right)$. The time interval of the rising section can be obtained by using this relation in reverse. Using F_{max} and t_{max} calculated with K_{e1}:

$$t_{e1} = \arcsin\left(\frac{F(t_{e2})}{F_{max}}\right) \cdot \frac{t_{max}}{\frac{\pi}{2}}$$

The area under the sinusoidal curve can be calculated by:

$$A = \frac{F_{max} \cdot t_{max}}{\frac{\pi}{2}}\left(1 - \cos\left(\frac{t \cdot \frac{\pi}{2}}{t_{max}}\right)\right)$$

This area can be calculated for the rising section (A_1) and the restitution section (A_2).

The total area under the force-time diagram is supposed to be equal to the total momentum: $m \cdot v$. Therefore, the time interval of the (constant) middle section can be calculated by subtracting the areas of the rising and restitution section:

$$t_p = \frac{m \cdot v - A_1 - A_2}{F(t_{e2})}$$

The force-time relation is now fully captured and all sections could be plotted together in one figure, to create a graph similar to the one given previously, in Figure 4.14.

4.3 Comparison theoretical and empirical impact force

In this paragraph, the theoretical impact force, as determined in this MSc thesis, will be compared to the empirical impact force from the research by the CUR (1989 – 1).

Since the method in this MSc thesis results in just the peak force, it is most relevant to compare it only to the peak force in the force-time relation of the CUR report, which is given by:

$$F_{max} = \left(1.25 \cdot \alpha \cdot v^2 \cdot K^{\frac{2}{3}}\right)^{\frac{3}{5}}$$

Where $\frac{m_1}{2} \leq \alpha \leq m_1$, depending on the mobility of the stricken unit, as treated in the previous paragraph, and m_1 is the mass of the moving element.

The CUR found a value of K = 175 N/mm² for their test with diameter D = 420 mm, plus they determined that the contact parameter K for larger/smaller elements can be calculated from:

$$K_{e1} = 175 \cdot \frac{D}{420}$$

With D as the diameter in mm of the spherical element that was used in their tests.

Since the concrete armour units are not spherical, but more cubical, the spherical diameter will be converted into a cubical diameter, based on their volumes: $V_{sphere} = \frac{4}{3}\pi r^3 = \frac{\pi}{6} D_{sphere}^3$ and $V_{cube} = D_{cube}^3$, so $D_{sphere} = \sqrt[3]{\frac{6}{\pi}} \cdot D_{cube}$, where D_{cube} is equal to d_n for cubes, so:

$$K_{e1} = 175 \cdot \frac{d_n[mm] \cdot \sqrt[3]{\frac{6}{\pi}}}{420}$$

Since d_n is generally given in metres, this is rewritten to:

$$K_{e1} = 175 \cdot \frac{d_n[m] \cdot \sqrt[3]{\frac{6}{\pi}}}{0.420}$$

$$K_{e1} = 516.96 \cdot d_n[m]$$

Note that this is an empirical relation; K_{e1} [kN/mm$^{3/2}$] and d_n [m] do not have the same unit.

Now, for the comparison, it is important to try to get the two situations as close as possible, as it would otherwise be an unfair comparison. That is difficult though, due to the origin of both methods: the theoretical method observes an Xbloc®, while the empirical method observes a certain test setup. In order to align the two situations as much as possible, both are viewed as having a clamped stricken element, thus the velocity of block 2, $v_2 = 0$ m/s and the effective mass, $\alpha = m_1$. For the comparison, the spring of the bed is excluded, and the force is determined solely based on the stiffness of the leg. Furthermore, the elements are the same size and have the same impact velocity. A few plots are made, where the impact force is plotted against the impact velocity, for a certain block size, given in Figure 4.15 to Figure 4.17. A distinction is made between the spiky leg and the cubic leg of the Xbloc®s, since they result in different forces.

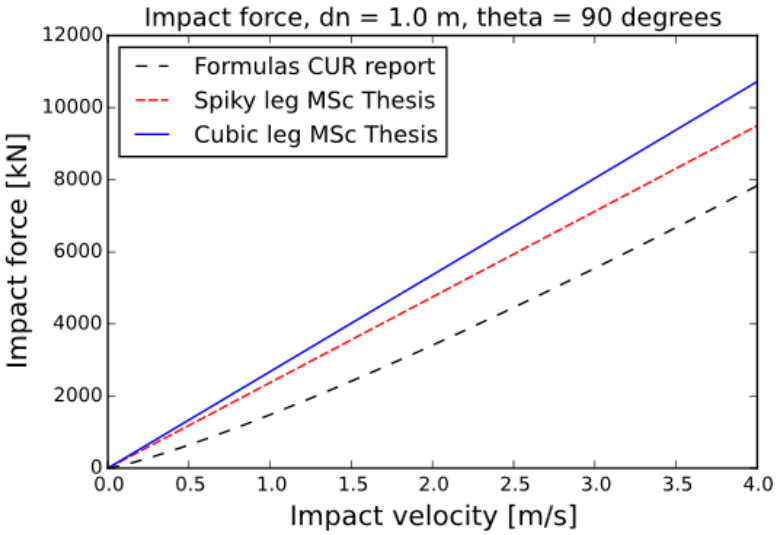

Figure 4.15: Comparison impact forces, dn = 1.0 m, θ = 90°

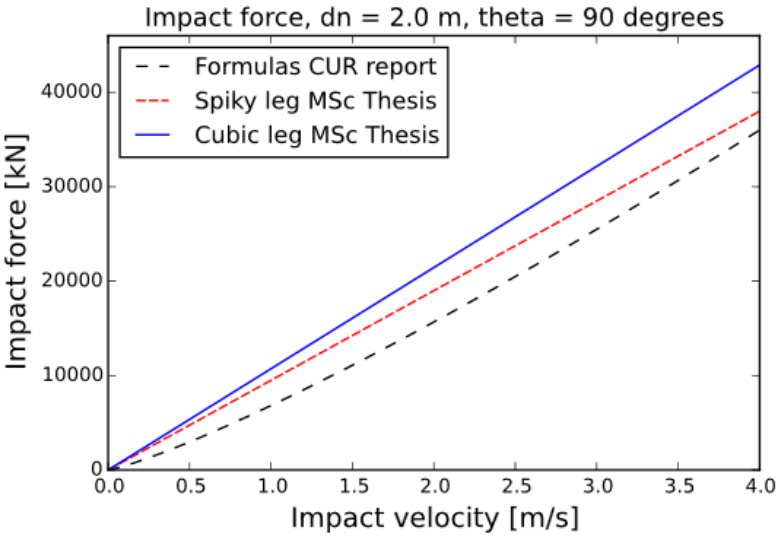

Figure 4.16: Comparison impact forces, dn = 2.0 m, θ = 90°

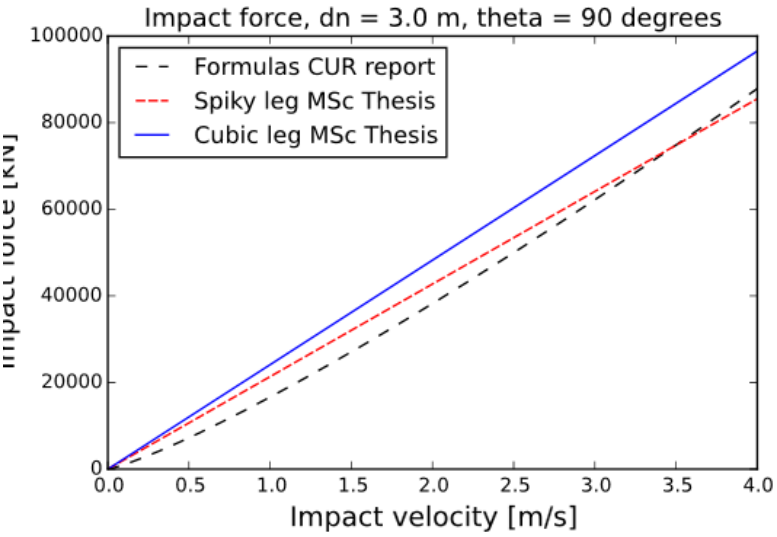

Figure 4.17: Comparison impact forces, dn = 3.0 m, θ = 90°

It is important to realise that the incoming angle of the force also has a large effect on the value of the force. The legs are much stiffer against compression than against bending, and it is generally said that “stiffer elements attract more of the load”, thus logically, if the leg is loaded in compression, it will attract a higher force, than when it is loaded in bending. This is visualised in Figure 4.18, where the impact force is plotted against the angle of the incoming force. Note: 0° is pure compression, 90° is pure bending. The force in case of pure compression is roughly twice as much as the force in case of pure bending.

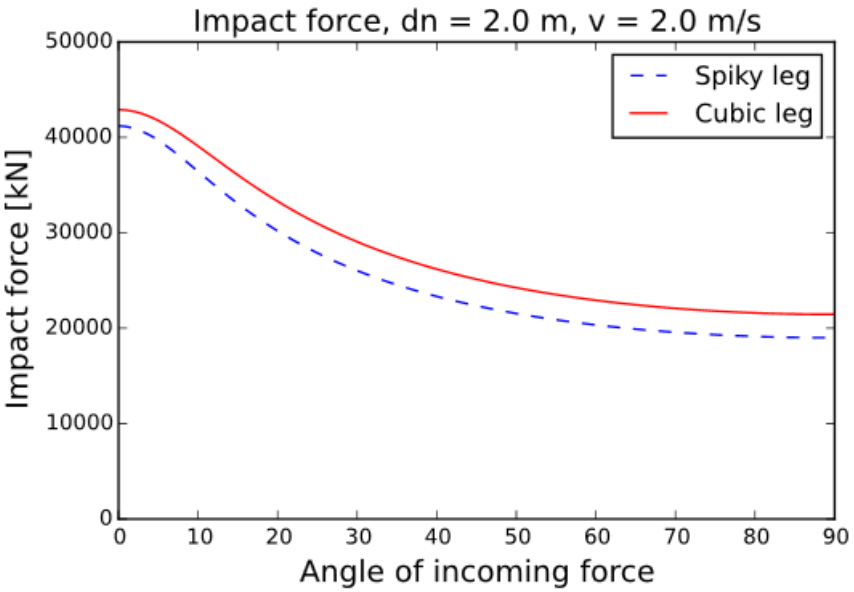

Figure 4.18: Impact force versus incoming angle

Conclusions

Based on Figure 4.15 to Figure 4.17, the theoretically determined impact force is generally higher than the empirically determined impact force from the CUR report. The theoretical and empirically determined values tend to be closer to each other for larger armour units, and also for larger impact velocities, which are luckily the most important regions, with larger chance of breakage. Still, the theoretically determined forces can get higher when changing the incoming angle of the force. This may seem problematic with respect to breakage, but higher forces occur when the legs are loaded more in compression, while compressive loads generally cause less trouble for concrete than bending and tension.

All in all, the theoretical forces are relatively high with respect to the empirical forces, but it is important to note that the situation is treated as if the stricken block is not going to move, since it is unknown how much of the kinetic energy of the moving block would be converted into kinetic energy of the stricken block. Though, it is likely that the stricken block will also move, which reduces the impact force. There is so much diversity in the force for different situations, that it is difficult to say that the force is determined correctly in this MSc thesis. However, what can be said, is that the force is at least in the right order of magnitude, based on the comparison with the CUR test results.

5. Failure

This chapter deals with determining whether a concrete unit will break or not. Failure is a matter of strength versus stresses, so those are important to determine. Though, first of all, it is important to identify the failure mechanism, in order to know which locations are critical, and in what way the concrete will fail. When the failure mechanism is known, the occurring stresses can be compared to the concrete strength, to predict concrete failure. The concrete strength is thus very important as well, so the second paragraph of this chapter is dedicated to finding a valid strength of concrete under impact loading. To conclude this chapter, it will shortly be described what the model results mean with regard to actually breaking the concrete armour unit.

5.1 Failure mechanisms

In this paragraph, several possible failure mechanisms of a concrete armour unit will be evaluated. This will be done for the case of an Xbloc®, but most failure modes are similar for other types of armour units. It is important to also keep in mind which failure mechanisms would have the most severe effect on the overall state of the breakwater, since failure of the concrete does not necessarily lead to failure of the breakwater as a whole. The stability of the armour units is governed by their weight and interlocking, so reducing the weight and interlocking. Furthermore, in nearly all cases, the legs of the Xbloc® are involved in the impact, not the body of the Xbloc®. Therefore, the observed failure mechanisms will be mainly focussed on the legs. A short description of each failure mechanism will be given, accompanied by an illustration to show what the failure looks like. To conclude, the critical failure mechanism will be identified.

5.1.1. Description of failure mechanisms

Local crushing due to compression

The impact between the armour units leads to a concentrated load. This will locally cause high compressive stresses, around the location of the impact. Due to the enormous weight of the large armour units, the concentrated loads can be so high that the local stresses exceed the concrete strength, and the concrete will be crushed. A small part of the concrete will be crumbled to pieces, as illustrated in Figure 5.1 and Figure 5.2. This will weaken the leg of the armour unit, but the loss of weight is minor, probably even negligible. The armour unit will still be able to interlock with the surrounding units as well, thus the effect on interlocking is also negligible. However, during a storm, multiple high waves will induce motion of the block in a similar way, thus it is probable that a block is repeatedly loaded at almost the same location. Repeatedly crumbling some of the concrete will hollow out the leg, until a larger piece of the leg will eventually break off, in which case the loss of weight could surely be significant. Local crushing will likely occur frequently, since the forces can be huge when a large block has a significant impact velocity, and the impact force is concentrated. However, it is not easy to estimate up front how likely the occurrence of more severe failure due to repeated loading would be.

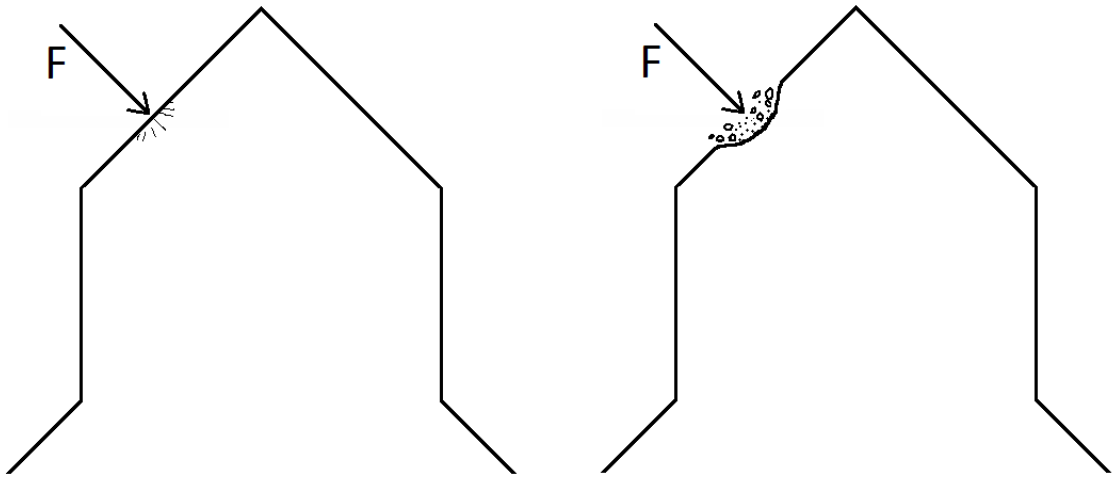

Figure 5.1: Schematisation of local crushing, spiky leg

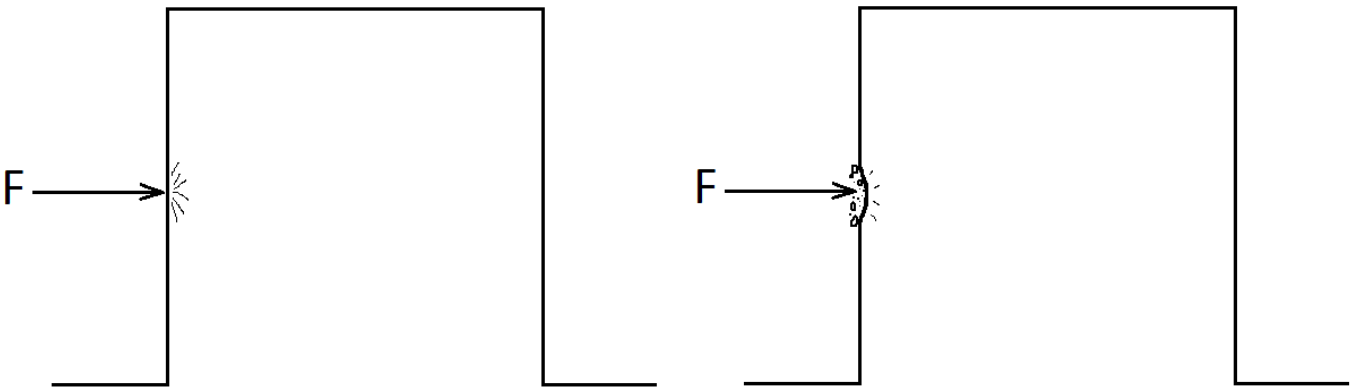

Figure 5.2: Schematisation of local crushing, cubical leg

Chipping off corners due to shear

When one of the legs is hit near the corner of the leg, under a specific angle, the impact induces a shear force, which locally leads to high shear stresses, since the effective area is small near the corner. The corner may then be chipped off, as illustrated in Figure 5.3 and Figure 5.4. The chipped piece has more weight than the previously observed crumbled concrete due to local crushing, but in most cases it is still a relatively small piece of the leg causing only a minor decrease of the weight of the armour unit. The interlocking capabilities will not be severely reduced either, by the loss of a corner. The likelihood of a corner being chipped off is rather large, if the force comes in at the right location and under the right angle. The situation of occurrence is thus very specific, so overall, it will probably not happen as frequent as local crushing.

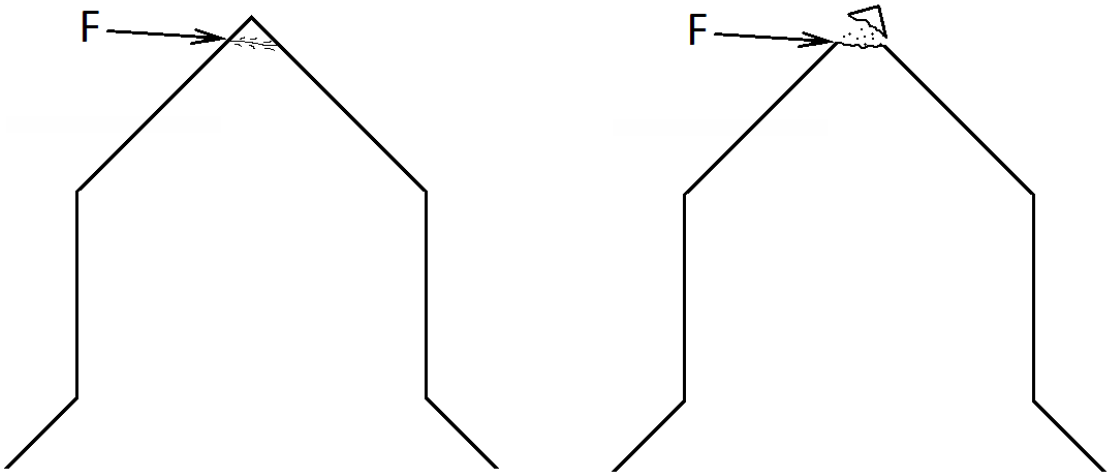

Figure 5.3: Schematisation chipped corner, spiky leg

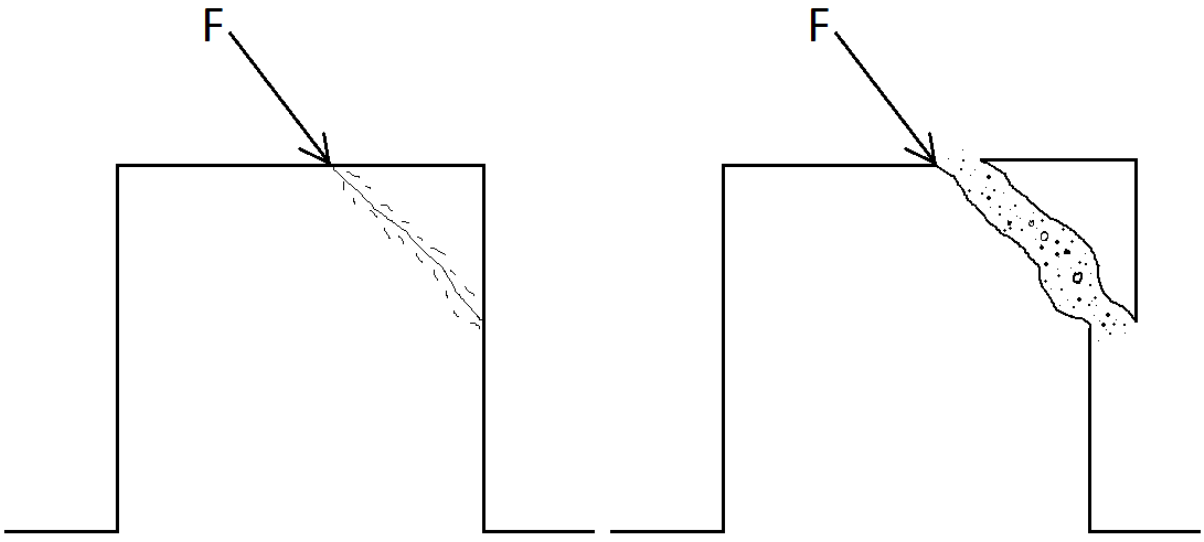

Figure 5.4: Schematisation chipped corner, cubical leg

Rupture of the leg due to bending

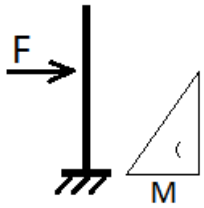

When regarding the leg as a cantilever beam, the impact force would induce a linear bending moment in the leg: zero at the location of the force, up till a maximum at the base of the leg, where it is attached to the body.

This bending moment may lead to cracks at the base of the leg, and due to the brittle behaviour of the concrete, the whole leg can be torn off, visualised in Figure 5.5 and Figure 5.6. This is the most severe failure mechanism, resulting in a significant loss of weight, while also losing a significant part of the interlocking capability. This type of failure is more likely to occur when the force acts on the upper part of the leg, such that it has a large arm, thus a large bending moment.

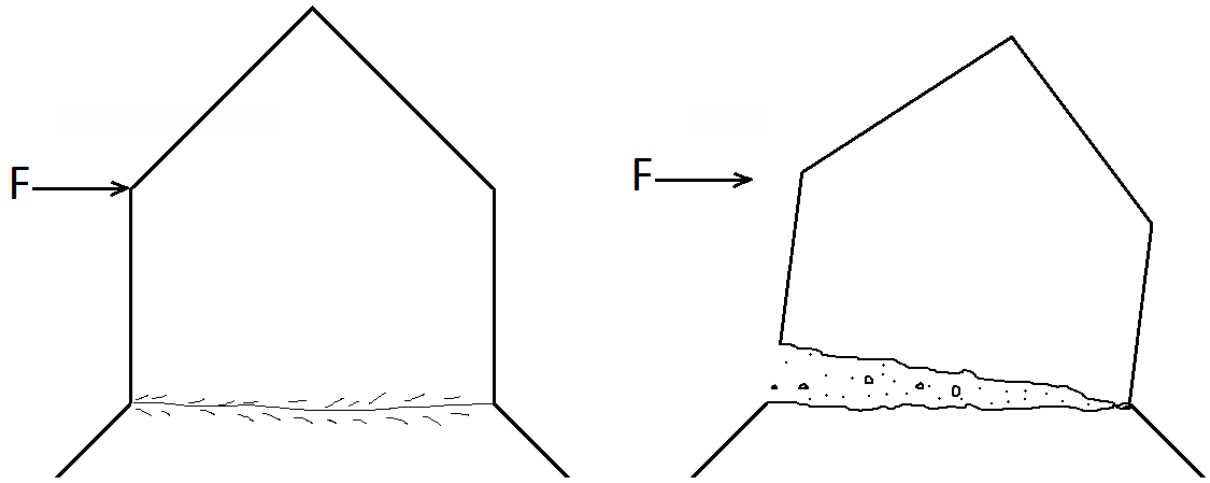

Figure 5.5: Schematisation ruptured leg due to bending, spiky leg

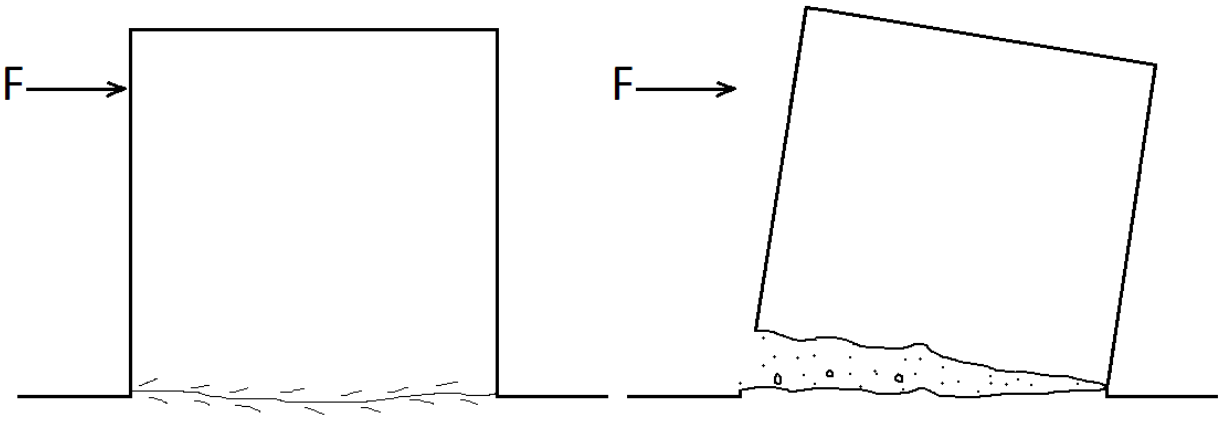

Figure 5.6: Schematisation ruptured leg due to bending, cubical leg

Rupture of the leg due to shear

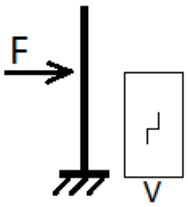

When regarding the leg as a cantilever beam, the impact force would induce a constant shear force in the leg, at the part of the leg between the force and the support.

From this visualisation though, the shear failure could happen at any plane between the force and the support. Since the shear force is constant, it will find its way to the weakest plane, where it will cause shear failure, thus complete rupture of the piece of the leg. Though, based on some photographs, for example the ones given in Figure 5.7, of broken breakwater armour pieces, rupture will normally occur at the base, and not somewhere halfway the leg, which could be an indication that rupture due to bending moments is governing.

Figure 5.7: Broken concrete armour units, Hofland et al. (2018)

Schematizations of rupture of the leg due to shear are given in Figure 5.8 and Figure 5.9.

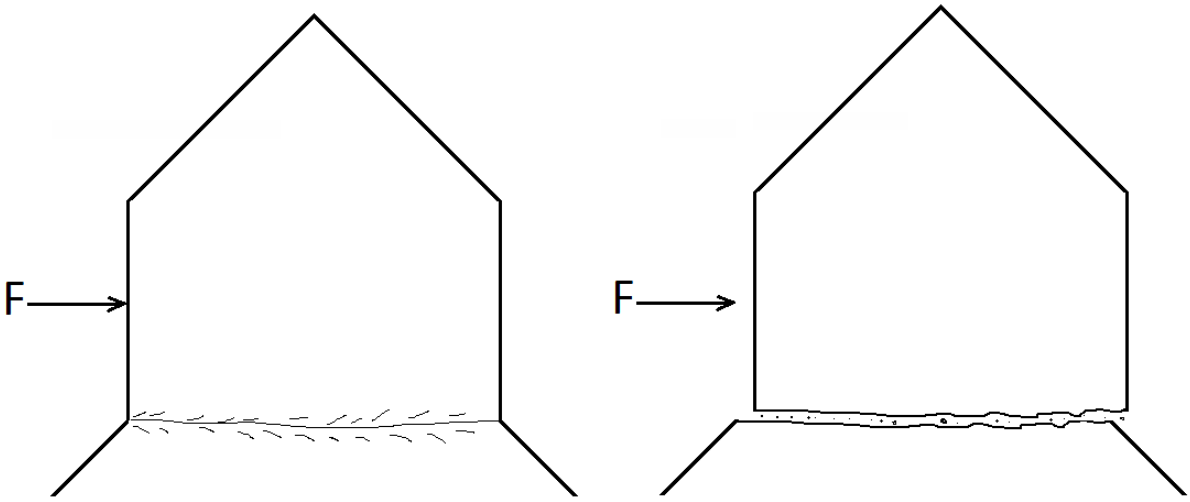

Figure 5.8: Schematisation ruptured leg due to shear, spiky leg

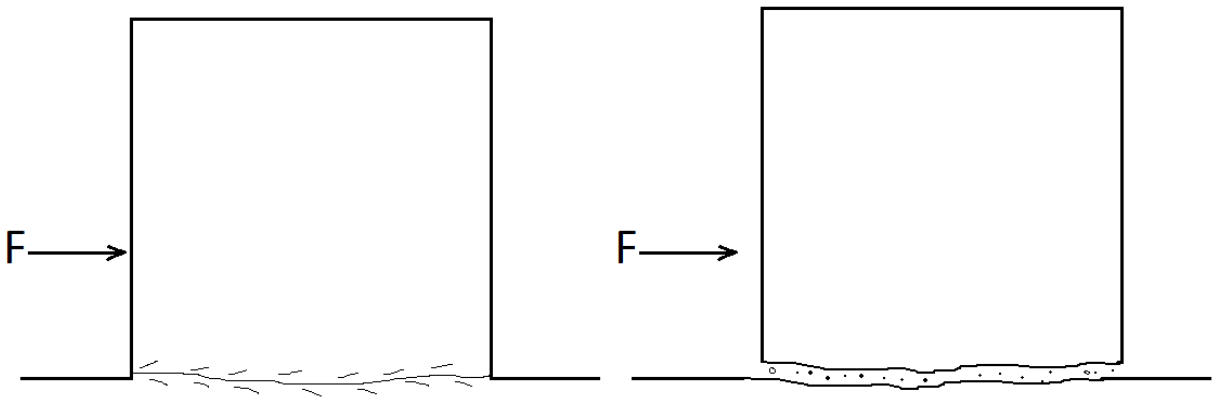

Figure 5.9: Schematization rupture leg due to shear, cubical leg

5.1.2 Discussion of critical failure mechanism

An overview of all failure mechanisms is given in Table 5.1.

Type of failure	Consequences	Likelihood of occurrence
Local crushing	Very minor weight loss, though repeated loading weakens the armour unit	Likely. The forces can be huge, causing locally high compressive stresses
Chipping off corners	Minor weight loss	Not very likely, since it only happens in very specific cases
Rupture due to bending	Severe weight loss	For large waves, and sufficient bending moment arm, it is quite likely to get bending failure, though this is likely only for a few percent of the blocks
Rupture due to shear	Severe weight loss	Unlikely, since rupture due to bending is governing in most cases

Table 5.1: Likelihood of occurrence and consequences of several failure mechanisms

Overall, rupture of the leg due to bending is the most interesting failure case to investigate, because it has severe consequences, plus a decent probability of occurrence. Rupture due to shear is potentially dangerous as well, but it is checked in Appendix C that shear over the full leg is normally not going to happen.

5.2 Concrete strength during impact load

Concrete is known to be stronger against short term loading than against long term loading. This effect is probably best known from creep, which causes the deflections to increase when a concrete member is loaded over a period of months or years. The opposite is also true: concrete has a higher strength against a very short impact load. The collision between two breakwater armour units is such a case of a short impact load. For this MSc thesis, it is thus important to take the impact strength of concrete into account, rather than the regular concrete strength.

The book Concrete Technology by Neville and Brooks (2010) shortly treats the impact strength of concrete. It is stated that there is no unique relation between the impact strength and the static strength of concrete. Instead, the impact strength depends among others on the type and size of aggregate, and on the storage conditions of the concrete. The impact strength of water-stored concrete is somewhat lower than when the concrete is dry, which is disadvantageous for breakwater armour units, with the abundance of water nearby. The aggregate affects the impact strength in multiple ways. Using angular aggregate with a rough surface gives a higher impact strength than using rounded aggregate with a smooth surface. Furthermore, using a smaller maximum size of the aggregate significantly improves the impact strength. Aggregate with a low modulus of elasticity and a low Poisson's ratio are also found to improve the impact strength.

This MSc thesis does not aim to find the best way to make concrete armour unit with a high impact strength, but rather to find a useable value for the impact strength, relative to the static strength values defined by the concrete classes. Neville and Brooks (2010) refer back to a German research by Popp (1977), where the relation between the compressive strength and the rate of loading was investigated. It was found that the strength increases greatly when the load is applied faster, leading to an impact strength that is more than double the strength at normal rates of loading, even roughly 2.5 times as large.

All in all, it is clear that there is not a single expression that can relate the impact strength to the static strength of concrete. In order to use the impact strength in this MSc thesis, a reasonable value must be estimated. Therefore, it is assumed that the impact strength of the observed concrete armour units is twice as large as the static strength.

$$f_{c,impact} = 2 \cdot f_c$$

Now, the probabilistic distribution of the concrete strength will be based on the commonly used characteristic strength and mean strength, illustrated in Figure 5.10. Most importantly, the deviation between characteristic strength and mean strength is $1.64 \cdot \sigma$.

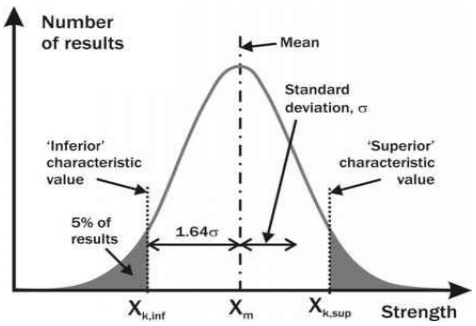

Figure 5.10: Characteristic strength and mean strength, Eurocode (n.d.)

In the standard concrete classes, for class C30/37, the mean tensile strength is $f_{ctm} = 2.9\ N/mm^2$, while the characteristic tensile strength is $f_{ctk0.05} = 2.0\ N/mm^2$. Therefore, the standard deviation can be estimated as: $\sigma = \frac{f_{ctm} - f_{ctk0.05}}{1.64} = \frac{2.9-2.0}{1.64} = 0.549\ N/mm^2$.

Since the impact strength is estimated as twice the static strength, the standard deviation will also be twice that of the static strength. Finally, the probabilistic distribution of the tensile impact strength is given by the following normal distribution:

$f_{ct,impact} = N\ (\mu = 5.8\ N/mm^2, \sigma = 1.098\ N/mm^2)$

5.3 Failure definition

This short paragraph is meant to explain what is regarded as failure of the concrete armour unit in this MSc thesis. The failure is very complex, while this MSc thesis uses a lot of assumptions and simplifications. It is therefore important to explain the actual meaning of the results of the model in this MSc thesis.

The stresses are determined in a linear elastic way. Therefore, it is possible to identify cases in which the linear elastic stresses exceed the strength of the concrete. In such cases, plastic deformations will occur, i.e. the concrete will start cracking. From that moment onward, the linear elastic models are no longer useful. In order to model plastic deformations, the stresses need to be determined by taking plasticity into account. That is something that is not done in this MSc thesis.

The results in this MSc thesis will therefore only show whether plastic deformations are expected to start, which is assumed to eventually lead to complete rupture of an armour unit leg. When the strength of the concrete is only barely exceeded by the determined stress, this might only result in a crack, and not in complete rupture of the leg at once. However, concrete armour units are loaded repeatedly during a storm. The movement of most of the armour units is prevented by its surroundings, but the ones that have sufficient movement space will likely experience multiple movements during a storm. Therefore, if the stresses exceed the strength to start cracks, it is likely that the stresses will exceed the strength again for the next large wave. This repeated loading weakens the concrete armour unit every time that the strength is exceeded, so it will eventually tear off the whole leg of the armour unit.

6. Stresses

The goal of this chapter is to find an expression to determine the maximum tensile stresses during the impact, which may lead to rupture of a leg of the armour unit. The starting point is to gain insight into the stress development in this leg, which is regarded as a deep beam. A better understanding of the behaviour helps to find an analytical expression for the stresses. A FEM model will be used to observe the stresses throughout the leg, and this can also be used to obtain the shape of the stress distribution at the critical location. Subsequently, a strut-and-tie model will be set up to represent the leg, from which a tie force is obtained at the same critical location. Now, an expression for the maximum tensile stress can be obtained, which can be implemented in the Monte Carlo simulation. The process covered in this chapter is visualised by a flow chart in Figure 6.1.

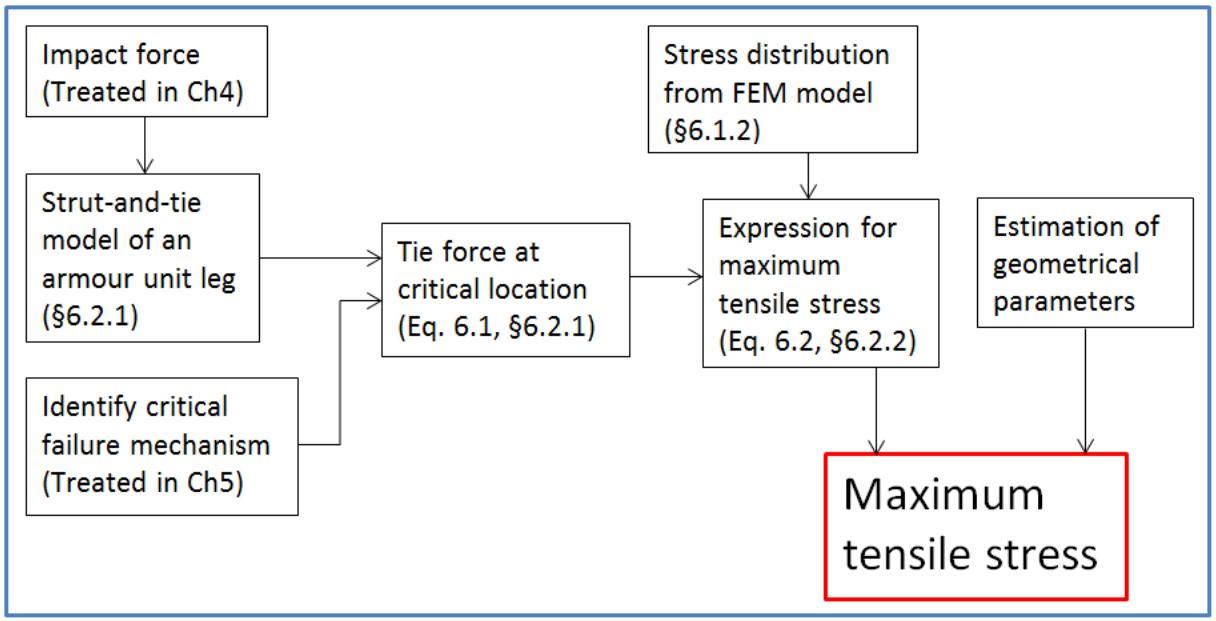

Figure 6.1: Flow chart chapter 6. Stresses

6.1 Behaviour of deep beams

The legs of an Xbloc® have a large depth with respect to their length, so they have to be treated as deep beams. The well-known formulas to determine the stresses in a beam are therefore not fully valid. Still, it is preferred to obtain a relatively simple equation to determine the maximum stresses in the beam, in order to incorporate it as the next step in Monte Carlo simulation of this MSc thesis. Therefore, an attempt is made to reduce the complex behaviour of a deep beam to a simple equation, that predicts the maximum stresses with acceptable accuracy.

6.1.1 Effect of depth to span ratio

The effect of the depth to span ratio on the behaviour of a beam is treated in an article by Patel, Dubey and Pathak (2014). They made several plots to show the stress distributions for various depth to span ratios of a simply supported beam, given in Figure 6.2 and Figure 6.3. Note that this situation differs from the cantilever beam that is treated in this MSc thesis, but it helps to understand the qualitative difference in stress development for deep beams.

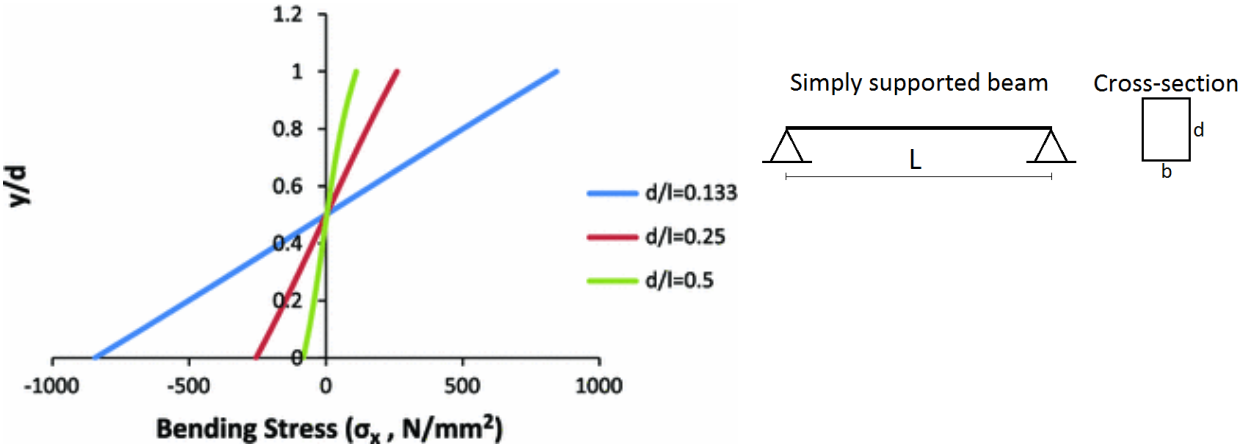

Figure 6.2: Bending stress distribution for a few depth to span ratios, Patel et al. (2014)

Figure 6.2 shows that the bending stresses are significantly lower in a deep beam (d/l=0.5) than in a regular beam (d/l=0.133). It is also clearly visible that the bending stress distribution is not linear over the beam depth, because the green line (d/l=0.5) is curved.

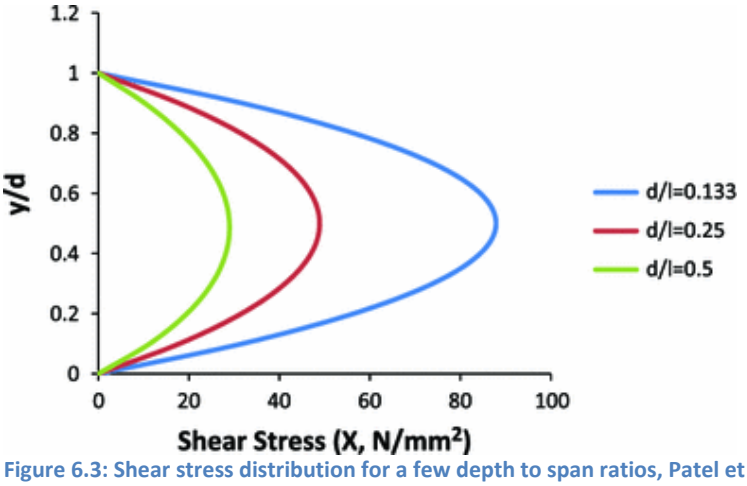

Figure 6.3: Shear stress distribution for a few depth to span ratios, Patel et al. (2014)

Figure 6.3 shows that the shear stress is also significantly lower in a deep beam than in a regular beam.

6.1.2. Finite-element model

In order to improve the understanding of the stress distributions in the legs of an Xbloc®, a finite-element model will be made using DIANA. The spiky leg and cubical leg will both be modelled, to check if they behave significantly different.

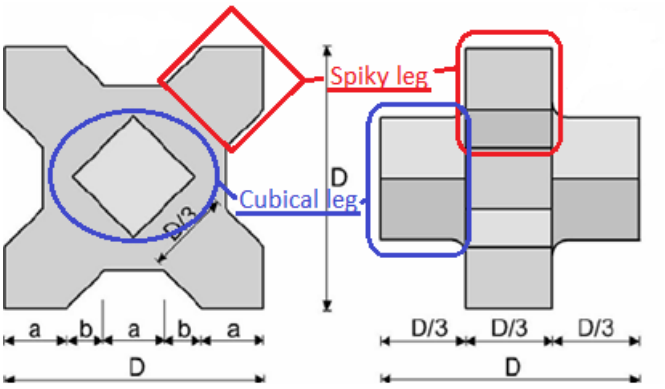

Figure 6.4: Xbloc® dimensions

A block of size D = 3 m will be modelled, to obtain a convenient value of D/3 = 1 m = 1000 mm. For both legs, the horizontal force has a value of 1000 kN and is applied at a height of 621 mm, to make it easier to compare them. First, the legs will be modelled with a clamped edge to the body. The relevant output of DIANA is shown in Figure 6.5 for a spiky leg, and in Figure 6.6 for a cubical leg. The applied force is drawn in these figures to make clear where the force was applied in the model.

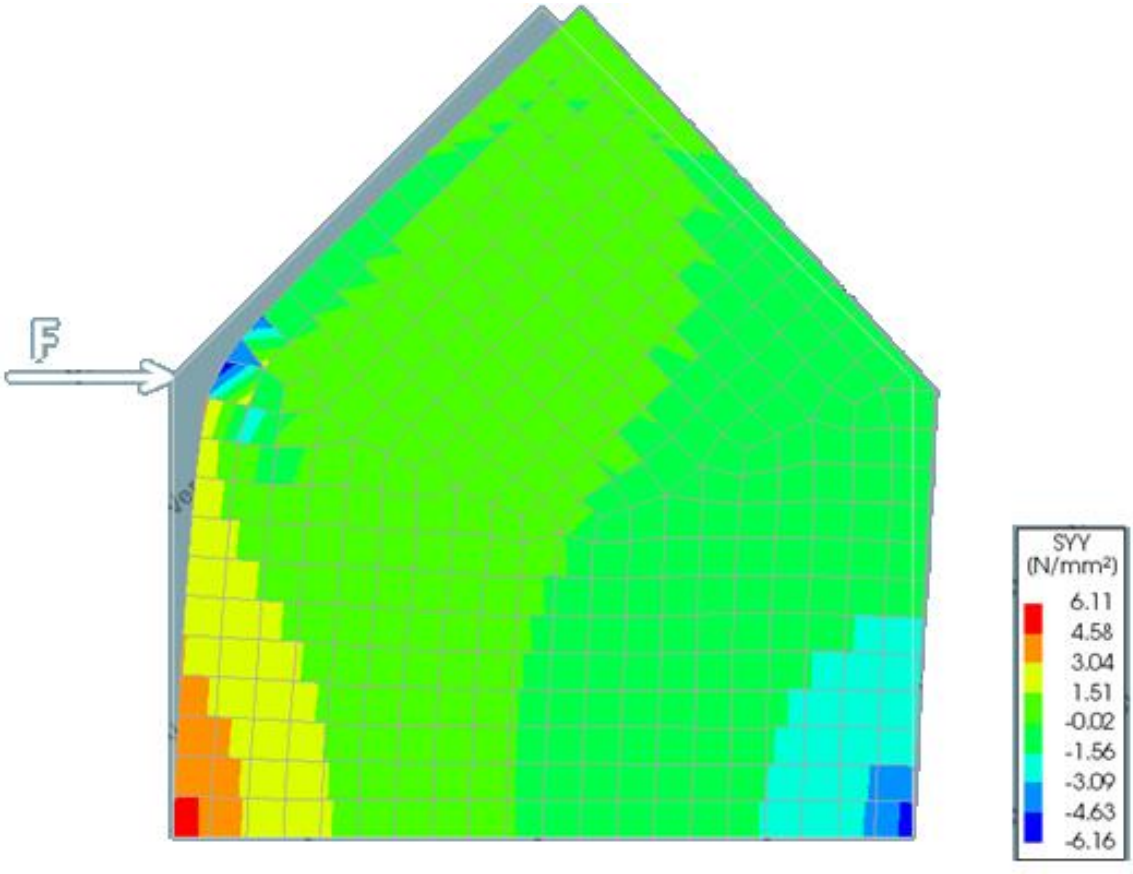

Figure 6.5: Finite element model, spiky leg, horizontal force at 621 mm

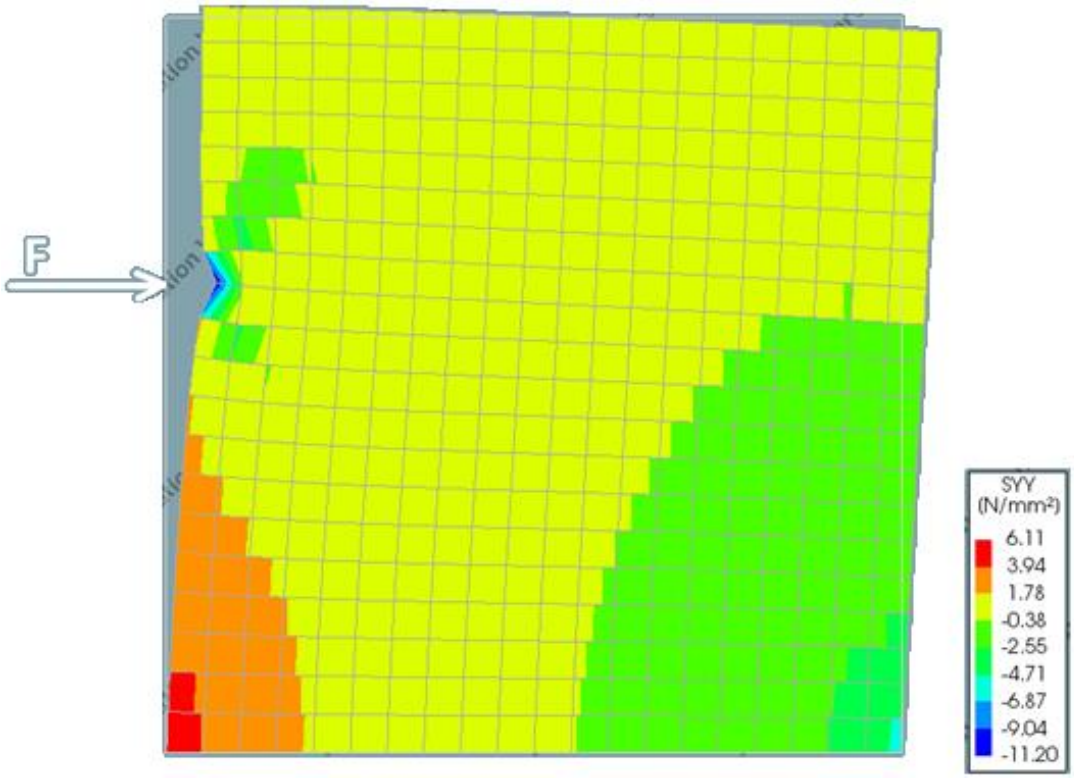

Figure 6.6: Finite-element model, cubical leg, horizontal force at 621 mm

It is also possible to obtain a table from DIANA with all the calculated values. This feature is used to obtain the stresses at the bottom of the leg, and the stress distribution at this edge is plotted in Excel, shown in Figure 6.7. Note that the stresses of the cubical leg are barely visible in this plot, because they are nearly identical to the stresses in the spiky leg. This leads to the belief that, when the force works on the lower part of the spiky leg, the behaviour is very similar to the cubical leg.

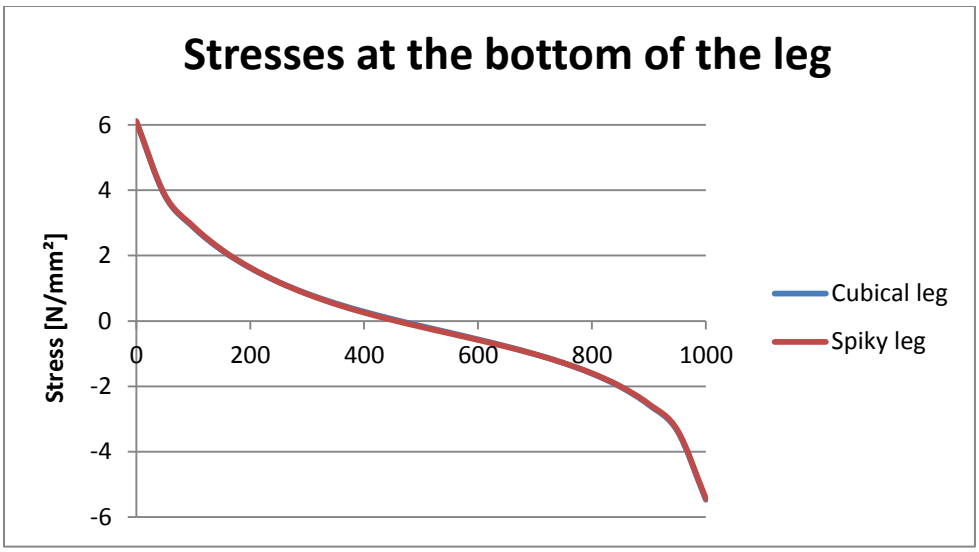

Figure 6.7: Stresses at the bottom of the leg

Note that the shape of the stress distribution obtained in Figure 6.7 is very similar to that of the bending stresses in a deep beam in Figure 6.2, by Patel et al. (2014).

To check the behaviour of the stresses into the body, another finite-element model check is performed, where the spiky leg is modelled with a part of the body. The result of this model is given in Figure 6.8, where it is nicely shown that there are high bending stresses at the junction of the leg to the body. This strengthens the belief that this is indeed the critical location, thus making it acceptable to check the stresses only on this location.

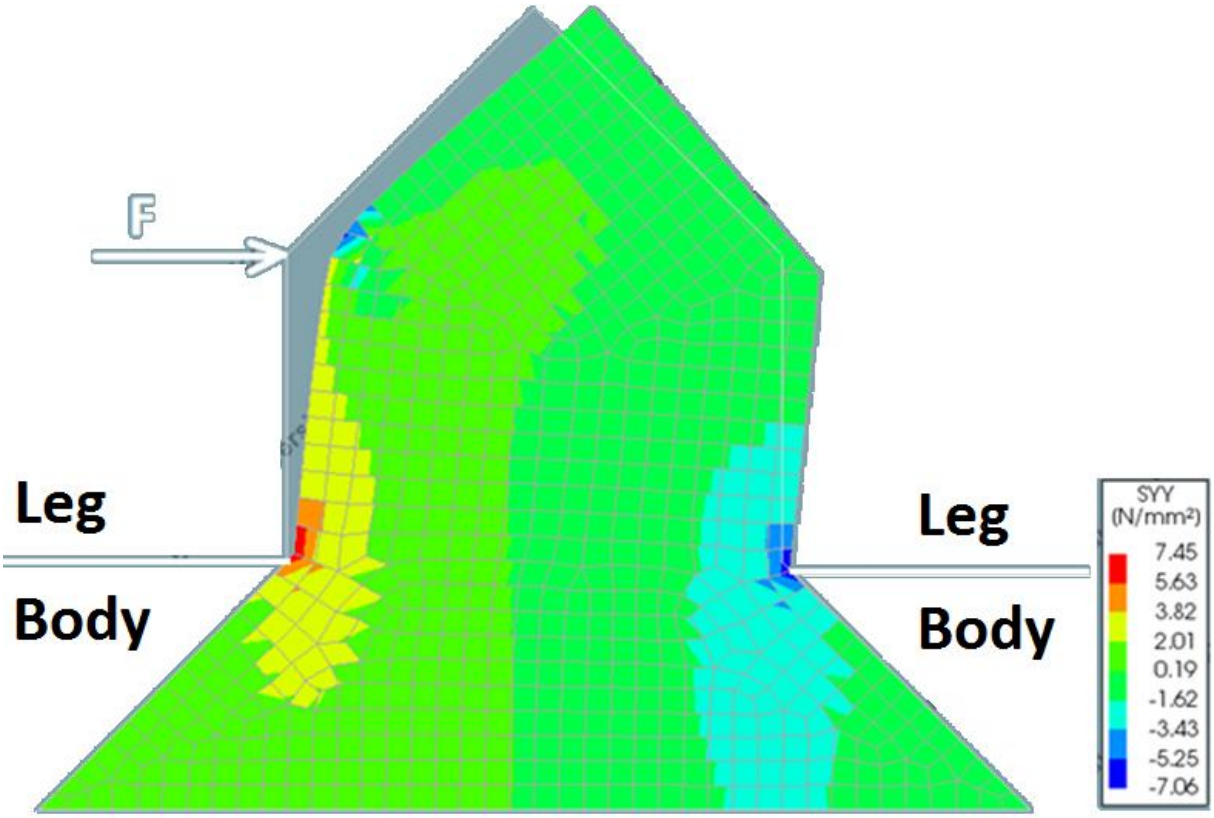

Figure 6.8: Finite element model, spiky leg with part of the body

6.2 Strut-and-tie model

This paragraph treats the determination of the maximum tensile stresses due to bending, via a strut-and-tie model. First, the strut-and-tie model will be set up. Then, the stresses will be determined from the force obtained from the strut-and-tie model. To conclude this paragraph, a quick validity check of the obtained stress equation will be performed.

6.2.1 Set up of strut-and-tie model

A strut-and-tie model is a method that can be used to determine the required amount and size of reinforcement in concrete structures that cannot be simplified as a beam or plate. An example of a strut-and-tie model in a concrete corbel is given in Figure 6.9. In the case of concrete breakwater armour units there is no reinforcement, but the obtained tensile force can be used to determine the stress distribution at a certain location, so the strut-and-tie method is still applicable.

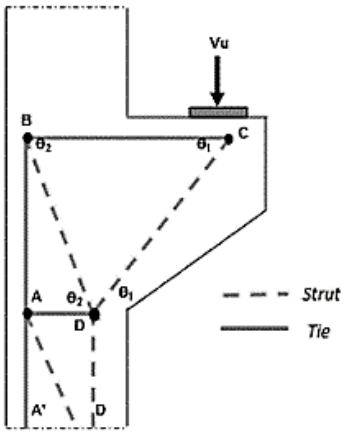

Figure 6.9: Example strut-and-tie model, Putri et al. (2018)

The strut-and-tie model that will be applied in the model in this MSc thesis is given in Figure 6.10. It is illustrated for the cubical leg, but the spiky leg will have a similar strut-and-tie model. The relevant location for determining the maximum tensile stress is highlighted in the lower left corner. Though the stress will only be determined in the leg, the strut-and-tie model is extended into the body, in order to reduce the importance of the choice of the supports, thereby reducing the error this choice causes. The force comes in under an angle, but can be decomposed in a horizontal and vertical component.

Note that this is a 2D representation with the force acting on the face of the leg. Oblique forces acting on the corner of the leg are therefore not included, though these are expected to mainly cause local failure of the concrete, instead of the more severe complete rupture of the leg.

It is commonly used in design practice that the angle of the concrete compressive strut must be between 21.8° and 45°, which is for example stated in the book 'Constructieleer Gewapend Beton', by Braam and Lagendijk (2011). The strut-and-tie model with a double layer, depicted at the left in Figure 6.10, is thus actually not valid when the force acts at a location near the base of the leg, since the angle would be too small. Therefore, it is opted to create a strut-and-tie model with a single layer, depicted at the right in Figure 6.10, which will be used in cases with a force acting near the base of the leg.

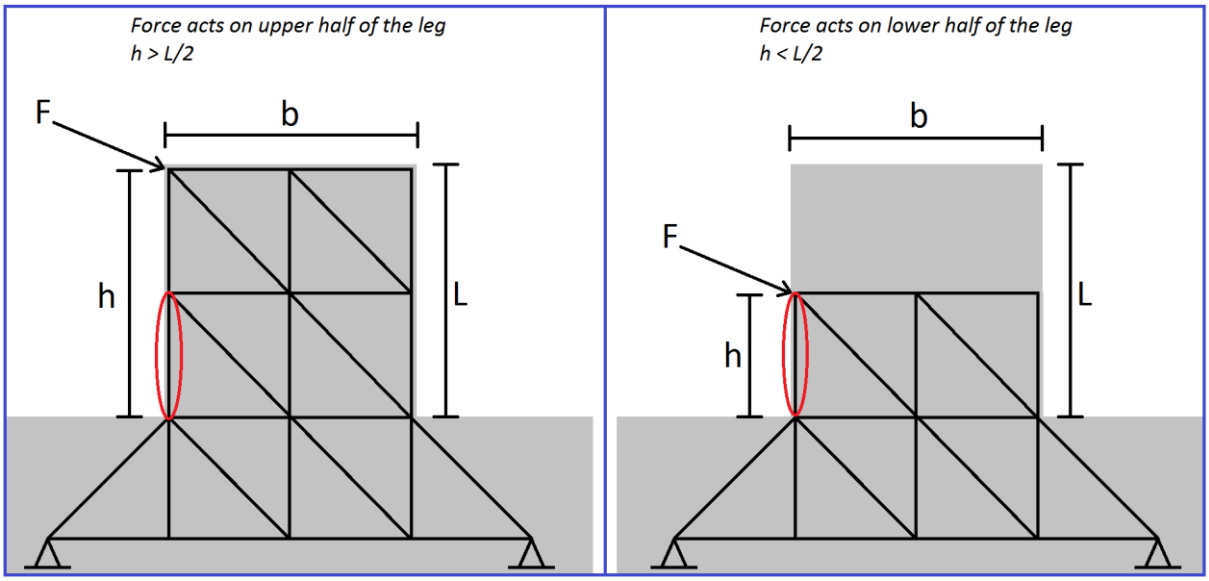

Figure 6.10: Strut-and-tie model in the cubical leg

Solving the strut-and-tie model can be done by setting up the equations for horizontal and vertical equilibrium for each of the nodes. The reaction forces in the supports can normally be solved by the outer equilibrium. However, since the system is statically indeterminate, it is more difficult to solve by hand.

Luckily, there is no need to solve it by hand, because there are nifty computer programs like MatrixFrame that are able to solve the bar forces in such systems. As an example, the double layer strut-and-tie model as it looks like in MatrixFrame is given in Figure 6.11, where tension is positive and compression is negative. A similar model can be made in MatrixFrame for the single layer strut-and-tie model.

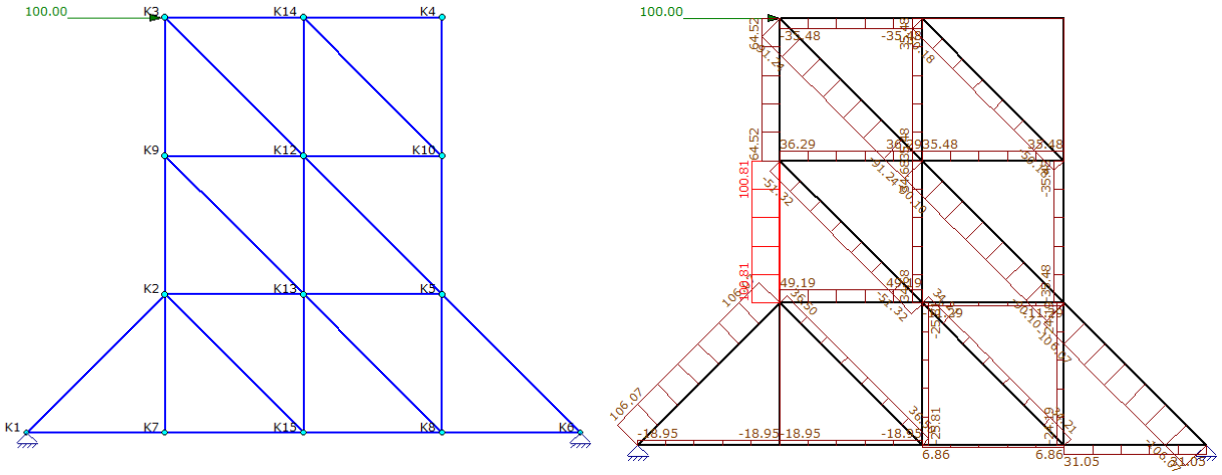

Figure 6.11: MatrixFrame input and results (tension is positive)

The model in MatrixFrame is ran for various heights of the acting force, in order to obtain an expression that is valid for random incoming forces. Since there is a different model when the force acts on the lower half of the leg, there is a slight deviation in the results there, as visible in the dashed line in Figure 6.12. Still, it is possible to fit a line that is a good approximation for both the single- and double layer model. This approximation is plotted in Figure 6.12 with the red line, and is given by:

$$N = \left(\frac{h}{b}\right)^{0.9} \cdot F_H - F_V$$ Equation 6.1

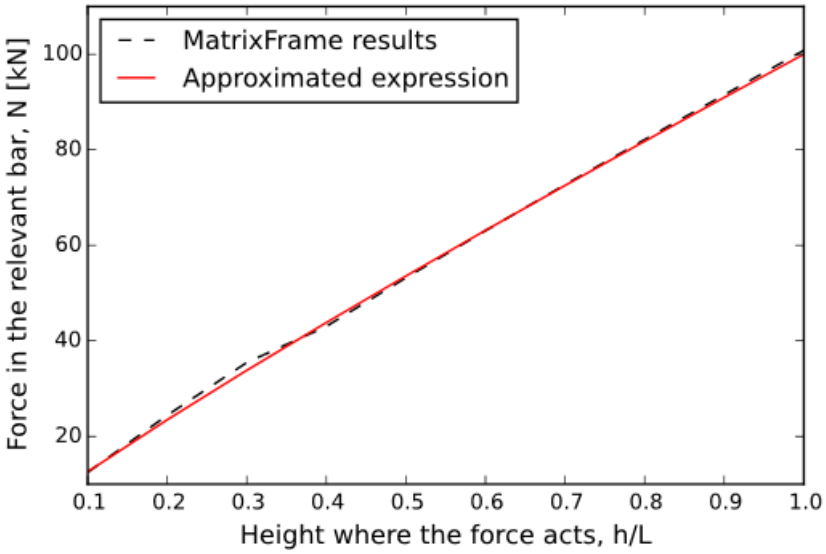

Figure 6.12: Comparison exact MatrixFrame results with the approximated expression

6.2.2 Stresses from the strut-and-tie model

Based on the force obtained from the strut-and-tie model, an equation to approximate the maximum tensile stress will be created. To do so, a stress distribution has to be determined. The stresses will be calculated from a linear distribution, even though it is earlier (in Figure 6.2 and Figure 6.7) already seen that the stress distribution over the depth of the cross section is curved, because of the deep beam behaviour. Therefore, a correction will be applied to compensate for this error.

To determine the correction needed, a linear approximation will be added to the graph of Figure 6.7. In this approximation, it is important to keep the integral of the stresses equal, such that the resulting force is equal. The integral of the positive part of the nonlinear curve is calculated numerically. This is set equal to the integral of the linear approximation, which is calculated as the area of the triangle. The linear approximation has a maximum tensile stress of $\sigma_{max,linear} = 3.5\ N/mm^2$, while for the nonlinear curve: $\sigma_{max,nonlinear} = 6.11\ N/mm^2$. Again, note that their area under the graph is equal, over the positive part of the stresses.

Based on this evaluation, by calculating the stresses in a linear way, a correction of $6.11/3.5 = 1.75$ is needed. This factor is visualised in Figure 6.13, where the y-axis of the graph is normalized.

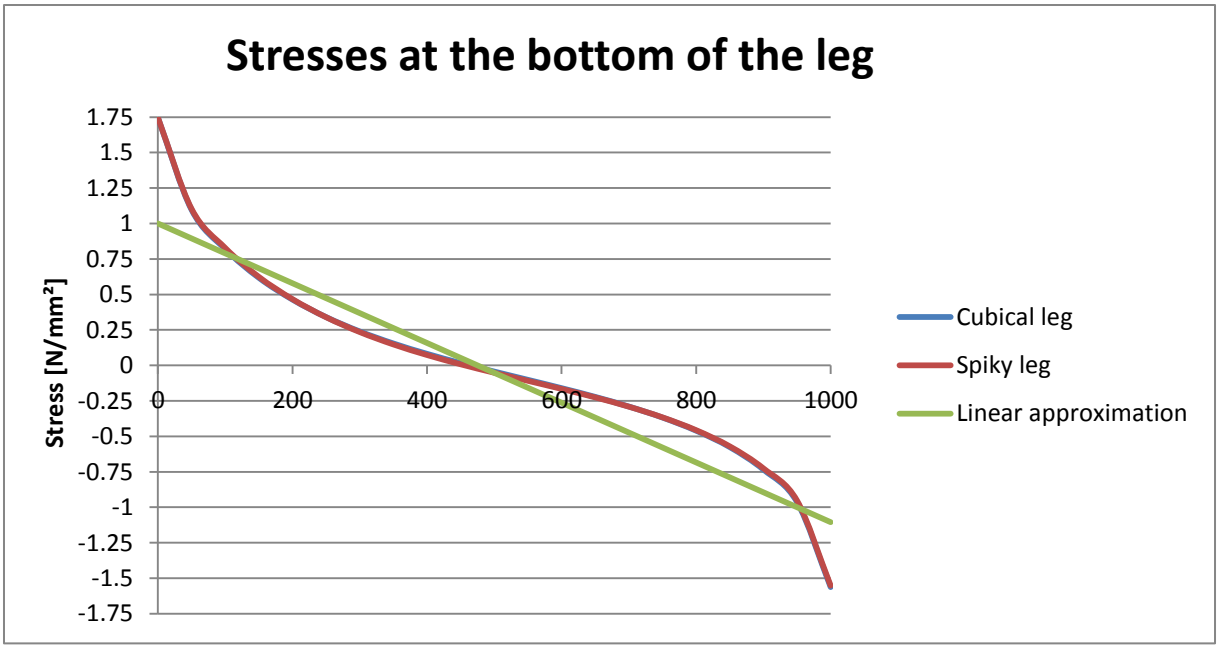

Figure 6.13: Normalized graph to show the correction factor for nonlinearity

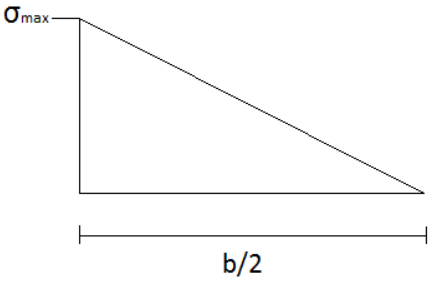

The calculation of the stresses will thus at first be based on a linear distribution, for which the resulting force can be calculated as the stress integrated over the area:

$$F_{stress} = \sigma_{avg} \cdot A = \frac{\sigma_{max}}{2} \cdot \frac{b}{2} \cdot width$$

For the squared cross section of the Xbloc® legs, $width = b$, which has a dimension of $D/3$:

$$F_{stress} = \frac{\sigma_{max} \cdot b^2}{4} = \frac{\sigma_{max} \cdot \left(\frac{D}{3}\right)^2}{4} = \frac{\sigma_{max} \cdot D^2}{36}$$

The resulting force of the stresses is equal to the force in the bar of the strut-and-tie model, which was determined as: $N = \left(\frac{h}{b}\right)^{0.9} \cdot F_H - F_V$

$$F_{stress} = N$$

$$\frac{\sigma_{max} \cdot D^2}{36} = \left(\frac{h}{b}\right)^{0.9} \cdot F_H - F_V$$

Now, add the previously determined correction factor for nonlinearity of 1.75, and rewrite it to d_n via $D = 1.443 \cdot d_n$ to finally obtain Equation 6.2. In this equation, F_H and F_V are in *N* and d_n is in *m*, so $\sigma_{t,max}$ follows in N/m^2.

$$\sigma_{t,max} = 30.3 \cdot \frac{\left(\frac{h}{b}\right)^{0.9} \cdot F_H - F_V}{{d_n}^2}$$

Equation 6.2

6.2.3 Validity check

A validity check of the obtained stress relation is performed by comparing it to a stress calculation via slender beam theory. For a regular slender beam, the following equations to determine the bending stresses are used:

$$M = F \cdot arm \qquad \sigma_{max} = \frac{M}{\frac{1}{6}bh^2}$$

The two methods to determine the stresses are plotted in the same graph, shown in Figure 6.14.

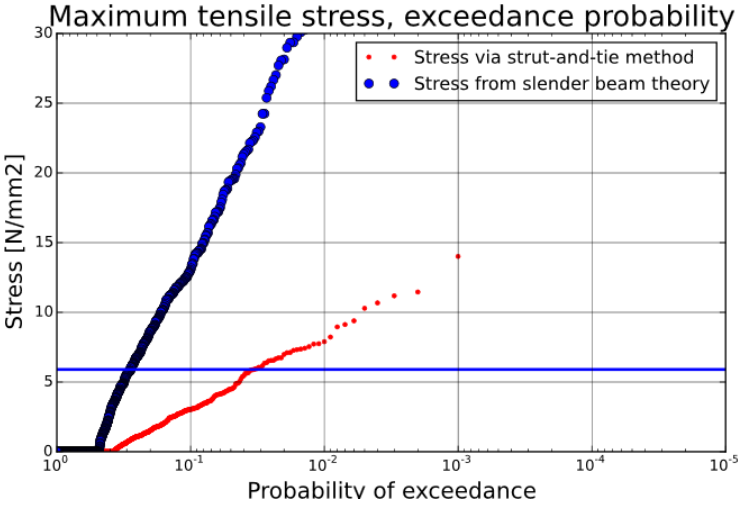

Figure 6.14: Comparison stresses from strut-tie model with slender beam theory

It is earlier noted that the stresses in a deep beam are much lower than in a regular beam, back in Figure 6.2, in paragraph 6.1.1 Effect of depth to span ratio. Now, Figure 6.14 clearly shows that the stresses from the strut-and-tie method are indeed much lower than the stresses from slender beam theory, as expected. Though, keep in mind that this is no solid proof that the values are actually correct, but it does show that it is at least in the expected range.

7. Final model

In this chapter, all individual parts of the model will be put together. First, the full methodology will be given, recapping the earlier determined individual parts of the model. Subsequently, the results of the model will be presented for a few cases, and the outcome will be discussed. To conclude this chapter, a sensitivity analysis will be performed, to identify the most important parameters and variables.

7.1 Presenting the complete model

The model requires the significant wave height H_s and the armour unit diameter d_n as input, while all other variables follow from these inputs, or were determined separately when the model was made. The model takes a random set out of the stochastic variables, to capture one specific situation with a certain wave acting on unit with a certain position. The model will then consecutively determine the impact velocity, the impact force, and the stresses at the critical location, to assess whether the concrete will crack. This simulation is carried out multiple times via a Monte Carlo simulation, resulting in exceedance probabilities and a failure percentage. The estimated values of the parameters and variables are given in the appropriate tables later in this section. A flow chart of the whole model is give in Figure 7.1, and shows which parameters and variables are needed in each step.

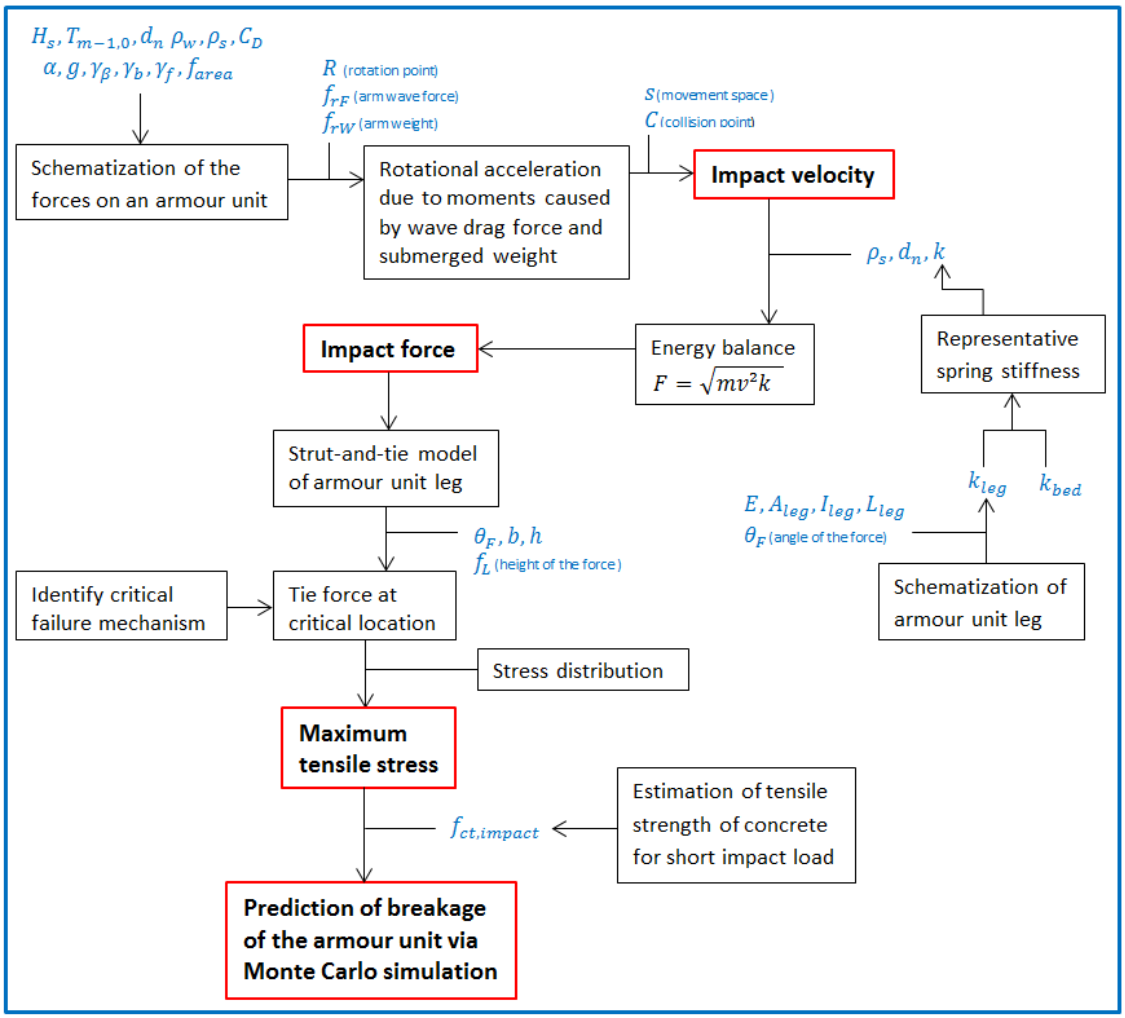

Figure 7.1: Flow chart of the whole model

Impact velocity

The first step in the model is to determine the impact velocity. This will be done by the following formula, that is based on the rotation of an armour unit due to the wave drag force. It is derived in chapter 3

$$v = f_{cor} \cdot \sqrt{2s\left(k_1 \frac{C_D u^2}{(\Delta+1)d_n} - k_2\left[1 - \frac{1}{\Delta+1}\right]g\right)} \qquad \text{Equation 3.1}$$

Where:

- f_{cor} is an empirical factor that corrects for the invalid assumption of constant acceleration, established in Appendix B as: $f_{cor} = 1 - \frac{\sqrt{s}}{4}$, for Xbloc®
- s is the available space between the blocks, i.e. the distance a block travels before it hits another block
- C_D is the drag coefficient of the armour unit
- u is the velocity of the water during run-up, determined as: $u = \sqrt{2g(R_u - z_A)}$, where z_A is the location on the slope relative to still water level, so $z_A = 0$ at the waterline, and run-up level R_u is determined by $\frac{R_{u2\%}}{H} = 1.75 \cdot \gamma_b \cdot \gamma_f \cdot \gamma_\beta \cdot \xi_{m-1,0}$
- d_n is the nominal diameter of the armour unit
- H_s is the significant wave height
- Δ is the relative density, $\Delta = \frac{\rho_s - \rho_w}{\rho_w}$, here: $\rho_s = 2400\ kg/m^3$, $\rho_w = 1025\ kg/m^3$
- g is the gravitational acceleration of 9.81 m/s²
- k_1 and k_2 are dimensionless variables, included to consider all the dimensionless parameters that are taken into account in the model.

These dimensionless factors are defined as:

$$k_1 = \frac{\frac{1}{2} \cdot f_{area} \cdot f_{rF} \cdot f_{hit}}{f_{inertia}} \qquad \text{and} \qquad k_2 = \frac{f_{rW} \cdot f_{hit}}{f_{inertia}}$$

Where:

- f_{area} is the fraction of the area that is subjected to the drag force, a fraction of d_n^2. For example if the affected area is $0.5d_n^2$, then $f_{area} = 0.5$
- f_{rF} is the arm of the wave force to the rotation point, as a fraction of d_n.
- f_{hit} is the distance of the collision point C to the rotation point R, as a fraction of d_n.
- $f_{inertia}$ is the dimensionless part of the mass moment of inertia, as $I = f_{inertia} \cdot m \cdot {d_n}^2$, where $f_{inertia}$ is then dependent on the type of armour unit and the rotation point
- f_{rW} is the arm of the weight to the rotation point, as a fraction of d_n.

Values and distributions for all of the parameters and variables that are needed to determine the impact velocity are given in Table 7.1.

	Values
Constants	
Mass density water, $\rho_w[kg/m^3]$	1025
Mass density concrete, $\rho_s\ [kg/m^3]$	2400
Slope angle, α	$3V:4H$
Berm coefficient, γ_b	1.0
Roughness coefficient, γ_f	0.45
Oblique wave coefficient, γ_β	1.0
Drag coefficient, C_D	1.20
Variables	
Arm of the wave force, f_{rF}	$0.96 + \sin(\alpha) \cdot R$
Arm of the weight, f_{rW}	R
Inertia factor, $f_{inertia}$	$0.7783 + R^2$
Stochastic variables	
Rotation point, R	Normal distribution: $N(\mu = 0\,; \sigma = 0.144)$
Movement space, s	Adjusted exponential distribution: $0 \quad for\ 50\%\ of\ the\ cases$ $Exp(\lambda = 0.0408) \quad for\ the\ other\ 50\%\ of\ the\ cases$
Collision point, f_{hit}	Uniform distribution: $U(\min = 0.58\,; \max = 1.44)$
Area subjected to wave, f_{area}	Normal distribution: $N(\mu = 0.381\,; \sigma = 0.083)$
Individual wave height, $H\ [m]$	Rayleigh distribution: $\sqrt{-\frac{1}{2}\ln\left(p(\underline{H} > H)\right)} \cdot H_s$
Spectral wave period, $T_{m-1,0}[s]$	Correlation with wave height: $\sqrt{5 \cdot H} + (H + 3) \cdot U(\min = 0, \max = 1)$

Table 7.1: Parameters and variables to determine the impact velocity

Impact force

The second step is to determine the impact force, using the previously calculated impact velocity. The impact force is based on an energy balance between the kinetic energy of a moving armour unit and the elastic energy absorbed by the stricken armour unit and the gravel bed. The following formula is derived in chapter 4:

$$F = \sqrt{m_1 v_1^2 k - m_2 v_2^2 k} \qquad \text{Equation 4.1}$$

Where:

- m_1 is the mass of object 1, the moving armour unit, $m_1 = \rho_s d_n^3$
- v_1 is the velocity of object 1 at the moment of impact
- k is the representative spring stiffness of the leg of the armour unit and the gravel bed
- m_2 is the mass of object 2, the stricken armour unit, and is equal to m_1
- v_2 is the velocity of object 2, which can be left out when it is unknown how much of the energy is converted into kinetic energy, reducing the formula to: $F = \sqrt{m_1 v_1^2 k}$

The representative spring stiffness is determined from the individual stiffness of the leg of the armour unit and the leg, which is regarded as a system in series, such that:

$$\frac{1}{k} = \frac{1}{k_{leg}} + \frac{1}{k_{bed}}$$

$$k = \frac{1}{\frac{1}{k_{leg}} + \frac{1}{k_{bed}}}$$

With: $k_{leg} = \frac{1}{\sqrt{\frac{\cos^2\theta_F}{\left(\frac{EA}{L}\right)^2} + \frac{\sin^2\theta_F}{\left(\frac{3EI}{L^3}\right)^2}}}$ and $k_{bed} = 69.4 \cdot 10^6 \cdot d_n^2$

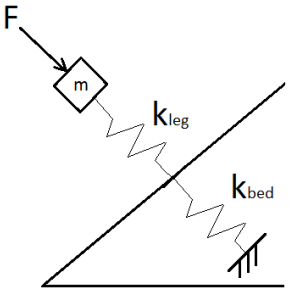

The parameters and variables required to determine the impact force are given in Table 7.2.

	Values
Parameters	
Young's modulus concrete (class C30/37), $E\ [N/mm^2]$	32837
Variables	
Area of the cross section, $A\ [m^2]$	$0.2297 \cdot d_n^2$
Area moment of inertia of the cross section, $I\ [m^4]$	$0.004461 \cdot d_n^4$
Full length of the leg, $L_{leg}[m]$	Spiky leg: $0.540 \cdot d_n$ Cubical leg: $0.481 \cdot d_n$
Stochastic variables	
Incoming angle of the force, $\theta_F[°]$	Special probabilistic distribution: $cdf = \frac{\theta_F^2}{8925}$, $for\ 0 \le \theta_F \le 85$ $0.1 \cdot \theta_F - \frac{\theta_F^2}{2100}$, $for\ 85 < \theta_F \le 105$
Location of the collision on the armour unit leg, relative to the leg length, i.e. the distance between the acting point of the force and the junction of the leg with the body, $f_L\ [1/d_n]$	Special probabilistic distributions: Spiky leg: $U(-0.1\,;0.9)$ but set all negative Cubical leg: $U(-0.4\,;0.6)$ values to zero
Tensile impact strength (class C30/37, $f_{ct,impact}\ [N/mm^2]$	Normal distribution: $N\ (\mu = 5.8\,, \sigma = 1.098\,)$

Table 7.2: Parameters and variables to determine the impact force and the stresses

Stresses

The final step is to determine the stresses due to the impact, and compare this to the impact strength of the concrete. Tensile failure due to bending is identified as the most important failure mechanism. The formula for the maximum tensile stresses is derived in chapter 6, given by:

$$\sigma_{t,max} = 30.3 \cdot \frac{\left(\frac{h}{b}\right)^{0.9} \cdot F_H - F_V}{{d_n}^2} \qquad \text{Equation 6.2}$$

With: $F_H = \sin\theta_F \cdot F$ and $F_V = \cos\theta_F \cdot F$

$$h = (1 - f_L) \cdot L_{leg}$$

$$b = \frac{D}{3} = 0.481 \cdot d_n$$

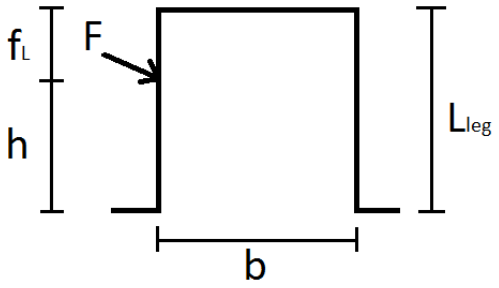

The parameters and variables required to determine the stress are given above, in Table 7.2.

7.2 Discussion of model assumptions and uncertainties

This paragraph is meant to give a recap of the most important assumptions, uncertainties and drawbacks in the model. It will be discussed how severe these are, starting by the assumptions in each step of the model, finalising by giving a list of uncertainties in parameters and variables.

The starting point of the model is the schematization of the forces acting on an armour unit. This is a 2D representation, where the wave drag force and the submerged weight of the unit are the relevant forces. The wave drag force is calculated with the fluid velocity around the water line, based on the run-up velocity. Note that for units above the waterline, the local fluid velocity will be smaller, resulting in a smaller wave drag force. Now, using the aforementioned forces, the acceleration of the armour unit is determined for a pure rotation, so no translation is considered. Rotation is generally considered to be the main movement, which is recently confirmed by Caldera (2019). To derive a formula for the impact velocity, it was first assumed that the acceleration is constant, which is actually not true. Therefore, a correction factor is established, to reduce this error.

With the impact velocity as input, the impact force is determined, based on an energy balance. This balance sets the kinetic energy of the moving unit equal to the potential energy in the form of a spring energy. Two possibly important components that are not included are the kinetic energy of the stricken unit, and the energy losses due to local crushing of the concrete and other sources of damping. These components would reduce the impact force, so it is conservative, but they are neglected because they are difficult to quantify without a detailed investigation. Also note that the damping due to local crushing is expected to decrease per loading cycle, which reduces the error of the model. The impact force is thus determined from the potential energy in the form of a spring energy, for which a representative spring stiffness must be determined. This spring stiffness is determined from two springs in series: a spring to represent the breakwater bed, and a spring to represent the stiffness of the armour unit leg against a combination bending and compression.

The impact force is then used as input to determine the tensile stresses at the base of the leg of the armour unit, based on a 2D schematization with the force acting on the face. Forces acting on the corners are not considered, though they are expected to mainly cause local failure, which is less severe than total rupture of the leg, the most important failure mechanism, as identified in chapter 5. Rupture to due bending is the only failure mechanism that is implemented in the model, though other failure mechanisms like local crushing and chipped off corners may happen as well, but these are less severe for the overall state of the breakwater. Now, to determine the stresses, the armour unit leg is regarded as a deep beam, for which strut-and-tie models are commonly used in design practice. However, this is usually done to determine the tensile force that must be taken by the reinforcement steel. In this case, this tensile force is used to determine the maximum stresses, based on a stress distribution that is obtained via a finite-element model. It is important to realise that some choices in the set-up of the strut-and-tie model, such as the type of supports, affect the end result. Different choices lead to slightly different answers, but it is important that the main errors are avoided here, by adding an extra row to reduce the effect due to the choice of the supports, and by taking the angle of the compressive concrete strut between 21.8° and 45° (Braam & Lagendijk, 2011). Once the stresses are determined, they are compared with the concrete strength. Since concrete is stronger for short impact loads (Neville & Brooks, 2010), an impact strength is estimated, which is much more uncertain than the regularly used static concrete strength, but it is the only way to truly assess whether the impact due to rocking will lead to failure of the concrete.

Essentially, what the final model does is to randomly pick an armour unit around the waterline, plus a random wave, and randomly positioned surrounding units. For this set of stochastic variables, a calculation will be performed, to check if the tensile impact strength will be exceeded by the peak stress, at the identified critical location at the base of the leg of the armour unit. If this strength is exceeded, it is said that cracks will start to form. Plastic behaviour is not included in the model, but instead it is assumed that crack formation leads to complete rupture of the leg, either immediately or due to cyclic loading. A breakage prediction is now made for one random case, but the model performs a Monte Carlo simulation of e.g. 100,000 cases, where a new set of stochastic variables is picked each time. The end result is a distribution of the impact velocity, impact force, and peak stresses, which can be used to determine exceedance probabilities and a prediction of the percentage of breakage of the armour unit legs.

There are uncertainties in various parameters and variables that had to be determined as input for the model. The following list provides an overview of the most important uncertainties of the parameters and variables:

- Many parameters and variables needed to determine the impact velocity (Equation 3.1) have some uncertainty, especially because some are specifically defined for this MSc thesis and there is no reference. However, it is only important that the impact velocity results are good, which can be validated by physical model tests, thereby reducing the uncertainty of all these variables without validating them separately.
- The model uses the significant wave height H_s as input to create a wave field. However, H_s itself is usually an important uncertainty in the design of breakwaters. This is therefore not necessarily a drawback of the model, since H_s is still widely used, but it does give some extra uncertainty in the results.
- The stiffness of the breakwater bed has a high uncertainty, which causes significant uncertainty in the impact force. As some form of validation, two estimations are made: one based on the subgrade modulus, and one based on the Young's modulus. Still, there is a lot of uncertainty, because it is uncommon to represent a soil as a single spring, so it is unknown if the applied method is correct. Additionally, the breakwater bed consists of pretty large rocks, so it likely behaves differently than regular soils.
- There are several variables regarding the position of the armour unit and its surroundings, such as the available movement space, the area affected by waves, and the location and angle of impact. All of these are estimated based on a single geometric lab experiment, and although it provides a much better estimation than random guesses, there is still a lot of uncertainty. Some of these are used as input for the impact velocity and, as mentioned above, their uncertainty can be reduced by measuring the impact velocity in physical tests.
- The impact strength of the concrete is another important uncertainty. Although the static strength of concrete is fairly well known, there is much less knowledge about the concrete strength under a short impact load. The implemented probabilistic distribution is based on the characteristic static strength provided in the standardised concrete classes, but the main uncertainty comes from translating that to a distribution for the impact strength. The impact strength depends on various factors, which makes it very difficult to determine it accurately.

7.3 Model results

Now that the model is completed, the results will be presented for several relevant cases.

7.3.1 Presenting the results

The model results will be presented for a few different cases. These cases are based on the Xbloc® guidelines by Delta Marine Consultants (2018), where a table of advised Xbloc® dimensions is given for varying wave heights. A few cases are picked, in order to check the model results for a range of wave heights and block dimensions. The cases that will be investigated are given in Table 7.3, where also the results of predicted breakage are given. For all of these investigated cases, the stability number is: $\frac{H_s}{\Delta d_n} \approx 2.75$.

Significant wave height, H_s [m]	Unit height, D [m]	Nominal diameter, d_n [m]	Percentage of simulations that predict breakage [%]
3.35	1.31	0.91	5.2
5.32	2.08	1.44	9.4
7.38	2.88	2.00	12.8
10.01	3.91	2.71	15.8

Table 7.3: Investigated breakwater cases

The full model is implemented in Python, where the results of each step of the model will be plotted. This will result in a plot of the impact velocity, a plot of the impact force, and a plot of the maximum tensile stresses, in which also the tensile impact strength is plotted, to visualise expected failure. The model performs a Monte Carlo simulation, in which the number of simulations is set to N = 100,000, but the runtime is still under a minute, so it is possible to increase N if one would be interested in checking the very small exceedance probabilities more accurately. The full Python script is given in Appendix D.

For an easy comparison, the results of the four investigated cases are plotted in the same figure. Plots of the impact velocity, impact force, and the maximum tensile stresses are given in Figure 7.2 to Figure 7.4 respectively.

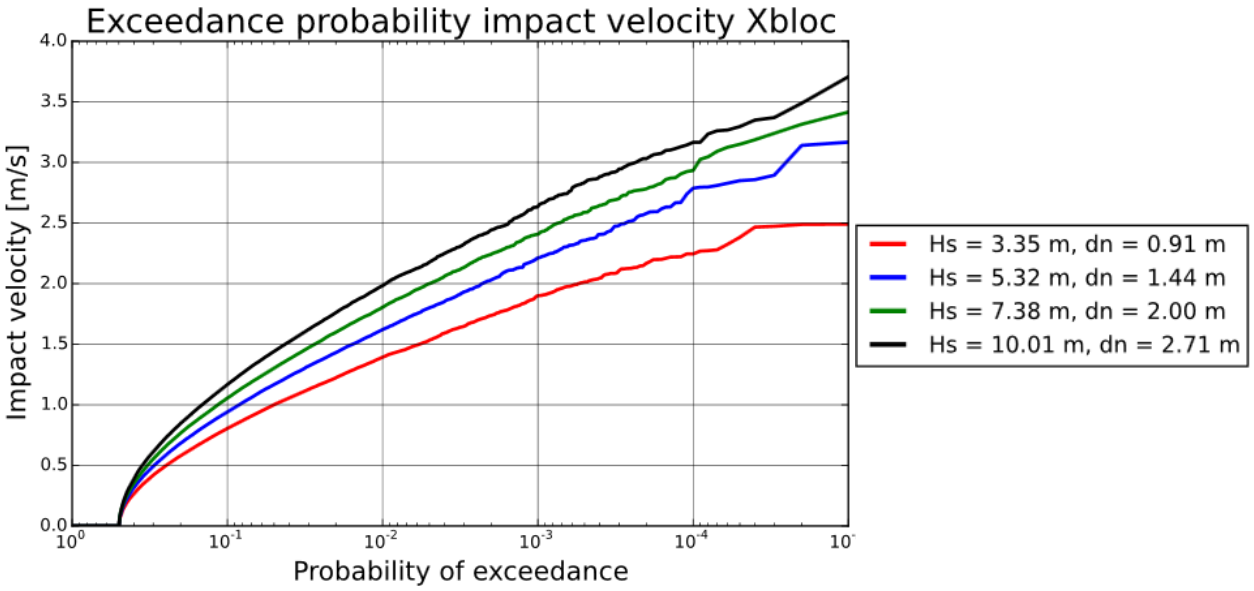

Figure 7.2: Model results impact velocity Xbloc

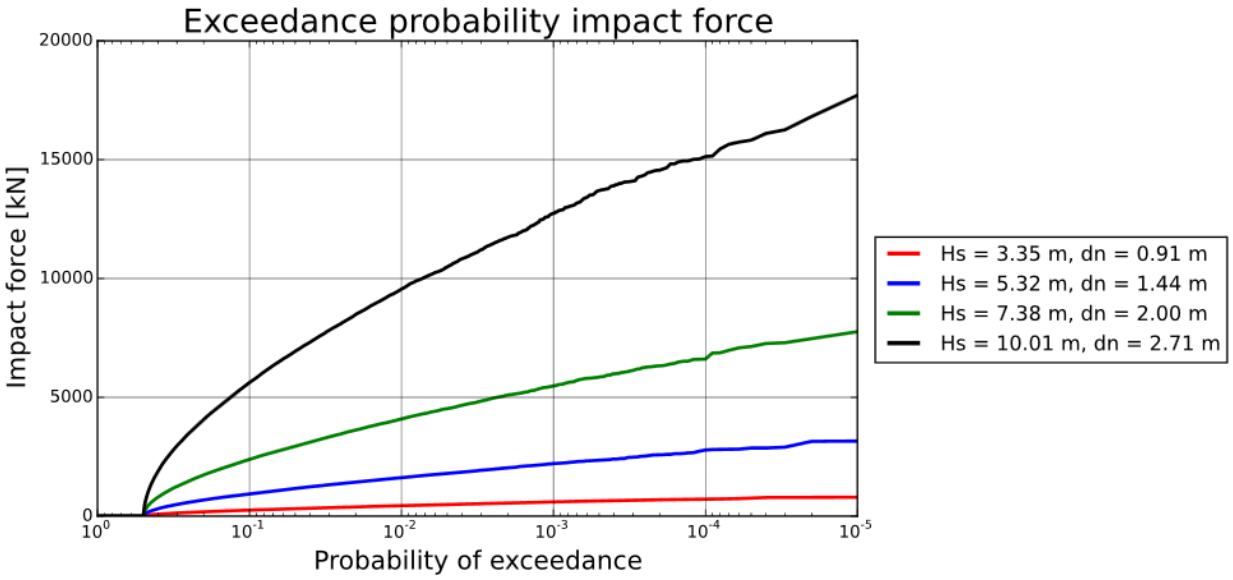

Figure 7.3: Model results impact force Xbloc

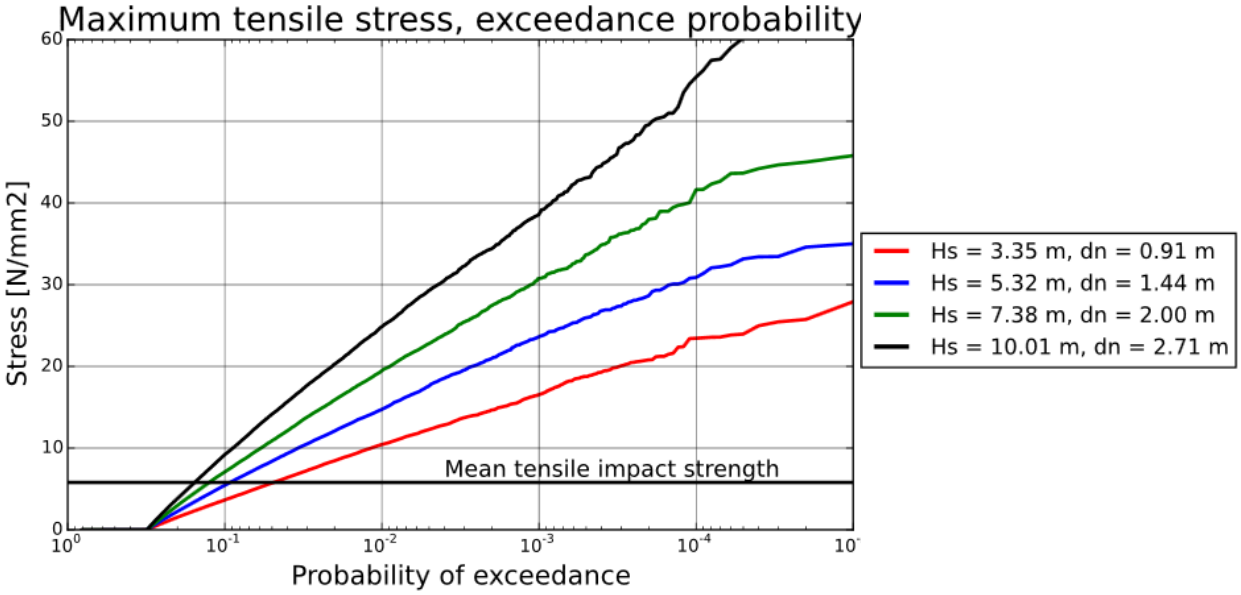

Figure 7.4: Model results maximum tensile stress Xbloc

7.3.2 Discussion of the results

First, a few notes about how to interpret the graphs.

- It can be seen that the velocity, force, and stress are all zero for the first part of the graph. This is solely due to the fact that it was specified that half of the units do not have any movement space, thus they will not move, thus no force and stress. This is based on a small scale lab experiment, where a small breakwater piece was recreated to obtain some information about the movement parameters of the Xbloc®.
- The graphs are plotted with the probability of exceedance on a logarithmic scale, in order to identify the extreme cases properly.
- For the Monte Carlo simulation, N = 100,000 is used, thus the 10^{-5} probability is based on a single randomly picked set of variables, so that value is random and will vary if the simulation is repeated. The values up to a probability of 10^{-3} should be decently stable though.
- The model simulates completely independent events, so it is only identified how many of these independent events experience an exceedance of the tensile impact strength. This is assumed to eventually lead to failure of the armour unit, since it will be weakened, so the required wave height to cause damage decreases.

Overall, the impact velocity, impact force, and the resulting stresses all get larger as the size of the waves and armour units increases. This leads to more broken armour units for larger waves/units. This tendency is as expected, since breakage of armour units is generally found to be more problematic in more severe conditions, with large waves and large armour units.

The model results are expected to be an upper limit of the percentage of completely broken armour units in a real situation. This is partially due to the fact that certain unknowns are left out of the energy balance to determine the forces. This energy balance is now treated as if the kinetic energy of the moving block is completely converted to the potential spring energy: $E_{kin} = E_{pot}$, leading to $F = \sqrt{m_1 v_1^2 k}$. However, it is possible that the stricken block will also move due to the collision, such that a part of the energy is converted into kinetic energy of the stricken block. Another form of energy losses is local crushing of the concrete, which is identified as a failure mechanism of the concrete, but is neglected because the consequences for the breakwater are negligible. The energy balance would then look like: $E_{kin,1} = E_{pot} + E_{kin,2} + E_{local\ crushing}$, which significantly reduces the eventually calculated force, and thus the occurring stresses, and the expected failure percentage. This may be one of the causes why the failure percentage is much higher for larger waves/units. The forces are much higher in those cases, so local crushing is much more likely to occur than for smaller waves/units, thus the energy losses due to local crushing would also be much higher, so the resulting stresses would be overall be somewhat levelled if energy losses due to local crushing would be taken into account. Another failure mechanism that is neglected is chipping off the corners. It might be that some cases that are identified to have tensile bending failure, will actually be cases of chipped off corners, which would immediately relieve the pressure and stop the stresses from developing. The concrete would then still fail, but it will be just a chipped off corner instead of complete failure of the leg.

7.4 Sensitivity analysis

In order to identify which variables have a significant effect on the impact velocity, force, and stresses, a sensitivity analysis will be performed. For this analysis, a single set of variables will be chosen, in which one variable at a time will be varied. That standard set of variables is chosen such that there will be significant movement of the armour unit, and consists of the following values:

- $d_n = 1.44\ m$, the nominal diameter of the armour unit
- $H = 5.32\ m$, the wave height of a single wave
- $f_{area} = 0.381$, the area subjected to wave attack
- $s = 0.05$, the movement space
- $R = 0.0$, the distance of the rotation point to the centre of gravity
- $f_{hit} = 1.0$, the distance between the collision point and the rotation point
- $f_L = 0.0$, the location of the impact on the stricken leg
- $\theta_F = 80°$, the angle of the incoming force

Now, each of these variables (except d_n) will be varied individually over a realistic range, while keeping all other at their chosen value. A plot of the variation in stresses will be given for the sensitivity check of each variable, while a plot of the impact velocity will also be given where relevant.

Wave height, H

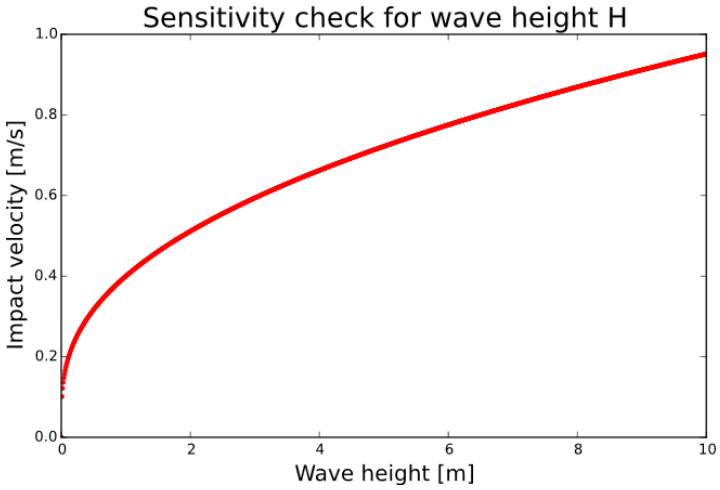

Figure 7.5: Sensitivity check wave height. Impact velocity

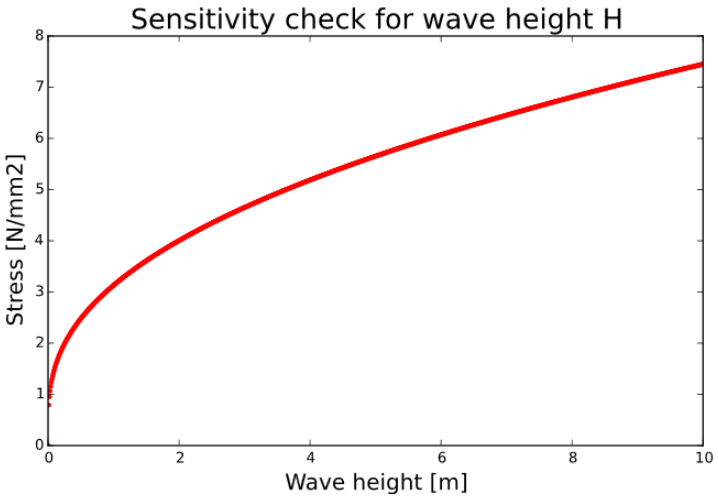

Figure 7.6: Sensitivity check wave height. Stresses

Fraction of area subjected to waves, f_{area}

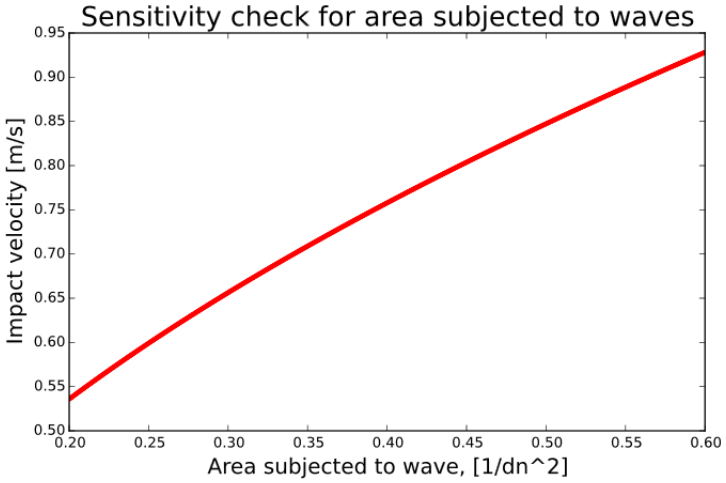

Figure 7.7: Sensitivity check area subjected to waves. Impact velocity

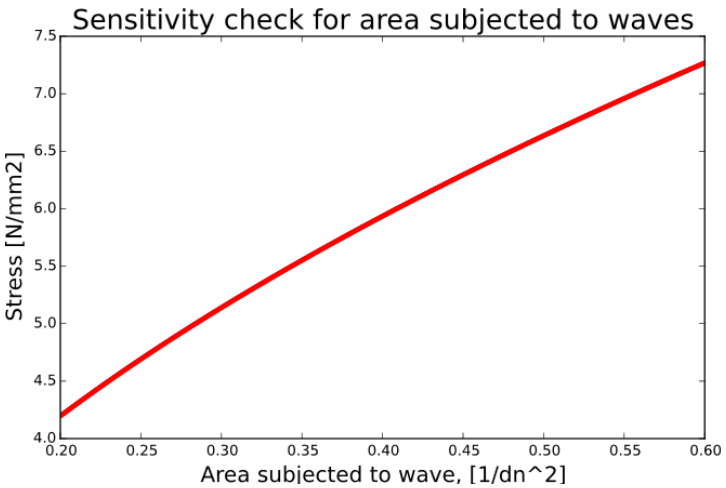

Figure 7.8: Sensitivity check area subjected to waves. Stresses

Movement space, *s*

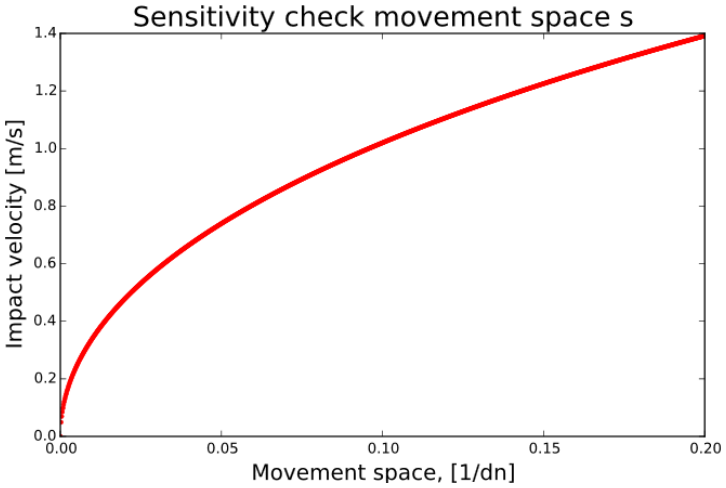

Figure 7.9: Sensitivity check movement space. Impact velocity

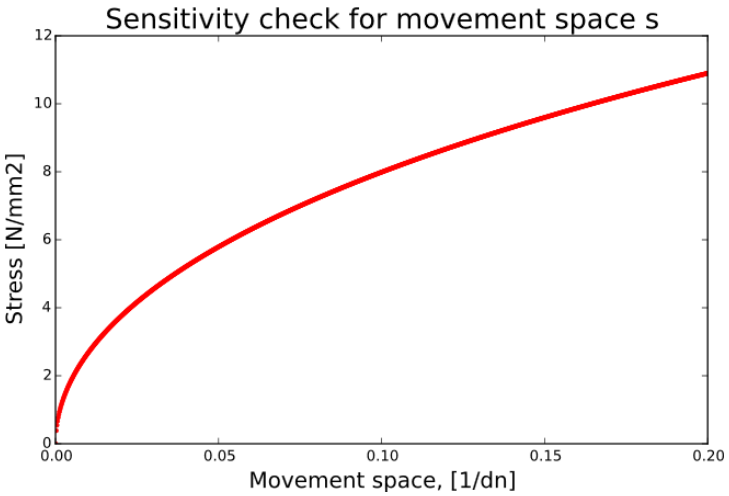

Figure 7.10: Sensitivity check movement space. Stresses

Distance of rotation point to centre of gravity, *R*

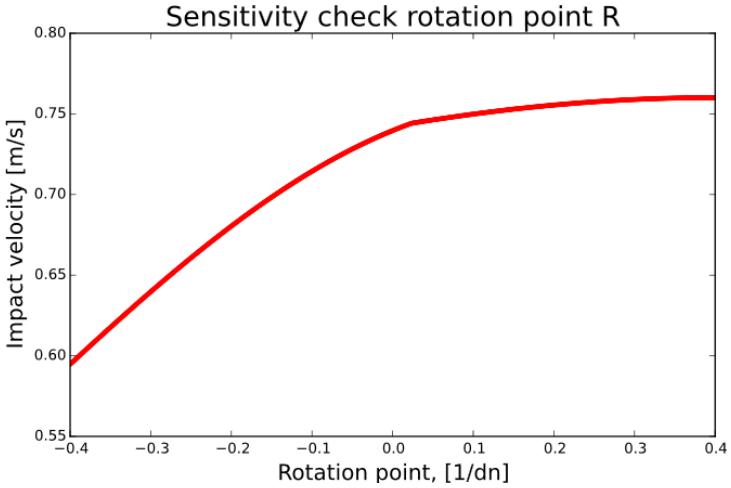

Figure 7.11: Sensitivity check rotation point. Impact velocity

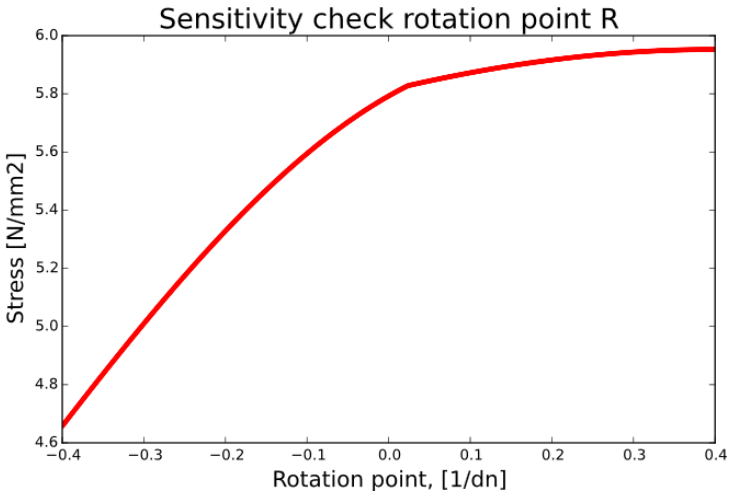

Figure 7.12: Sensitivity check rotation point. Stresses

Distance of the collision point to the rotation point, f_{hit}

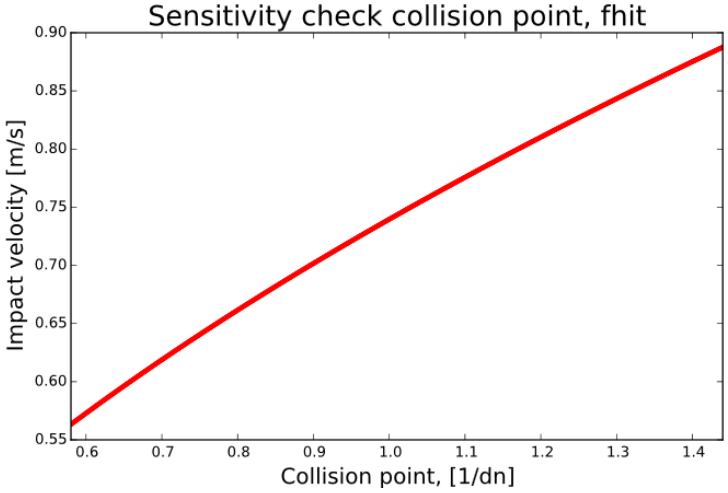

Figure 7.13: Sensitivity check collision point. Impact velocity

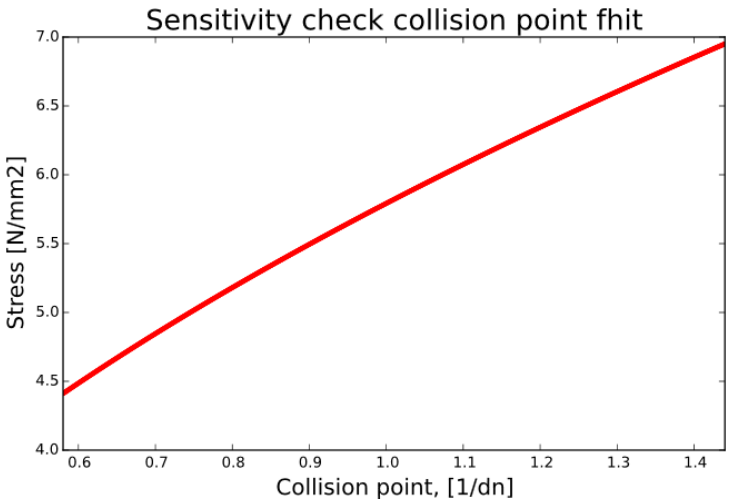

Figure 7.14: Sensitivity check collision point. Stresses

Impact location on the stricken leg, f_L

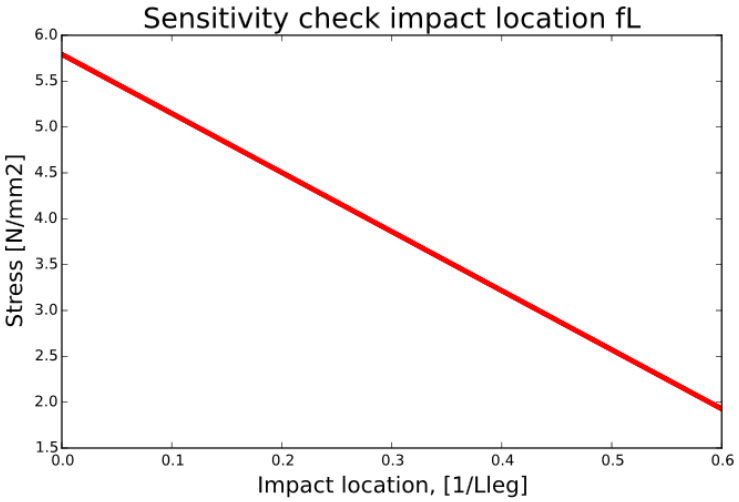

Figure 7.15: Sensitivity check impact location

Angle of the incoming force, θ_F

Note that 0° is parallel to the leg, thus full compression, and 90° is perpendicular to the leg, thus full bending. The angle can even go beyond 90°, such that the vertical component of the force causes tension instead of compression.

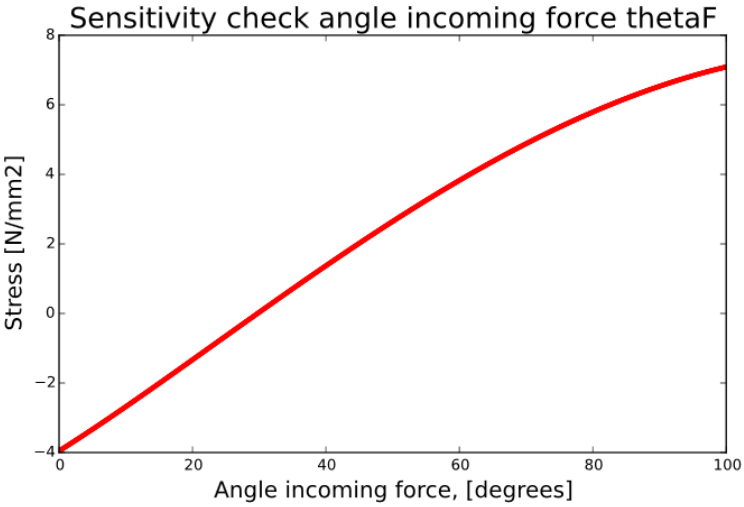

Figure 7.16: Sensitivity check angle incoming force

Discussion of sensitivity checks

For each variable it will shortly be described how sensitive the results are to varying that variable, and how much they contribute to uncertainties of the final result.

- H, the wave height of a single wave: since the wave height ranges essentially from zero to twice H_s, the resulting impact velocity and stresses also have a large range of magnitude. The wave height of a single wave is based on the significant wave height, H_s, which is a widely used variable, but it is still one of the most important uncertainties in breakwater design.
- f_{area}, the area subjected to wave attack: variations in f_{area} also cause significant variation in the resulting impact velocity and stresses. Getting either a low value of f_{area}or a high value, results in difference in impact velocity/stress of roughly a factor 2.0, which is in many cases decisive in whether a unit fails or not. Also, the distribution given to f_{area}might not be accurate, as it is solely based on one small lab experiment, in which it was difficult to estimate the values accurately.
- s, the movement space: just like the wave height, the movement space can also be zero and has a large range of resulting impact velocity/stress. The results is quite sensitive to the available movement space. Though, unlike the wave height, it is not certain that the applied distribution of the movement space is very accurate, so this causes a significant amount of uncertainty.
- R, the distance of the rotation point to the centre of gravity: the highest resulting impact velocity and stresses are roughly 30% higher than the lowest results. The variation rotation point does thus have a significant impact on the results, but less than most other variables. The distribution is not guaranteed to be correct, because it is based on a single small lab experiment, but it was possible to measure the location of the rotation point with satisfactory precision. This causes minor uncertainty.
- f_{hit}, the distance between the collision point and the rotation point: the highest resulting impact velocity and stresses are roughly 50% higher than the lowest results. The variation rotation point does thus have a significant impact on the results. Higher than for the rotation point, but less than most other variables. Again, the distribution is not guaranteed to be correct, because it is based on a single small lab experiment, but it was possible to measure the collision point with satisfactory precision. This causes minor uncertainty.
- f_L, the location of the impact on the stricken leg: the highest resulting stresses are roughly 3 times as high as the lowest stresses. The location of impact on the leg is thus very significant. Again, the distribution is not guaranteed to be correct, because it is based on a single small lab experiment, but it was possible to measure the collision point with satisfactory precision, but due to the large effect that f_L has on the results, it still causes some uncertainty.
- θ_F, the angle of the incoming force: the resulting stresses range from compressive stresses to tensile stresses. For small angles, the force will be mainly compressive, thus counteracting the tensile bending stresses. Therefore, the armour unit will likely never fail when the angle of the force is small enough. This angle has a large effect on the failure of the concrete armour units. The probabilistic distribution of the angle of the force is solely based on a single small lab experiment

Overall, the three most sensible variables are identified as: the wave height H, the movement space s, and the angle of the incoming force θ_F.

Sensitivity checks of some uncertainties

Though it is not treated as an independent variable, it still is interesting to investigate the sensitivity of the bed stiffness as a parameter, because it is highly uncertain if the determined spring stiffness to represent the bed is correct. Therefore, one more plot is made, with a range of k_{bed} from $10 \cdot 10^6\ N/m$ to $100 \cdot 10^6\ N/m$. It is seen in Figure 7.17 that the bed stiffness has a significant effect on the eventual stresses. Therefore, it would greatly improve the accuracy of the model if uncertainties of the bed stiffness can be taken away, by a more detailed investigation.

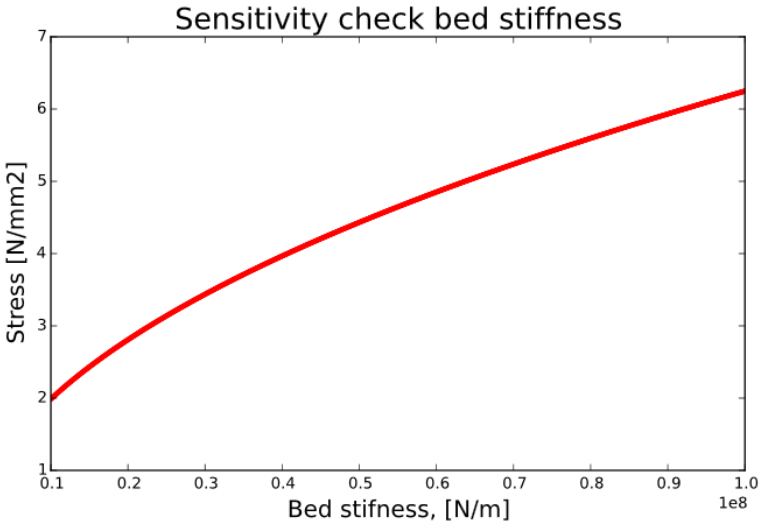

Figure 7.17: Sensitivity check bed stiffness

Another uncertainty is the amount of kinetic energy of the moving block that is converted into the potential spring energy. In the model, it is used that $E_{kin,1} = E_{pot}$, such that $F = \sqrt{m_1 v_1^2 k}$, but if the energy balance is treated as $E_{kin,1} = E_{pot} + E_{kin,2} + E_{losses}$, the formula to determine the force becomes: $F = \sqrt{m_1 v_1^2 k - m_2 v_2^2 k - 2 \cdot E_{losses} \cdot k}$, reducing the force, and thus the stresses. The effect of a reduction of the potential energy is plotted in Figure 7.18. Depending on how large the energy losses are, they may have a significant effect on the stresses.

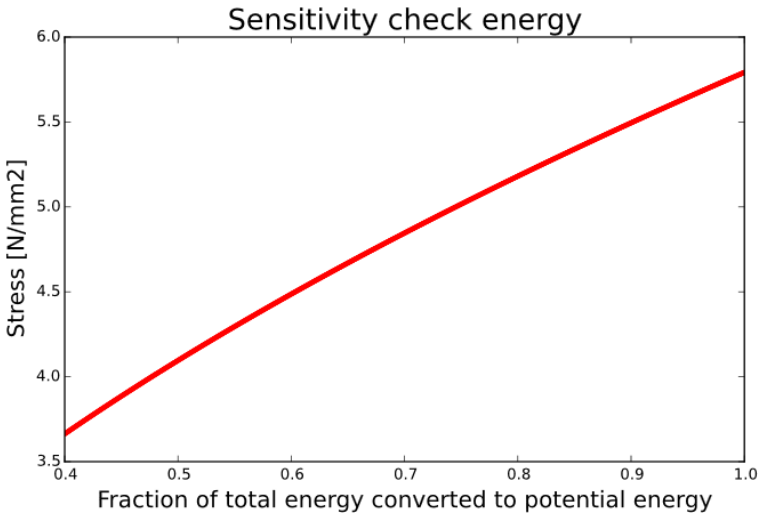

Figure 7.18: Sensitivity check energy

8. Conclusions

This chapter shortly treats the conclusions of this MSc thesis.

Conclusions of what is achieved in this MSc thesis

A functioning model is made, which produces a probabilistic distribution of the impact velocity, the impact force and the maximum stress due to rocking. Based on the distributions of the maximum stress and the concrete strength, a probability of failure is obtained. In this model, failure means that the concrete will start to crack at the base of the armour unit leg, which is assumed to eventually lead to complete rupture of the leg, due to the cycling loading by the waves. The probabilistic distributions are obtained via a Monte Carlo simulation performed in a Python script, where the velocity, force, and stress are calculated by using expressions that were derived in this MSc thesis.

The impact velocity formula is derived in such way that it can be used for any type of armour unit, and the formulas for the impact force and the stress are derived specifically for Xbloc®, for tensile failure at the base of a leg. These formulas require several uncommon variables as input. Some of these variables are stochastic, and have a probabilistic distribution instead of a single value. All required variables were determined during this MSc thesis. A lab experiment is performed to estimate the distributions of the geometrical stochastic variables. Physical model test results are used to validate the impact velocity for Xbloc® and for cubes, as well as the impact force for Xbloc®.

Conclusions from model results

The results show that the failure percentage becomes higher for larger waves and armour units, starting at a failure of 5% of the simulate cases for the situation of $H_s = 3.35\ m$ and $d_n = 0.91\ m$, up to a failure of nearly 16% of the simulated cases for the situation of $H_s = 10.01\ m$ and $d_n = 2.71\ m$. It was expected that a situation with larger waves and armour units leads to more breakage, so it is good to see this trend being represented by the model.

Some steps of the model are validated by means of test data, though it is sometimes difficult to interpret these validations as the tests represent different cases, which deteriorates the comparison. The impact velocity formula is checked for cubes, which gave comparable results. A validation of the impact velocity is also performed for Xbloc®s, leading to the conclusion that the highest impact velocities are modelled with reasonable accuracy. The impact force is validated with test data of concrete to concrete impact, but this test did not include the breakwater bed, so for a fair comparison, it was also excluded from the model. These results were relatively good, but it still leaves a large uncertainty in the effect of the breakwater bed on the impact force.

Neglecting local crushing may result in higher breakage percentages for larger waves and armour units, since the forces are just much larger in these cases, thus more frequent and larger energy losses due to local crushing are expected, relieving the tensile bending stresses. This may lead to an overestimation of the failure percentage, especially for cases of larger waves and armour units, which exaggerates the differences between small and large waves and armour units.

Conclusions from model setup

During the development of the model, it was apparent that rocking-induced stresses are very complex. In order to be able to model the impact velocity, the impact force, and the resulting stresses, many assumptions had to be made to simplify the complexity. Every assumption adds some uncertainty or error to the model, but this is reduced where possible. E.g. the assumption of constant acceleration, that was necessary to obtain the impact velocity formula, is compensated by a correction factor. A similar correction is applied to take the nonlinear stress distribution into account. Furthermore, uncertainties in the input variables are reduced by performing a lab experiment to determine distributions for the geometric variables.

It is noted from the sensitivity analysis that there are many factors that have a significant effect on the end results, further proving the complexity of the subject. Throughout the development of the model, several parameters and variables were defined, for which the values had to be determined. Many of these were estimated with reasonable accuracy in the aforementioned lab experiment, but the lack of other results to compare with still leaves some uncertainty. Repeating the lab experiment will likely give slightly different results, because the blocks are positioned randomly.

9. Recommendations

This chapter treats some recommendations to improve or valid the model that is developed in this MSc thesis, as well as some ideas for other research.

Usage of the model

Although the model is not yet ready to use in design practice, it is interesting to think about the possible uses of the model. A few possibilities will shortly be treated below:

- After the initial design stage, where the breakwater is designed for hydraulic stability, a prediction of rocking-induced breakage can be performed. A certain percentage of armour units is expected to break, and it is then up to the engineers to decide whether this is acceptable, or it would be better to increase the size of the units to reduce movement.
- Another interesting possibility is to assess existing breakwaters. Wave heights are increasing due to climate change, which might endanger some existing breakwaters in the future. By assessing this up front, measures can be taken before the breakwater fails completely.

Extending the model

The current model predicts breakage of Xbloc®s around the water line, due to tensile bending stresses, which can be extended in three ways:

- Predict breakage for other types of armour units. The impact velocity formula is derived independently from the armour unit type, so it can also be used for other types of armour units. There are other types of armour units with legs that have a risk of breaking, for which the failure types are similar. There are parameters that are determined specifically for Xbloc®, so these need to be determined for another type of armour unit, if one would be interested in using the model for a different type of armour unit.
- Involve armour units that are located higher up the slope. The impact velocity is based on the run-up velocity of the water on the slope. The run-up velocity is now solely calculated at the water line, but can be easily be calculated at different heights on the slope as well. This extension is relatively easy to implement, but requires validation to see if the results are actually correct.
- Add other failure mechanisms. Right now, the only implemented mechanism is failure due to tensile bending stresses at the base of the leg. While less severe, there are other mechanisms leading to failure of the concrete, and they can potentially threaten the safety of the breakwater.

Investigate the energy balance

The impact forces are based on an energy balance, in the form of: $E_{kin,1} = E_{pot}$. The kinetic energy of the moving unit, block 1, is converted into a potential spring energy, which determines the force. Actually, the energy balance looks more like: $E_{kin,1} = E_{pot} + E_{kin,2} + E_{losses}$. The stricken unit, block 2, might move due to the impact, in which case a part of the energy will be converted into kinetic energy of block 2. There are also other forms of energy losses, most notably local crushing of the concrete. Crushing the concrete requires energy, which reduces the energy that is converted into the potential energy that eventually leads to the tensile bending stresses. Since the kinetic energy of block 2 and the other energy losses are unknown, they are left out of the model, but they can give a significant reduction of the stresses. A better understanding of the amount of energy that is truly converted into potential energy will therefore significantly improve the accuracy of the model.

Investigate the stiffness of the bed

The stiffness of the bed is now represented by a spring, for which the stiffness is estimated. This estimation is not claimed to be accurate at all, so a closer investigation could improve this estimation, thereby improving the model results.

Further validation of the impact velocity

Although some validation is already performed in this MSc thesis, to show that the modelled impact velocity is in the right order of magnitude, it is still good to do further validation. So far, the validation is based on measurements of a single unit, under attack by many waves. It would be interesting to do similar tests with multiple measurement units, to get variation in the position parameters of the armour units, similar to what it is done this MSc thesis, where new random position parameters are picked for each simulation.

It is also possible to adjust the output of the model in order to make a better comparison with test results. For example, the position parameters of the block can be picked up front, such that a field of random waves is modelled on a single unit. This can even be extended to include multiple units with varying position parameters. An example is given in Figure 9.1, where four blocks are picked with increasing available movement space, and mean values for the other position parameters. A large number of random waves is modelled, resulting in a plot of the exceedance probability.

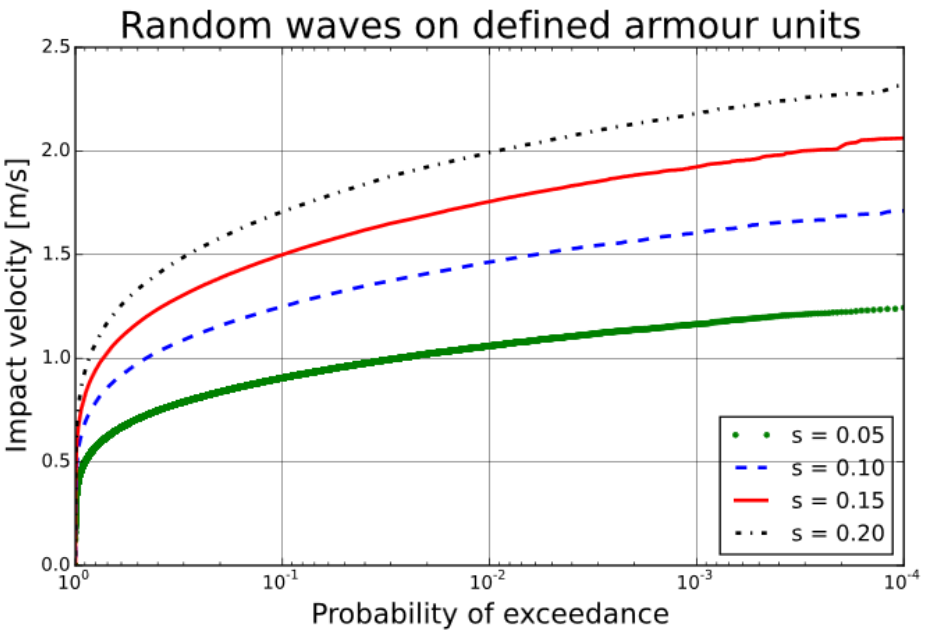

Figure 9.1: Impact velocity for several defined units under random wave attack

Ideally, if all position parameters of the measurement unit would be determined, it is possible to recreate the exact same situation in the model simulation, thus being able to truly make an accurate comparison. However, it is not even known if the position parameters are actually constant during heavy wave conditions. Due to the movement of the blocks, their position might change.

Even without knowing the position parameters during physical model tests, the results will still give insight in the probabilistic distribution of the impact velocity. If the measurement units are placed completely randomly, there will likely be several units that will not move at all, since it was estimated in this MSc thesis, that half of the units have no space to move. Though, it would be interesting to validate how much units move, it is more efficient for the higher impact velocities to ensure that all measurement units have at least a tiny amount of movement space. An impression of the amount of testing needed for a certain validation level is given below, under the assumption that half of the units move, so ensuring that all measurement units move doubles the efficiency. Note that it is also possible to use a single unit under 10000 waves to reach a 1/10000 exceedance probability, but for a truly accurate result, it is important to vary the position of the measurement unit as well.

	Number of different unit positions	Exceedance probability up to
10 random units, 1 test, 1 wave	10	1/10
10 moving units, 1 test, 1 wave	10	1/20
10 random units, 10 tests, 1 wave	100	1/100
10 moving units, 10 tests, 1 wave	100	1/200
10 random units, 10 tests, 100 random waves per test	100	1/10000
10 moving units, 10 tests, 100 random waves per test	100	1/20000

Literature list

Avci, B., Gurbuz, A. (2018) Modulus of subgrade reaction that varies with magnitude of displacement of cohesionless soil. Published in the Arabian Journal of Geosciences.11.10.1007/s12517-018-3713-1. Retrieved from: https://www.researchgate.net/publication/326141380_Modulus_of_subgrade_reaction_that_varies_with_magnitude_of_displacement_of_cohesionless_soil, last consulted on 05-12-2019

Braam, C.R., Lagendijk, P. (2011) Constructieleer Gewapend Beton. Published by Aeneas

Caldera, H.G.P.M. (2019) Rocking of Single Layer Armour Units. Rocking revisited III. MSc thesis TU Delft

CUR (1989 - 1) Golfbrekers; sterkte betonnen afdekelementen - kracht-tijdrelaties van beton op beton impact-schaaleffect, werkgroep I “Onderzoek”

CUR (1989 - 2) Golfbrekers; sterkte betonnen afdekelementen - integratie van fasen 1-3, werkgroep I “Onderzoek”

CUR (1990 - 1) Golfbrekers; sterkte betonnen afdekelementen – werkgroep II “Toepassingen”

CUR (1990 - 2) Golfbrekers; sterkte betonnen afdekelementen - samenvatting onderzoek

Delta Marine Consultants (2004) Structural integrity of Xbloc® breakwater armour units. Prototype and numerical drop tests

Delta Marine Consultants (2018) Guidelines for Xbloc® Concept Design. Retrieved from: https://www.Xbloc®.com/sites/default/files/domain-671/documents/Xbloc®-guidelines_2018-671-1532949730287638300.pdf, last consulted on 15-11-2019

Delta Marine Consultants, BAM (2019) Choose Xbloc®. https://www.Xbloc®.com/en/choose-Xbloc®/Xbloc®, last consulted on 08-03-2019

DIANA FEA BV (2017) DIANA Finite Element Analysis. Retrieved from: https://dianafea.com/sites/default/files/2018-03/DIANA-10-1-Brochure-Oct-2017-Print-Version.pdf, last consulted on 29-03-2019

DIANA FEA BV (2019) Dams and dykes. https://dianafea.com/index.php/solutionsdamsdikes, last consulted on 29-03-2019

Elger, D.F., Williams, B.C., Crowe, C.T., Roberson, J.A. (2014) Engineering Fluid Mechanics, tenth edition. Published by Pearson

EurOtop (2018) Manual on wave overtopping of sea defences and related structures. An overtopping manual largely based on European research, but for worldwide application. Van der Meer, J.W., Allsop, N.W.H., Bruce, T., De Rouck, J., Kortenhaus, A., Pullen, T., Schüttrumpf, H., Troch, P. and Zanuttigh, B., www.overtopping-manual.com.

Geotechdata.info (2013) Soil elastic Young’s modulus, retrieved from http://www.geotechdata.info/parameter/soil-young's-modulus.html, last consulted 05-12-2019

Holthuijsen, L.H. (2010) Waves in Oceanic and Coastal Waters. Published by Cambridge University Press

Hudson, R.Y. (1953) Wave forces on breakwaters, Proceedings-Separate ASCE, no 113

Hofland, B., Arefin, S. S., Van der Lem, C., Van Gent, M. R. A. (2018). Smart rocking armour units. In Proc. 7th international conference on the application of physical modelling in coastal and port engineering and science.

Iribarren Cavanilles, R. (1938) Una formula para el calculo de los diques de escollera, M. Bermejillo-Pasajes

Neville, A.M., Brooks, J.J. (2010) Concrete Technology, Second Edition. Published by Pearson

Patel, R., Dubey, S.K., Pathak, K.K. (2014) Effect of depth span ratio on the behaviour of beams. Published in the International Journal of Advanced Structural Engineering 6: 3. Retrieved from https://doi.org/10.1007/s40091-014-0056-3, last consulted on 29-11-2019

Popp, C. (1977) Untersuchen über das Verhalten von Beton bei schlagartigen Beanspruchung

Schiereck, G.J. , updated by Verhagen, H.J. (2016) Introduction to Bed, bank and shore protection. Published by Delft Academic Press / VSSD

Ten Oever, E. (2006) Theoretical and experimental study on the placement of Xbloc®. MSc thesis TU Delft

Van den Bos, J.P. , Verhagen, H.J. (2018) Breakwater design – Lecture notes CIE5308 TU Delft

Van der Meer, J. (1988 - 1) Rock slopes and gravel beaches under wave attack. Doctoral thesis TU Delft

Van der Meer, J. (1988 - 2) Application and stability criteria for rock and artificial units. Retrieved from : http://www.vandermeerconsulting.nl/downloads/stability_b/1998_vandermeer_ch11.pdf, last consulted on 20-03-2019

Van der Meer, J. (2011) The Wave Run-up Simulator. Retrieved from: http://www.vandermeerconsulting.nl/downloads/stability_a/2011_wave_run_up_simulator.pdf, last consulted on 25-04-2019

Images

Corredor, A. et al. (2010) Concrete cube [photograph]. Retrieved from https://pdfs.semanticscholar.org/54dc/787eeb32a180bc8b720308d8b82b2ecd274c.pdf , consulted on 01-04-2019

Delta Marine Consultants, (n.d.) Xbloc®s on a breakwater, [photograph]. Retrieved from https://www.Xbloc®.com/en/projects/port-of-poti-georgia , consulted on 01-04-2019

Eurocode (n.d.) *Characteristic strength* [image]. Retrieved from https://www.eurocode.us/structural-design-eurocode-7/material-properties-and-resistance-resistance.html, consulted on 14-01-2020

Hofland, B., Arefin, S. S., Van der Lem, C., Van Gent, M. R. A. (2018). *Smart rocking armour units. In Proc. 7th international conference on the application of physical modelling in coastal and port engineering and science.* [photograph]

Putri, M., Sulistyo, D., Triwiyono, A. (2018) *Reinforced Concrete Corbel's Behavior using Strut and Tie Model.* Journal of the Civil Engineering Forum. 4. 97. 10.22146/jcef.28221., [image] Retrieved from https://www.researchgate.net/publication/325126216_Reinforced_Concrete_Corbel's_Behavior_using_Strut_and_Tie_Model , consulted on 06-12-2019

Van Gent, M.R.A., Van der Werf, I.M. (2017) *Breakwater with cubes in a single layer*, [photograph], Retrieved from https://www.researchgate.net/publication/320415867_Single_layer_cubes_in_a_berm , consulted on 01-04-2019

Appendix A. Mass moment of inertia, Xbloc®

This appendix deals with the determination of the mass moment of inertia of an Xbloc®.

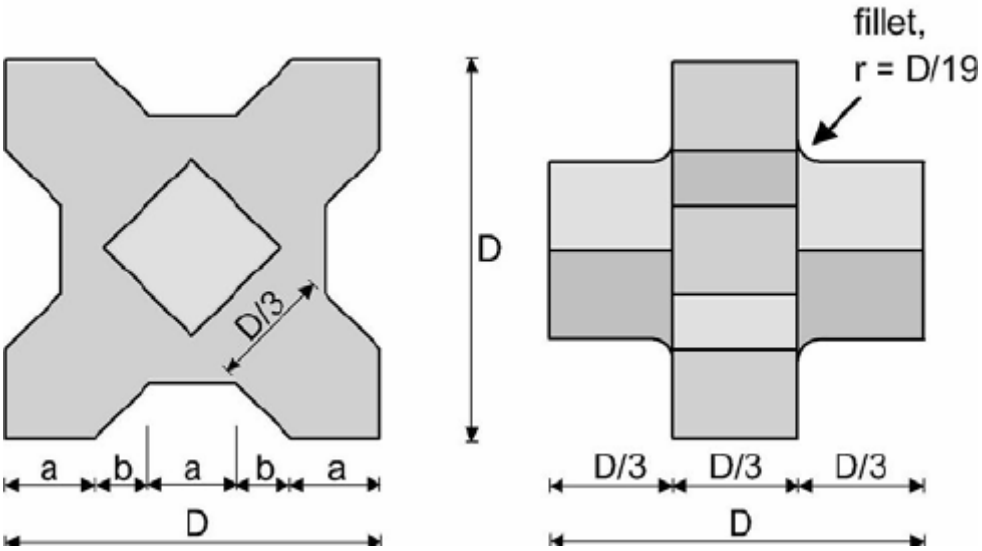

Figure A.0.1: Main dimensions Xbloc®

The shape of the Xbloc® makes it difficult to do an integration. Therefore, the block is divided in several rectangles and triangles, as shown in Figure A.0.2, for which the mass moment of inertia will be determined individually. The total mass moment of inertia can then be determined as the sum of the mass moment of inertia of all individual parts, plus the contributions from Steiner's theorem.

The Xbloc® is divided in the following pieces:

1. Core of the block, *3a* by *3a* by *D/3*

2. Cubical leg, *D/3* by *D/3* by *D/3*, appears 2 times (at the front and at the back)

3. Rectangular, *b* by *b* by *D/3*, appears 4 times

4. Rectangular, *b* by *a – b* by *D/3*, appears 8 times

5. Triangular, base *b*, height *b*, by *D/3*, appears 8 times

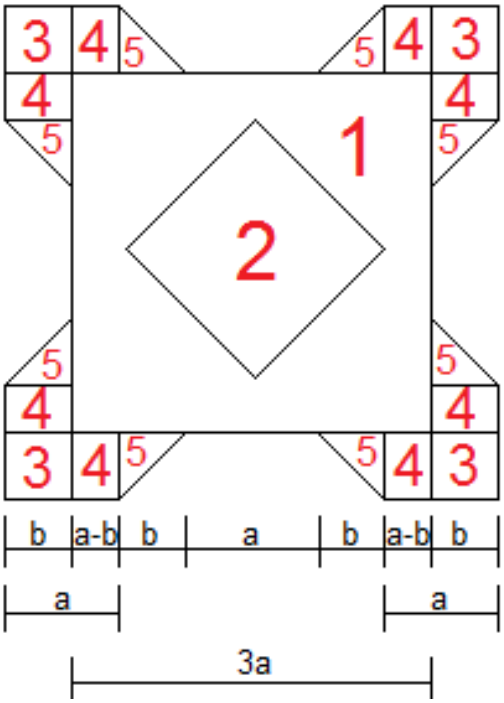

Figure A.0.2: Division of Xbloc® in several pieces

Steiner's theorem, also called parallel axis theorem, is a well-known principle to determine the mass moment of inertia of an object about any axis. It can thus be used to determine the mass moment of inertia about an axis that does not go through the centre of gravity of the object. This rule states that: $I = I_{cg} + md^2$, where I_{cg} is the moment of inertia about the centre of gravity of the object, m is the mass of the object, and d is the distance between the centre of gravity and the new axis. This principle can be used to determine the moment of inertia of pieces of the Xbloc® about the axis that goes through the centre of gravity of the Xbloc® as a whole. The distances are shown in Figure A.0.3, for which d_3, d_4, and d_5 can be calculated by applying Pythagoras' theorem:

$$d_3 = \sqrt{\left(\frac{3}{2}a + \frac{b}{2}\right)^2 + \left(\frac{3}{2}a + \frac{b}{2}\right)^2}$$

$$d_4 = \sqrt{\left(\frac{3}{2}a + \frac{b}{2}\right)^2 + \left(\frac{3}{2}a - \frac{a-b}{2}\right)^2}$$

$$d_5 = \sqrt{\left(\frac{3}{2}a + \frac{b}{3}\right)^2 + \left(\frac{a}{2} + \frac{2}{3}b\right)^2}$$

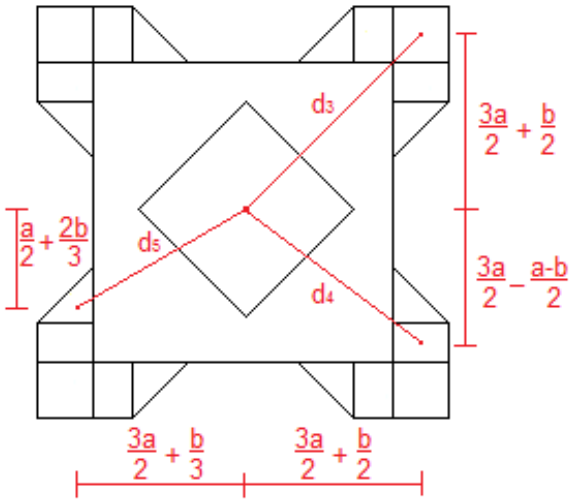

Figure A.0.3: Distances for Steiner's theorem contributions

The mass moment of inertia for a rectangle, about its centre of gravity, can be calculated as:

$$I_{cg_{rectangle}} = \frac{1}{12}m(B^2 + H^2)$$

where m is the mass of the rectangle, B is the width, and H is the height

The mass moment of inertia for a triangle, about its centre of gravity, can be calculated as:

$$I_{cg_{triangle}} = \frac{1}{18}mH^2$$

where m is the mass of the triangle, and H is the height

The mass moment of inertia of the whole Xbloc® about its centre of gravity will be written below as the summation of the mass moment of inertia of each of the pieces, plus the contributions of Steiner's theorem. Note that the centres of gravity of piece 1 and 2 go through the same axis as the centre of the whole Xbloc®, so there is no additional term from Steiner's theorem there. Furthermore, several pieces appear multiple times, which can be accounted for by simply multiplying by the number of times the piece appears.

$$I_{cg_{Xbloc}} = \frac{1}{12}\rho \cdot 3a \cdot 3a \cdot \frac{D}{3} \cdot ((3a)^2 + (3a)^2) \qquad 1_{cg}$$

$$+ 2 \cdot \frac{1}{12}\rho \cdot \frac{D}{3} \cdot \frac{D}{3} \cdot \frac{D}{3} \cdot \left(\left(\frac{D}{3}\right)^2 + \left(\frac{D}{3}\right)^2\right) \qquad 2_{cg}$$

$$+ 4 \cdot \frac{1}{12}\rho \cdot b \cdot b \cdot \frac{D}{3} \cdot (b^2 + b^2) \qquad 3_{cg}$$

$$+ 4 \cdot \rho \cdot b \cdot b \cdot \frac{D}{3} \cdot \left(\left(\frac{3}{2}a + \frac{b}{2}\right)^2 + \left(\frac{3}{2}a + \frac{b}{2}\right)^2\right) \qquad 3_{Steiner}$$

$$+ 8 \cdot \frac{1}{12}\rho \cdot (a-b) \cdot b \cdot \frac{D}{3} \cdot ((a-b)^2 + b^2) \qquad 4_{cg}$$

$$+ 8 \cdot \rho \cdot (a-b) \cdot b \cdot \frac{D}{3} \cdot \left(\left(\frac{3}{2}a + \frac{b}{2}\right)^2 + \left(\frac{3}{2}a - \frac{a-b}{2}\right)^2\right) \qquad 4_{Steiner}$$

$$+ 8 \cdot \frac{1}{18} \cdot \rho \cdot \frac{b \cdot b}{2} \cdot \frac{D}{3} \cdot b^2 \qquad 5_{cg}$$

$$+ 8 \cdot \rho \cdot \frac{b \cdot b}{2} \cdot \frac{D}{3} \cdot \left(\left(\frac{3}{2}a + \frac{b}{3}\right)^2 + \left(\frac{a}{2} + \frac{2}{3}b\right)^2\right) \qquad 5_{Steiner}$$

From Figure A.0.1 also follows that: $\sqrt{2} \cdot a = \frac{D}{3}$, so $a = 0.2357 \cdot D$. Then, from $3 \cdot a + 2 \cdot b = D$ follows that: $b = \frac{3 \cdot a + D}{2} = 0.14645 \cdot D$

By filling in $a = 0.2357 \cdot \mathrm{D}$ and $b = 0.14645 \cdot \mathrm{D}$, the only variables left to determine $I_{cg_{Xbloc}}$ are ρ and D. Each term can be elaborated to:

$$I_{cg_{Xbloc}} = 0.013889\,\rho D^5 + 0.00137\,\rho D^5 + 1.022 \cdot 10^{-4}\,\rho D^5 + 0.01042\,\rho D^5 + 8.544 \cdot 10^{-5}\,\rho D^5$$
$$+ 0.009675\,\rho D^5 + 3.407 \cdot 10^{-5}\,\rho D^5 + 0.005957\,\rho D^5$$

And this summation ultimately gives:

$$\boxed{I_{cg_{Xbloc}} = 0.041531\,\rho D^5}$$

Now, it would be useful to rewrite this to $I = factor \cdot \rho d_n^5$, with the nominal diameter d_n instead of the outer dimension D of the Xbloc®. Since $m_{Xbloc} = \rho d_n^3 = \rho V_{Xbloc}$, d_n and D can be related when the volume of the Xbloc® is known in terms of D. This can be calculated from the same division in pieces as earlier, see Figure A.0.2, which gives:

$$V_{Xbloc} = 3a \cdot 3a \cdot \frac{D}{3} + 2 \cdot \frac{D}{3} \cdot \frac{D}{3} \cdot \frac{D}{3} + 4 \cdot b \cdot b \cdot \frac{D}{3} + 8 \cdot b \cdot (a-b) \cdot \frac{D}{3} + 8 \cdot \frac{b \cdot b}{2} \cdot \frac{D}{3}$$

Again, fill in $a = 0.2357 \cdot \mathrm{D}$ and $b = 0.14645 \cdot \mathrm{D}$, which gives:

$$V_{Xbloc} = 3 \cdot 0.2357 \cdot D \cdot 3 \cdot 0.2357 \cdot D \cdot \frac{D}{3} + 2 \cdot \frac{D}{3} \cdot \frac{D}{3} \cdot \frac{D}{3} + 4 \cdot 0.14645 \cdot D \cdot 0.14645 \cdot D \cdot \frac{D}{3}$$

$$+ 8 \cdot 0.14645 \cdot D \cdot (0.2357 \cdot D - 0.14645 \cdot D) \cdot \frac{D}{3} + 8 \cdot \frac{0.14645 \cdot D \cdot 0.14645 \cdot D}{2} \cdot \frac{D}{3}$$

And eventually:

$$V_{Xbloc} = 0.33279\, D^3$$

Then, by definition of d_n, $V_{Xbloc} = d_n^3$, so:

$$d_n^3 = 0.33279\, D^3$$

$$d_n = 0.693\, D \quad ; \quad D = 1.443\, d_n$$

Therefore:

$$I_{cg_{Xbloc}} = 0.041531\, \rho D^5 = 0.041531 \cdot (1.443\, d_n)^5 = 0.25988\, \rho d_n^5$$

The mass moment of area of the Xbloc® about its own centre of gravity is thus given by:

$$\boxed{I_{cg_{Xbloc}} = 0.25988\, \rho d_n^5}$$

Note the Xbloc® will normally not rotate around its centre of gravity, but will more likely rotate around a point somewhere at the edge of one of the legs. The mass moment of inertia around any rotation point can again be determined from Steiner's theorem:

$$I_{Xbloc} = I_{cg_{Xbloc}} + md^2 = 0.25988\, \rho d_n^5 + \rho d_n^3 \cdot d^2$$

Ultimately, by determining d as a $factor \cdot d_n$, the mass moment of inertia of the Xbloc® can be written as $I_{Xbloc} = factor \cdot \rho d_n^5$

Appendix B. Velocity correction factor

This appendix deals with the determination of a velocity correction factor, which is eventually established as: $f_{cor} = 1 - \frac{\sqrt{s}}{4}$

In the derivation of the impact velocity formula, it was assumed that the acceleration of the armour unit is constant, in order to be able to determine the impact velocity directly from an analytical expression. However, the acceleration is not constant! The acceleration is based on the moments caused by the wave force and the own weight of the block, and these change during the motion.

The wave force is based on a velocity difference between the water and the armour unit: $F_{wave} = ½\,\rho_w C_D A(\Delta u)^2$, where $\Delta u = u - v$, $u =$ the fluid velocity, and $v =$ the velocity of the object, i.e. the armour unit. Initially, the water has a certain velocity, while the armour unit is at rest. The velocity of the water will decrease when the wave loses energy, though that is mainly when the wave runs up on the slope, and is probably negligible during the motion of the observed armour unit around the water line. Though, during this motion, the armour unit is accelerating, increasing its velocity, thus decreasing the velocity difference between the fluid and the armour unit. Therefore, the wave force decreases, so the acceleration of the armour unit will decrease, during the motion of the armour unit. Note that the armour unit does not a have a uniform velocity due to the rotation, so the velocity v must be determined at a point where the wave force acts. It is chosen to do this at a height of $\frac{2}{3}D$, or $0.96 \cdot d_n$, because the wave force mainly acts on the upper part of the block.

The weight of the armour unit does not change during the motion, but when it rotates, the arm between the centre of gravity and the rotation point does change. Therefore, there will still be a change in moment, and thus a change in the acceleration as well. This effect leads to a higher sum of moments, thus a higher acceleration, counteracting the effect of the decrease in wave force, when the armour unit gains velocity.

To account for the change in acceleration when the armour unit gains velocity and rotates, a looped calculation can be performed, where the acceleration, the velocity, and the angular rotation are updated after each time step Δt. This concept will be sketched here. The acceleration is assumed to be constant over this time step, which is an acceptable assumption as long as the time step is very small. Initially, the armour unit is at rest ($v_0 = 0\ m/s$), while the arm of the weight force is determined from geometry, thus the initial acceleration a_0 can be calculated, leading to a certain velocity after the first time step $v_1 = a_0 \cdot dt$. Then, for the next time step, the velocity difference $\Delta u = u - v$, must be updated, based on the new v. The arm of the weight force (r_W, a fraction of d_n) will be updated as well, based on the rotation of the block during the previous time step. This leads to a new acceleration a_1, which can be used to calculate the new velocity, $v_2 = v_1 + a_1 \cdot dt$.

The development of the velocity is now captured, so the last step is to define when to stop the loop. To determine the impact velocity, the loop must be stopped when the impact takes place, so when the travelled distance exceeds or is equal to the available movement space, s_{max}. Therefore, the travelled distance must be updated during each time step as well, based on the average velocity during this time step: $s[i] = s[i-1] + \frac{1}{2}(v[i] + v[i-1]) \cdot \Delta t$. Then, as soon as $s[i] \geq s_{max}$, the loop will be stopped and the last calculated value of the velocity is the impact velocity.

An example script is given below, written in Python. The velocity correction is determined for a case with $d_n = 2.5\ m, H = 6.0\ m, R = 0.0, f_{area} = 0.8, C1 = 1.0$ and a range of values is given for s in this example. Later, other variables will be varied to check their influence on the corrected velocity, for which $s = 0.1$ will be set as the standard value.

```
#check the effect of movement space
N = 200
sp = np.linspace(0.001,0.25,N)
v = np.zeros(N)
vc = np.zeros(N)
#Regular velocity calculation
for i in range(N):
    H = 6.0     #Wave height
    R = 0.0     #Rotation point, as a horizontal distance from the centre of gravity
    farea = 0.8         #Area subjected to wave
    s = sp[i]         #Travel distance
    C1 = 1.0           #Collision point moving block, distance to rotation point

    T = np.sqrt(5*H)+(H+3)*0.5 #Wave period Tm-1,0, linked to the wave height in a wonky way
    Ru = 1.75*yf*np.sqrt(H)*np.tan(alpha)/np.sqrt((2*np.pi)/(g*T)) #Run-up
    u = np.sqrt(2*g*Ru) #Fluid velocity, based on run-up

    frW = R  #Arm of weight
    frF = 0.96 + np.sin(alpha)*R #Arm of the wave force
    f_inertia = 0.776 + R**2   #Area moment of inertia as a fraction of dn^5

    k1 = 0.5*farea*frF*C1/f_inertia
    k2 = frW*C1/f_inertia
    if (k1*rhow*cd*u**2) /(rhos*dn) - k2*(rhos-rhow)*g/rhos >= 0.0:
        v[i] = np.sqrt( 2*s*((k1*rhow*cd*u**2) /(rhos*dn) - k2*(rhos-rhow)*g/rhos ) )
        #The derived formula for impact velocity
    else:
        v[i] = 0.0   #Set v to zero if sum of moments is negative
#Velocity correction
    #Make some arrays to store variables for each time step
    ar = np.zeros(2000)
    dt = 0.001
    ar[0] = (0.5*rhow*cd*farea*dn**3*u**2*frF - (rhos-rhow)*g*dn**4*frW)/(f_inertia*rhos*dn**5)
    vcor = np.zeros(len(ar))
    scor = np.zeros(len(ar))
    ucor = np.zeros(len(ar))
    vr = np.zeros(len(ar))
    thetacor = np.zeros(len(ar))

    frWcor = np.zeros(len(ar))

    for j in range(len(ar)):
        vcor[j] = vcor[j-1] + ar[j-1]*C1*dn*dt  #  a = ar * C1 * dn
        ucor[j] = u - vcor[j]/C1*0.96

        vr[j] = vr[j-1] + ar[j-1]*dt

        thetacor[j+1] = thetacor[j] - vr[j]*dt

        frWcor[j] = R + np.sin(thetacor[j])*0.77*dn  #0.77 dn = 1/2 D


        ar[j] = (0.5*rhow*cd*farea*dn**3*ucor[j]**2*frF - (rhos-rhow)*g*dn**4*frWcor[j])/(f_inertia*rhos*dn**5)

        scor[j] = scor[j-1] + 0.5*(vcor[j] + vcor[j-1])*dt
        if scor[j] > s:
            break

    if vcor[j] > 0:
        vc[i] = vcor[j]

    else:
        vc[i] = 0

x = vc/v
plt.plot(sp,x)
plt.xlabel('Movement space s, [1/dn]',size=12)
plt.ylabel('Ratio v_corrected / v',size=12)
```

The time step needs to be small in order to get an accurate impact velocity, so this method will not be implemented in the Monte Carlo simulation during this MSc thesis, since that makes it computationally heavy. If a large computation time is no problem, or you have very large computational capacity, it is an option to implement the velocity correction in the Monte Carlo simulation, but that will not be done here. Instead, a correction factor will be determined, to account for the decreasing acceleration, without having to perform a loop.

To determine a correction factor, the ratio between the impact velocity with correction of acceleration and the impact velocity without correction will be determined. Ideally, this ratio would be constant for all cases, but sadly there are differences for different combinations of the variables that affect the impact velocity. The main variables are: the diameter d_n, the wave height H, the area subjected to the wave f_{area}, the travel distance s, the collision point C, and the rotation point R.

Using the previously given example script, the velocity correction can be compared to the uncorrected velocity by means of a plot.

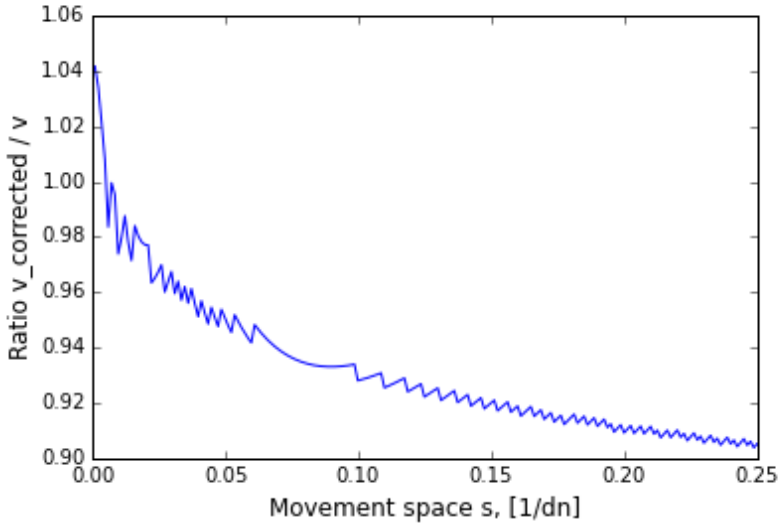

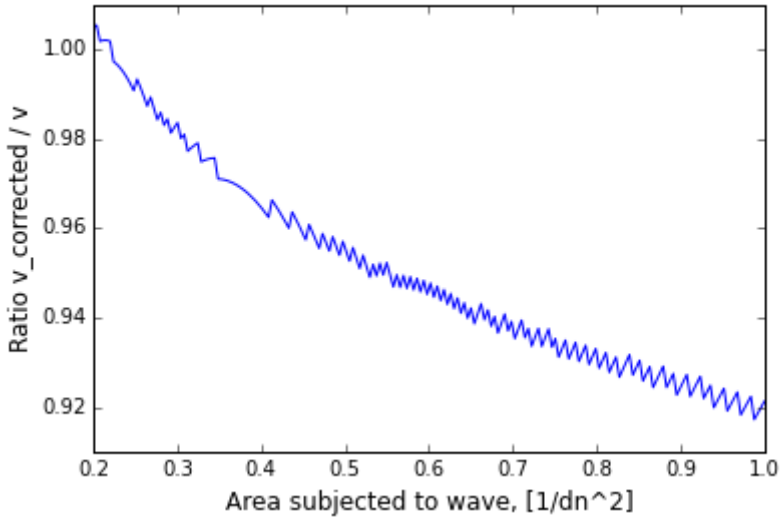

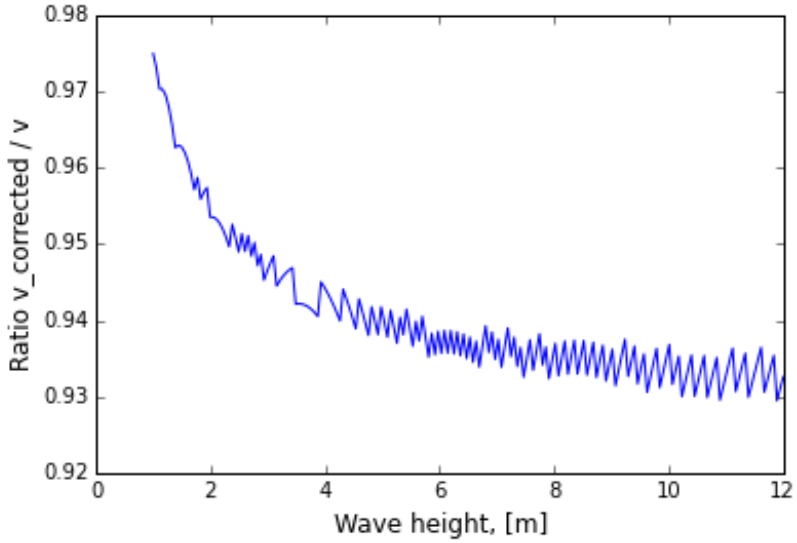
Ratio v_corrected / v
Wave height, [m]
0.98
0.97
0.96
0.95
0.94
0.93
0.92
0
2
4
6
8
10
12

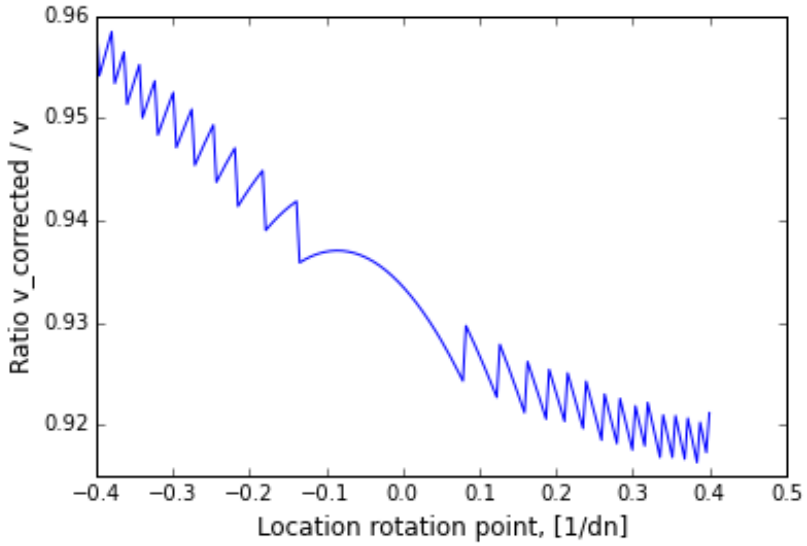
Ratio v_corrected / v
Location rotation point, [1/dn]
0.96
0.95
0.94
0.93
0.92
−0.4
−0.3
−0.2
−0.1
0.0
0.1
0.2
0.3
0.4
0.5

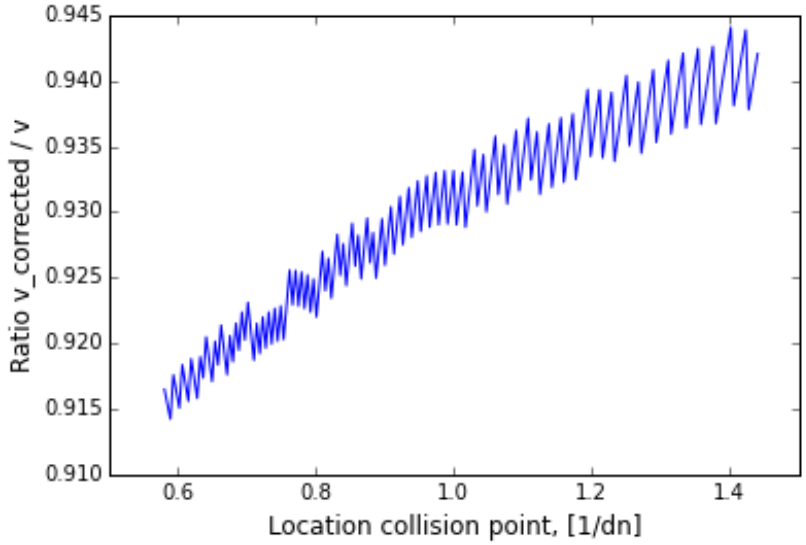
Ratio v_corrected / v
Location collision point, [1/dn]
0.945
0.940
0.935
0.930
0.925
0.920
0.915
0.910
0.6
0.8
1.0
1.2
1.4

The plots show that each variable affects the velocity correction. It is therefore difficult to create a single expression for a correction factor, as each variable should actually be included in that expression. Also, it would be interesting to see how much correction would be needed in all variables are varied together, to get to the limit of the required correction. This is done in the final plot, where all of the earlier variations are included. Note that the variation of the location of the collision point is reversed, in order to obtain the most unfavourable case, since that variable was the only one that showed an upward trend.

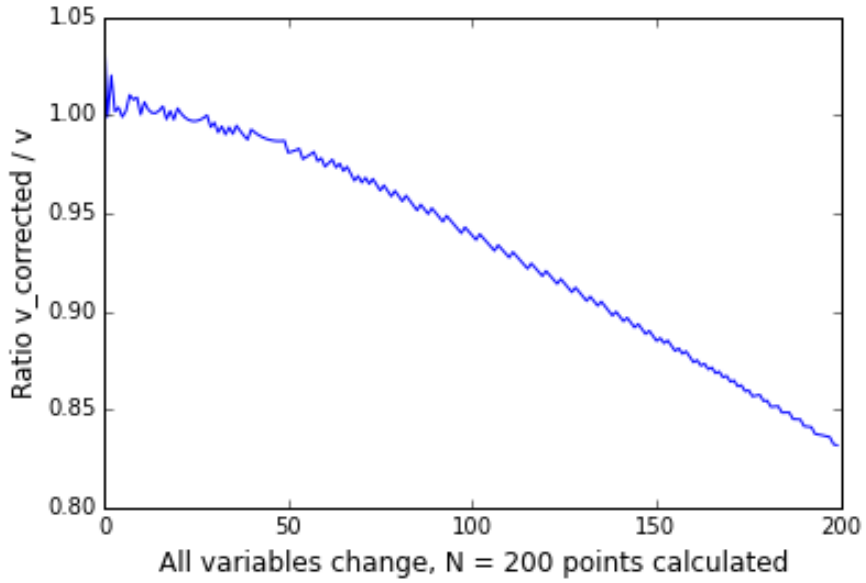

Eventually, a final value of 0.832 is obtained, so in any case, the required velocity correction will be less than 20%. Also note that this most unfavourable case is extremely rare; rarer than one in a billion. Still, there are also much more probable cases that still require a correction of around 10%.

To be able to incorporate the velocity correction in the Monte Carlo simulation, a simple correction factor will be established. This correction factor will be based solely on the available movement space, which is an arbitrary, but necessary in order to keep it simple. The movement space is evaluated as the most important variable, since it has a big influence on the travel time, as well as on the change of the arm of the weight. Looking back at the plot of the movement space variation, the correction factor seems to be proportional to s via a square root, more specifically, in the form of: $f_{cor} = 1 - x \cdot \sqrt{s}$, where $x = 1/4$ is found as a reasonable fit.

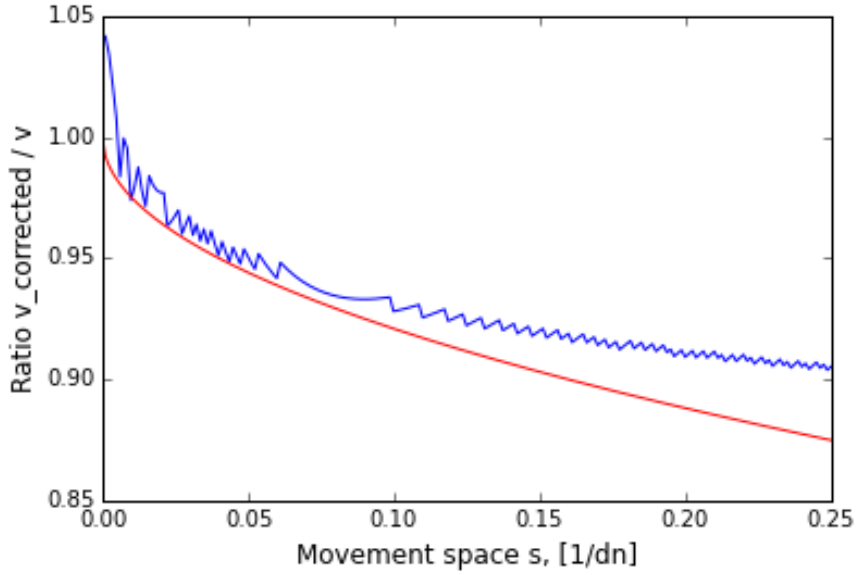

Note that the fitted line deviates from the calculated velocity correction, but this is done intentionally, to account for the variation of the other variables. The velocity correction factor is thus not perfect, but it will help to decrease the error.

Eventually, the velocity correction factor is determined as:

$$f_{cor} = 1 - \frac{\sqrt{s}}{4}$$

Appendix C. Shear strength check

This appendix is meant to prove that the shear strength is not governing for rupture of a breakwater leg at its base. It was earlier identified that failure due to bending was most likely the governing case, but this appendix attempts to prove that this is indeed true.

The shear strength of concrete can be determined according to:

$$v_{Rd,c}\ [N/mm^2] = 0.035 \cdot k^{3/2} \cdot f_{ck}$$

with: $k = 1 + \sqrt{\frac{200}{d}}$

Where: f_{ck} is the characteristic concrete strength, and d is the effective height of the cross section.

Note that d is generally used regarding reinforced concrete, for which, as a rule of thumb, $d = 0.81 \cdot h$, with h as the full height of the cross section. Since there is no reinforcement in this case, it seems appropriate to just use $d = h$ instead.

The allowable shear force can then simply be determine by multiplying with the cross section area. Note that the impact strength is assumed to be approximately twice as high as the regular strength, which leads to:

$$V_{Rd,c,impact}[N] = 2 \cdot v_{Rd,c} \cdot b \cdot d$$

The forces at the base of the leg are determined with the strut-and-tie model, which is shown once more in Figure C.0.1 and Figure C.0.2.

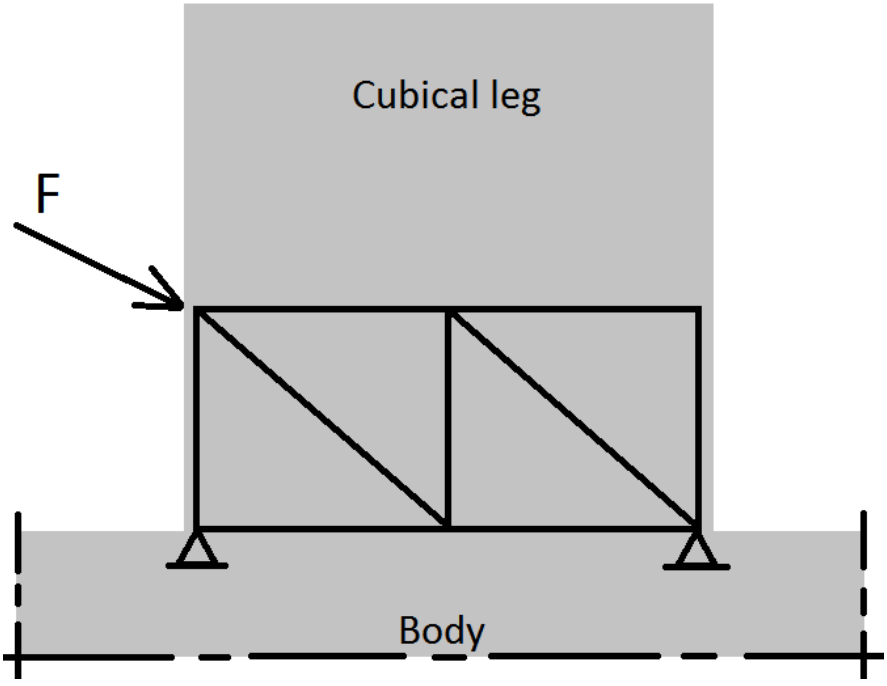

Figure C.0.1: Strut-and-tie model, example for a cubical leg

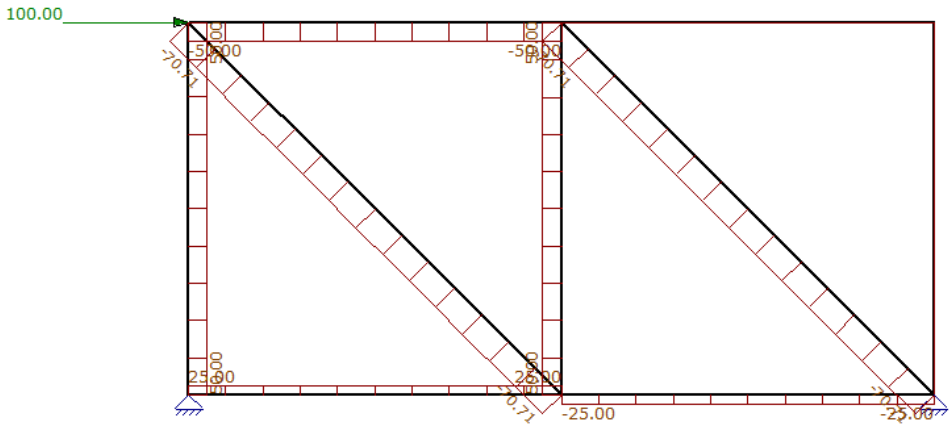

Figure C.0.2: Strut-and-tie model results from MatrixFrame

From the strut-and-tie model, the shear force at the bottom of the leg is identified as:

$$V = F_H/2$$

In Figure C.0.3, the shear force determined from the model is plotted against the probability of exceedance. To show that the shear resistance is not exceeded, a horizontal line that represents the shear resistance is drawn in the same graph. The shear resistance is not a exceeded a single time, proving that shear failure over the full leg is not a governing failure case.

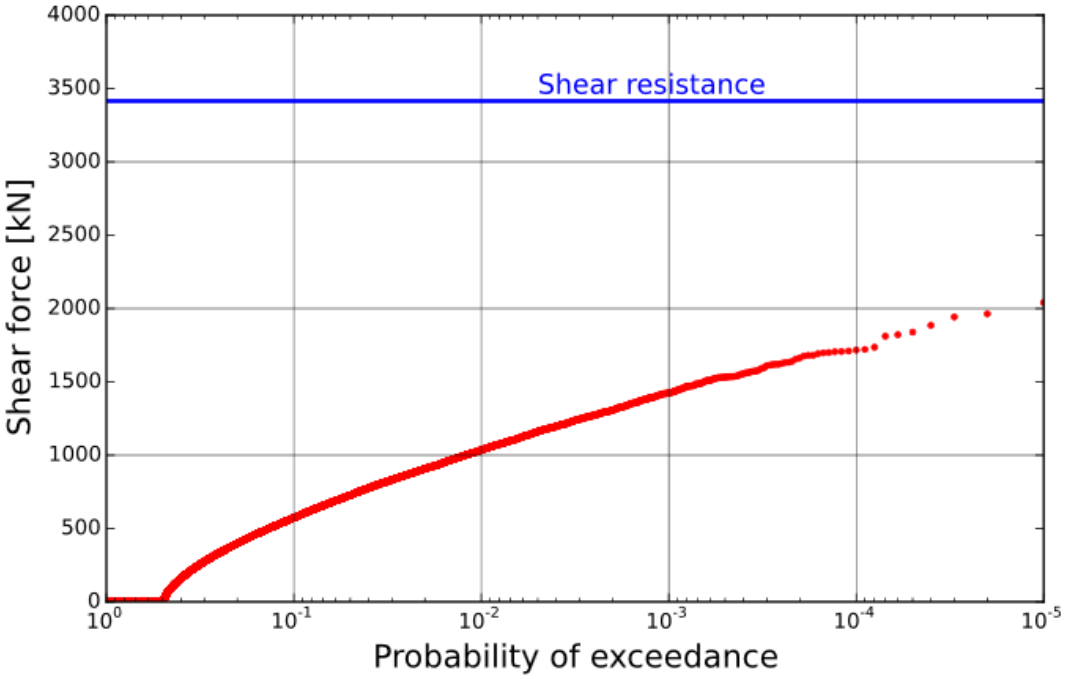

Figure C.0.3: Plot of the calculated shear force, plus the shear resistance

Note that in other cases, with extremely large waves and very large armour units, the shear resistance will eventually be exceeded for some units, but even then, the tensile strength is already exceeded due to the bending stresses, so shear over the full leg is still not the governing failure mechanism.

Appendix D. Python script of the model

The model is implemented in a Python script. The code is given in this appendix.

```
import matplotlib.pyplot as plt
import numpy as np
%matplotlib inline
```

Input

```
dn = 2.71 #m        INPUT VARIABLE
Hs = 10.01 #m        INPUT VARIABLE


rhow = 1025.0 #kg/m
rhos = 2400.0 #kg/m³
g = 9.81 #m/s²
alpha = np.arctan(3.0/4.0) #Slope 3V:4H
cd = 1.20 #Drag coefficient Xbloc
yf = 0.45 #Roughness coefficient Xbloc

#Create a wave height distribution, Rayleigh distribution for significant wave height Hs
p = np.linspace(1.0/10000,1,10000)
H_distribution = np.sqrt(-0.5*np.log(p))*Hs
H_distribution = np.sort(H_distribution)

#Create the travel distance/movement space distribution
s_dist = np.zeros(1000000)
for i in range(len(s_dist)):
    if i > 500000:
        s_dist[i] = np.random.exponential(0.0408)
```

Impact velocity, Monte Carlo simulation

Simulates N independent events, where a new wave and new block positioning parameters are picked for each event

```
N = 100000
v = np.zeros(N)
for i in range(N):
    H = np.random.choice(H_distribution)#Pick a random wave from the earlier created wave height distribution
    R = np.random.normal(0,0.144)       #Rotation point, as a horizontal distance from the centre of gravity
    farea = np.random.normal(0.381,0.083)           #Area subjected to wave
    s = np.random.choice(s_dist)*dn           #Travel distance
    C1 = np.random.uniform(0.58,1.44)              #Collision point moving block, distance to rotation point

    T = np.sqrt(5*H)+(H+3)*np.random.uniform(0,1) #Wave period Tm-1,0, linked to the wave height in a wonky way
    Ru = 1.75*yf*np.sqrt(H)*np.tan(alpha)/np.sqrt((2*np.pi)/(g*T)) #Run-up
    u = np.sqrt(2*g*Ru) #Fluid velocity, based on run-up

    frW = R  #Arm of weight
    frF = 0.96 + np.sin(alpha)*R #Arm of the wave force
    f_inertia = 0.7783 + R**2   #Area moment of inertia as a fraction of dn^5

    k1 = 0.5*farea*frF*C1/f_inertia
    k2 = frW*C1/f_inertia
    if (k1*rhow*cd*u**2) /(rhos*dn) - k2*(rhos-rhow)*g/rhos >= 0.0:
        #The derived formula for impact velocity
        v[i] = (1.0 - 0.25*np.sqrt(s)) * np.sqrt( 2*s*((k1*rhow*cd*u**2) /(rhos*dn) - k2*(rhos-rhow)*g/rhos ) )
    else:
        #Set v to zero if the moment caused by the wave is not larger than the moment due to the own weight
        v[i] = 0.0
#Sort the impact velocities from low to high
v = np.sort(v)
```

```
#Plot with the probability logarithmic on x-axis
plt.figure(figsize=(8,5))
for i in range(9):   #Add a raster to make it easier to read the plot
    plt.axvline(10**(-i-1),color = 'k', linewidth = 0.3)
    plt.axhline(i*0.5,color='k',linewidth = 0.3)
plt.plot(cp,v[::-1],'r.')
plt.xscale('log')
plt.xlim(1,10**-5)
plt.xlabel('Probability of exceedance',size=15)
plt.ylabel('Impact velocity [m/s]',size=15)
plt.title('Exceedance probability impact velocity Xbloc',size=19)
plt.savefig('excplot.svg',format='svg');
```

Impact force and stresses

```
#Create the distribution of the angle of the incoming force
p = 85.0
pt = np.linspace(0,1,10000)
thetaf = np.zeros(len(pt))
for i in range(len(thetaf)):
    thetaf[i] = np.sqrt(8925*pt[i]) #First part of the line

    a = -1.0/2100  #a in the abc formula ->  a*x^2 + b*x + c = 0, x = (-b +- sqrt(b^2 - 4*a*c))/(2*a)
    b = 0.1        #b in the abc formula
    if thetaf[i] > p:
        c = -4.25 - pt[i] #c in the abc formula
        thetaf[i] = (-b + np.sqrt(b**2 - 4*a*c))/(2*a)   #Second part of the line
```

```
#F = np.sqrt(m1 * v1^2 * k - m2 * v2^2 * k)   m1 = mass block 1, the moving blok
                                    #   v1 = velocity block 1
                                    #   k = "stiffness"
                                    #   m2 = mass block 2, the stricken blok, which moves due to the impact
                                    #   v2 = velocity block 2
#If v2 is unknown, just say it's zero and remove the part of -m2 * v2^2 * k
m1 = dn**3*rhos
v1 = v #np.linspace(0.1,2.0,10) #m/s, the previously determined impact velocity
thetaF = np.zeros(len(v1))

E = 32837e6 #N/m²  Young's modulus concrete

As = 0.2297*dn**2
Is = 0.004461*dn**4

Ac = 0.2297*dn**2
Ic = 0.004461*dn**4
```

```
F = np.zeros(len(v1))
leg = len(v1)*(['leg'])

for i in range(len(v1)):
    #"Stiffness" combination of: k = EA/L and  k = 3EI/L³
    thetaF[i] = np.random.choice(thetaf) #degrees  Angle of the force - 0° = parallel to leg/ straight on the leg, 90° = perpendicular to leg
    thetaF[i] = thetaF[i]/360.0*2*np.pi  #Angle can be anywhere inbetween 0° and 90°
    leg_det = np.random.uniform(0,1) #To randomly determine which leg is hit: as spiky leg or a cubical leg
    if leg_det <= 2.0/3:
        #Spiky leg
        leg[i] = 's'
        Ls = 0.540*dn

        kleg = 1.0/np.sqrt( ((np.cos(thetaF[i]))**2 / (E*As/Ls)**2 )  +  ((np.sin(thetaF[i]))**2 / (3*E*Is/Ls**3)**2) )
        kbed = 69.4e6*dn**2
        ks = 1.0 / (1.0/kleg + 1.0/kbed)

        F[i] = np.sqrt(m1*v1[i]**2*ks)

    if leg_det > 2.0/3:
        #Cubic leg
        leg[i] = 'c'
        Lc = 0.481*dn

        kleg = 1.0/np.sqrt( ((np.cos(thetaF[i]))**2 / (E*Ac/Lc)**2 )  +  ((np.sin(thetaF[i]))**2 / (3*E*Ic/Lc**3)**2) )
        kbed = 69.4e6*dn**2
        kc = 1.0 / (1.0/kleg + 1.0/kbed)


        F[i] = np.sqrt(m1*v1[i]**2*kc)


#Now on to determining the stresses
FH = F*np.sin(thetaF)
FV = F*np.cos(thetaF)
```

```
#Strut-and-tie model - Horizontal force
b = 1443*dn/3
h = np.zeros(len(leg))
for i in range(len(leg)):
    if leg[i] == 's':
        fL = np.random.uniform(-0.1,0.9)
        if fL < 0:
            fL = 0
        h[i] = (1-fL)*481*dn
    if leg[i] == 'c':
        fL = np.random.uniform(-0.4,0.6)
        if fL < 0:
            fL = 0
        h[i] = (1-fL)*481*dn

sig = 2*1.75* (FH*(h/b)**0.9 - FV) / (115680.5*dn**2)
sig = np.sort(sig)

#Percentage of broken blocks
broken = 0
for i in range(len(sig)):
    fct = np.random.normal(5.8,1.098)
    if sig[i] > fct:
        broken += 1.0
percentage_broken = round(broken/N*100 , 1)

print percentage_broken,'% of the armour units is expected to break'
```

```
#Plot the figures

F = np.sort(F)
F = F/1000
plt.figure(figsize=(8,5))
p = np.linspace(0,1,len(v1))
for i in range(5):   #Add a raster to make it easier to read the plot
    plt.axvline(10**(-i-1),color = 'k', linewidth = 0.3)
    plt.axhline(i*10000,color='k',linewidth = 0.3)
plt.plot(p,F[::-1],'r.')
plt.xscale('log')
plt.xlim(1,10**-5)
plt.xlabel('Probability of exceedance',size=15)
plt.ylabel('Impact force [kN]',size=15)
plt.title('Exceedance probability impact force',size=19)
plt.savefig('forceplot.svg',format='svg');


plt.figure(figsize=(8,5))
plt.plot(p,sig[::-1],'r.')
#plt.plot(p,sigma[::-1],'bo')
plt.xscale('log')
plt.axhline(5.8,color ='b',linewidth=2.0)
plt.text(0.005,6.5,'Mean tensile impact strength',color='b',size=13)
plt.text(percentage_broken/150,4.5,percentage_broken,color='r',size=12)
plt.text(percentage_broken/300,4.5,'% fails',color = 'r',size=12)
for i in range(7):   #Add a raster to make it easier to read the plot
    plt.axvline(10**(-i-1),color = 'k', linewidth = 0.3)
    plt.axhline(i*10,color='k',linewidth = 0.3)
plt.xlim(1,10**-5)
plt.ylim(0,50)
#plt.legend(['Stress via strut-and-tie method','Stress from slender beam theory'])
plt.xlabel('Probability of exceedance',size=15)
plt.ylabel('Stress [N/mm2]',size=15)
plt.title('Maximum tensile stress, exceedance probability',size=19)
plt.savefig('stressplot.svg',format='svg');
```